409 321

6342

BOEING

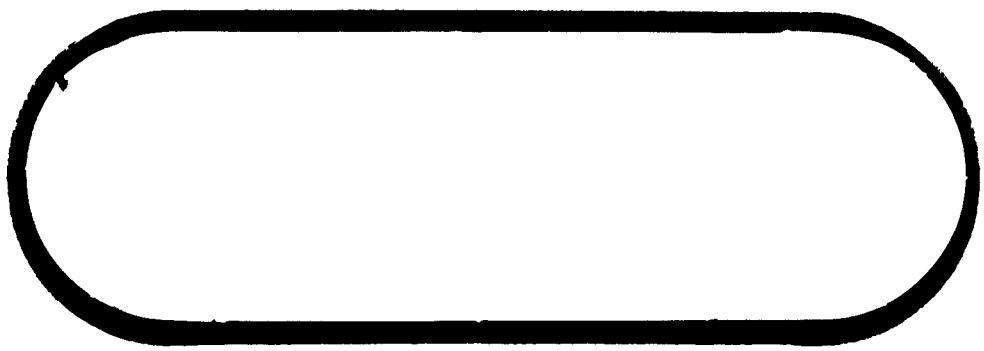

SEATTLE, WASHINGTON

THE BOEING COMPANY

NUMBER D2-80085

UNCLASSIFIED TITLE Leading Edges Development - Dyna Soar

MODEL NO. X-20A CONTRACT NO. AF33(657)-7132

ISSUE NO. 5 ISSUED TO Armed Services Tech. Dig.

CLASSIFIED TITLE
(STATE CLASSIFICATION)

See Sub-sections
CHARGE NUMBER

PREPARED BY D. A. Bowers 6/7/63 Paul H. Esch 6/20/3
D. A. Bowers P. G. Esch ARS

SUPERVISED BY A. K. Hepler 6/22/63
A. K. Hepler MA-11 dcln

APPROVED BY A. K. Hepler for 6/24/63
M. A. Nelson MA-11 dcln

CLASS. & DISTR. APPROVED BY A. K. Hepler for 6/25/63

RELIABILITY APPROVAL 6-26-63
(DATE)

VOL. I NO. D2-80085
SEC. PAGE 1 OF

2-3142

DOCUMENT, TITLE PAGE U3 4297 9000 REV. 1/61

DOCUMENT DISTRIBUTION

Aeronautical Systems Division (ASZRA)
Air Force Systems Command
Wright-Patterson Air Force Base, Ohio (3cys)

Armed Services Technical Information Agency
Arlington Hall Station
Arlington, Virginia (10cys)

AFFR (RWRSB)

CONTRACT REQUIREMENT

This document is submitted in partial fulfillment of paragraph B(1.1.1.1.9.2) of Statement of Work, System 620A, Exhibit 620A-62-2, dated 26 January 1962, revised 1 August 1962.

SUMMARY

This document reports on the facilities development and test results from the Dyna Soar Leading Edge Development Program.

The leading edge development program was undertaken: (1) to evaluate experimentally five leading edge and attachment scheme designs proposed for use on the glider and (2) to establish the reliability and structural integrity of the most promising design. All designs tested were evolved from the thin shell, coated molybdenum alloy leading edge concept which was proved feasible during Phase I of the Dyna Soar program.

A series of tests were begun by subjecting each specimen of the five design concepts to an acoustical vibration test performed at room temperature to simulate the boost trajectory sonic environment. Following these tests all specimens were exposed to elevated temperature tests in still air utilizing quartz radiant heating lamps. Each leading edge was subjected five times to time variable thermal environments simulating maximum heating rates, maximum temperature including exposure to design temperature overshoot, and maximum thermal gradients anticipated during re-entry along Dyna Soar trajectories.

Following a repetition of the initial acoustical vibration test on each specimen, four of the designs, using the above-mentioned specimens, were loaded statically to destruction at room temperature employing conventional loading rates. Two of the designs tested at conventional rates were also statically loaded to destruction at rapid loading rates.

Subsequent to the above series of tests, the double shell leading edge design was selected as the most promising design concept for additional testing. A specially designed plasma jet arc chamber and shroud was developed and calibrated to test the full-scale leading edge segment in an environment combining variable heat flux, temperature, pressure, surface airflows, and erosion conditions. Under these combined conditions the structural integrity and reliability was established for the double shell design.

All tested leading edge designs performed satisfactorily from the strength standpoint. No structural failures were caused by sonic testing, thermal stresses resulting from thermal gradients and heating rates, or plasma testing of the double shell design. All designs supported significantly higher loads than predicted during static tests. Although oxidation failures occurred through the molybdenum disilicide coatings during the radiant heat and plasma jet tests, the extent of these failures did not prevent the specimens from meeting the design requirements.

Because many of the parameters required for an analytical solution could not be defined with sufficient accuracy, the effects of boundary layer gas leakage on temperatures of the leading edge structural components were evaluated experimentally under EWA 5-609*. The double shell leading edge evaluated during the EWA 5-617 concept evaluation incorporated maximum inherent sealing capability. To determine if this sealing capability was adequate, a full-scale specimen was subjected to a simulated re-entry environment utilizing the plasma jet and shroud nozzle previously developed. Time history recordings were obtained for the leading edge shell temperatures, leakage flow rate, and leading edge support structure temperatures to evaluate leakage effects. Initial runs were performed on calibration models to establish the required test environment.

This document is published in three sections. Section 1 reports the leading edge plasma jet and shroud development program of EWA 5-615*. Section 2 reports the leading edge plasma jet seal evaluation test program of EWA 5-609*. Sections 1 and 2 are contained in Volume 1. The work of EWA 5-617* to develop the leading edge preliminary concepts and attachment schemes is reported under Section 3 and published in three volumes under separate covers. Volume 2 describes the test program in detail; Volumes 3 and 4 contain the recorded thermal data in the form of computer tabulations.

* Refer to D2-6783-1 Structural Integrity Development and Test Program - Detail Plan - Structures Technology

TABLE OF CONTENTS

* Refer to D2-6783-1 Structural Integrity Development and Test Program - Detail Plan - Structures Technology

INTRODUCTION

This report is the result of work accomplished on Dyna Soar EWAs 5-609*, 5-615*, and 5-617*. The development test work was required to obtain empirical data to supplement and check analytical procedures for the prediction of various environmental effects on proposed leading edge and attachment structural designs. Each design tested was evolved from the thin shell Mo - 0.5% Ti leading edge protected by molybdenum disilicide oxidation-resistant coating; a concept proved feasible during Phase I of the Dyna Soar program.

Prime objectives of this program were to establish and improve the reliability and structural integrity of a leading edge design which would be acceptable for use on the Dyna Soar glider.

Emphasis during testing was directed toward the following problem areas which were considered critical to the leading edge design. The reliability and integrity of leading edges depends on maintaining the continuity of the oxidation protective coating while being subjected to high heat flux, temperatures, thermal stresses, and stream flows. A leading edge design must account for the brittle effects of coating penetration and grain growth in the basic structural material. Since leakage of hot boundary layer gas into the leading edge cavity poses a threat of excessive temperature on various structural components, the joints between adjacent leading edge segments must restrict this leakage without imposing undue restraints on relative motions of the segments. And last, the attachment of the leading edge segments to the support beam must be adequate for airload and sonic vibration environments without significantly restraining differential thermal expansion between the leading edge segments and supporting structure.

EWA 5-617*, the initial portion of the leading edge development program, was formulated to determine the most promising leading edge design configuration and attachment scheme warranting more refined testing and evaluation. Full-scale test specimens, representing five leading edge and attachment scheme combinations, were fabricated and subjected to room temperature sonic tests, thermal gradient tests utilizing radiant heat, and room temperature static load tests to destruction. Measurements recorded included vibration response amplitudes, structural temperature distribution time histories, and load strains and deflections. Test results were analyzed and compared with preliminary theoretical analyses.

Qualification of a leading edge design for flight required testing under combined environmental conditions. Plasma jet testing presented a feasible method of simulating the temperature, pressures, and surface airflow conditions of hypersonic re-entry flight. To run concurrently with EWA 5-617*, EWA 5-615* was established to develop a plasma jet arc chamber and a specially designed shroud-nozzle that would permit tests on full-scale leading edge segments. Construction techniques and methods of control were developed to obtain the required test duration, range of test parameters, and time variable control of the test parameters.

* Refer to D2-6783-1 Structural Integrity Development and Test Program - Detail Plan - Structures Technology

THE BOEING COMPANY

NUMBER D2-80085 MODEL NO. DYNA-SOAR

TITLE LEADING EDGES DEVELOPMENT

	V. Gladstone V. M. Gladstone	4/24/63
	W. G. Oakes W. G. Oakes	4/26/63
PREPARED BY	T. Namatame T. Namatame	4/26/63
SUPERVISED BY	W. Rose W. K. Rose	4/26/63.
APPROVED BY	J. R. Glynn J. R. Glynn	4/29/63
RELIABILITY APPROVAL		(DATE)

A. K. Hopkins 4/29/63

AF 33(657)-7132
CONTRACT NO.

CHARGE NUMBER

VOL.
SEC. 2

NO. D2-80085
PAGE
2-1 of 93

2-5142

SECTION TITLE PAGE U3 4285 6000 REV. 2/61

2.1 SUMMARY

This work was undertaken to evaluate the double shell leading edge design considered for use on the X-20 glider and determine its sealing capabilities during simulated re-entry environment. An arc plasma jet with an associated shroud nozzle was constructed to apply the environmental conditions.

Checkout runs were conducted on an improved arc plasma jet with an integrated shroud nozzle to determine facility response to various combinations of airflow, power settings and electrode locations. Three full scale leading edge models including one graphite model and two disilicide coated Mo +.5Ti single shell models were used to obtain pressure and temperature gradients under various airflow and power levels. A fourth model, a disilicide coated Mo +.5Ti double shell design was utilized to evaluate the amount and effect of hot gas leakage through that leading edge configuration.

During the calibration runs stagnation pressures from less than 0.1 to 1.82 psig were obtained in conjunction with stagnation temperatures from 2300°F to approximately 3000°F. The test facility demonstrated capability to simulate glider re-entry conditions including transient maneuvers from the equilibrium glide line.

2.2 TABLE OF CONTENTS

2.2 CONTENTS (Continued)

2.10 FIGURE LIST

2.2 CONTENTS (Continued)

2.2 CONTENTS (Continued)

2.2 CONTENTS (Continued)

2.3 REFERENCES

A. D2-6783-1, "Structural Integrity Development and Test Program - Detail Plan - Structures Technology" Boeing Company, December, 1960

B. Boeing Drawing 25-17648, "Riveted Leading Edge, Assembly of"

C. Boeing Drawing 25-20378, "Leading Edge Segment - Forward Body Double Shell - Short"

D. Boeing Drawing 25-20375, "Leading Edge Installation Forward Body"

E. Boeing Drawing 25-20372, "Leading Edge Segment Forward Body"

F. Boeing Drawing 25-17647, "Support Structure, Leading Edge Segment"

G. Boeing Drawing 25-20314, "Leading Edge Installation"

H. Boeing Drawing 25-17649, "Leading Edge Segment Assembly, Graphite"

I. Boeing Drawing 25-17648, "Riveted Leading Edge, Assembly of"

J. Boeing Drawing 25-20355, "Support Assembly of Leading Edge Segment, Forward Body"

K. D2-11104, "Simulation Capabilities of the Boeing Arc Jet Facilities" Boeing Company, June 1962

2.4 INTRODUCTION

This work was accomplished on EWA 5-609.*

During the boost phase and re-entry maneuvers of the X-20 glider, the leading edges will experience aerodynamic heating. Due to the pressure difference between the outer and inner surfaces of the leading edges, the hot boundary layer gases will leak into the space between the leading edge and the leading edge beam. The amount of leakage is affected by both the pressure differential and the leading edge sealing capability. If excessive hot gas leakage occurs, the leading edge beam could be heated to the point where its structural strength would be seriously reduced.

It was necessary to experimentally measure the amount of leakage through a typical leading edge configuration under re-entry temperatures and pressures. Structural and thermal effects on the leading edge and leading edge beam caused by the simulated re-entry environment were evaluated.

The flight environment of the leading edges of the X-20 glider was simulated by a plasma arc chamber in conjunction with a water cooled copper shroud-nozzle. The arc chamber was used to heat the air to a desired temperature and energy level and the shroud-nozzle was used to contain the flow around the leading edge for proper temperature and pressure distribution. Three calibration models were used to check out the shroud-nozzle capability as well as establishing arc chamber operating parameters to achieve test model environment requirements. A section of the forward body leading edge was selected as the test model for this program.

* See Reference A.

2.5 TEST SPECIMENS AND INSTRUMENTATION

2.5.1 Test Specimens

Three calibration models, designated pressure, thermal distribution, and leakage control models, and one segmented double shell forward body leading edge specimen were tested during this program. The three calibration models were originally used in the development phase of the plasma arc chamber authorized under a different test program. These models were retested to substantiate the attainability of test conditions by the arc chamber facility because it was updated to the final configuration.

Dimensionally, the test specimens were representative of the forward body contour. Each of the models were 12 inches long with a 6.5-inch cylindrical radius and a 10.5-inch chord length.

2.5.1.1 Pressure Model (Figure 2-1)

The pressure model was fabricated from a solid ATJ graphite block. The entire surface of this model was siliconized to prevent any oxidation in the high temperature environment. Siliconizing, a proprietary process developed by the National Carbon Company, provides a silicon-carbon composition on the surface approximately .10-inch deep with no apparent change in contour. The model was mounted on a water-cooled copper simulated back-up structure and heat shields.

"Glasrock" end blocks, located at the ends of the shroud-nozzle and the model, were installed to provide material evaluation for end blocks to be used in subsequent models. End blocks are used to block flow of the hot gases around the ends of the models and offset the thermal gradient created by the water-cooled end walls of the shroud-nozzle. Molybdenum-0.5% titanium straps, loaded in tension by springs helped seal the ends at the skin and end block interfaces.

2.5.1.2 Thermal Distribution Model (Figure 2-2)

The thermal distribution model was a 12-inch long molybdenum-disilicide coated molybdenum-0.5% titanium shell segment 0.030 inch thick. The shell was stiffened with molybdenum-0.5% titanium formed angles and mounted on a René 41 back-up structure with molybdenum-0.5% titanium heat shields.

Glasrock end blocks with the coated molybdenum-0.5% titanium straps were used to seal the ends.

2.5.1.3 Leakage Control Model (Figure 2-3)

The leakage control model was a single sheet 0.05 thick coated molybdenum-0.5% titanium shell formed to match the contour of the forward body leading edge. The contoured skin was attached to a water-cooled copper back-up structure. The back-up structure was constructed to make a box to collect the leakage gases. The contoured shell was closed off with "glasrock," to fit the ends of the model. An integral part of the back-up structure was a Rene 41 beam assembly located to simulate the front spar in the flight article. The beam assembly included only the web and the stiffeners. The top and bottom chords were not included in the test set-up.

Heat shields of 0.012 gage coated molybdenum-0.5% titanium were installed immediately aft of the specimen along the upper and lower contour surface. The shields were also attached to the copper simulated back-up structure.

Straps made of disilicide coated molybdenum-0.5% titanium were installed at the ends of the model surface. The straps served to seal the model at the ends because of the thermal expansion lag between the skin and the end blocks.

2.5.1.4 Segmented Double Shell Model (Figure 2-4)

The test specimen consisted of an outer skin made of 0.012 gage coated molybdenum-0.5% titanium. The skin was made in four segments, each approximately 3.00 inches wide and were assembled to have an 0.02 gap at the circumferential butt joints. The outer skin made faying surface seals with the inner shell at the butt joints.

The inner shell of the leading edge assembly was made from 0.030 gage coated molybdenum-0.5% titanium sheet. Five separate segments were used to form the inner shell. Each of segments had integrally formed stiffeners for added strength. Siliconized ATJ graphite end blocks were fabricated to fit the ends of the model to seal the cavity between the leading edge skin and the front spar web assembly and thus prevented the hot gases of the arc chamber from flowing around the ends of the model.

The skin assembly was mounted on a water-cooled copper back-up structure. The box-like back-up structure also served as a leakage collection box for the hot gases leaking into the cavity immediately aft of the leading edge. The box was formed on five sides by the copper plates with the sixth side formed by the front spar web assembly which was exposed to the hot leakage gases.

2.5.1.4 (Continued)

Heat shields of 0.012 gage coated molybdenum-0.5% titanium were installed immediately aft of the specimen along the upper and lower contour surface. The shields were attached to the back-up structure.

The skin to end block seals were maintained by the coated molybdenum-0.5% titanium tension straps.

2.5.2 Instrumentation

Specimen instrumentation consisted of pressure transducers and high temperature thermocouples located within the specimen. In some instances, the specimen support structure was instrumented with thermocouples and pressure pick-ups to record data required for leakage rates and to analyze the thermal environment at the front spar.

A total radiation pyrometer was used, during some test runs, to supplement thermocouple stagnation point temperature data.

All of the recording instruments were calibrated prior to each test. Transducers were calibrated by the appropriate calibration laboratories.

The detailed description of the instrumentation are given below for each of the specimens as well as for the test facility.

2.5.2.1 Test Specimen Instrumentation

2.5.2.1.1 Pressure Model Instrumentation

The graphite model had twenty pressure ports drilled through the surface (see Figure 2-5). Ceramic tubings were inserted in the drilled holes and connected to a 48-channel pressure scanner (Figure 2-6). This pressure scanner was used to obtain many pressure readings from one transducer thus, greatly reducing transducer calibration requirements prior to test. The pressure ports were connected to the scanner at circumferential locations. A rotating pick-up aligned with each of these locations and the pressure data is recorded via the transducer. The output of the transducer was recorded on a two-axis graphic recorder, Autograf, serial number 428, J. F. Moseley Company, which utilizes standard Cartesian coordinate paper.

There were ten pressure ports in the shroud-nozzle in addition to those in the model.(see Figure 2-5). These pressures were recorded in the same manner as those in the model.

2.5.2.1.2 Thermal Distribution Model Instrumentation

A total of twenty thermocouples were installed for testing of the thermal distribution model (see Figure 2-7). Fourteen platinum/platinum 13% rhodium thermocouples were located on the surface of the leading edge skin. Since it was prohibitive for these thermocouples to contact the molybdenum skin the junctions were attached to platinum discs and flame spray coated with aluminum oxide. A spring-loaded arrangement allowed the thermocouple to maintain contact with the inner skin when thermal expansion occurred during the heating cycle.

Two platinum/platinum-13% rhodium thermocouples were attached to the outstanding leg of one stiffener angle used to strengthen the leading edge skin.

Three chromel/alumel thermocouples were attached to the leading edge beam assembly that formed part of the back-up structure.

One platinum/platinum-10% rhodium thermocouple was located on the lower heat shield.

A total radiation pyrometer was installed to supplement the stagnation thermocouple data.

The thermocouple data were recorded on the Heiland oscillograph and Leeds and Northrup or Bristol recorders.

2.5.2.1.3 Leakage Control Model Instrumentation

The leakage control model was instrumented to determine surface and back-up structure temperatures at specific test conditions. Leakage gas flow rates and temperatures were recorded simultaneously.

The inner surface of the leading edge skin was instrumented with six coated disc type platinum/platinum-13% rhodium thermocouples shown on Figure 2-8. Again, the thermocouples were spring-loaded so that they maintained contact as the model experienced thermal growth.

A total radiation pyrometer was used to supplement the stagnation line thermocouple data.

The René 41 beam assembly located in the back-up structure to simulate the front spar beam was instrumented with five chromel/alumel thermocouples.

2.5.2.1.3 (Continued)

The temperature of leakage gases were measured in front of the beam assembly (in the leading edge cavity) as well as behind the beam with platinum/platinum-10% rhodium thermocouples.

A coated disc type platinum/platinum-13% rhodium thermocouple was used to obtain temperature data in the area of the lower heat shield.

Static pressures in the leakage collection box (box formed by the back-up structure) were recorded.

Initially, a system of three rotameters installed in parallel with a wet test gas meter (Figure 2-9), measured the leakage gas flow rates. When it was found that the mass flow rates were very small, a system using only the wet test gas meter was used. The two measuring devices closely repeated flow rates so the gas meter was chosen in favor of the rotameters because of the ease in read-outs.

2.5.2.1.4 Segmented Double Shell Model (Figure 2-10)

The segmented double shell model was instrumented in the same manner as the leakage control model.

2.5.2.2 Shroud-Nozzle Plasma Jet Facility Instrumentation

The plasma arc chamber was instrumented to ensure that facility calibration conditions were achieved for the desired test conditions. The calibration test runs were made to determine the arc chamber parameters that are required to be varied during the course of a test run to produce the varying conditions defined in the test requirements.

Arc voltage and current recordings were made for power calculations.

One water flowmeter and one differential temperature thermocouple in the cooling water were used to measure the energy absorbed by the arc chamber water coolant.

Four water flowmeters and differential temperature thermocouples individually measured the energy loss of the working fluid to the cooling water of the nozzle-shroud components.

In order to maintain surveillance on the separate parts that comprise the arc chamber, ten iron/constantan differential temperature thermocouples were installed in the cooling water of the individual components.

2.6 TEST SET-UP

The Boeing-developed shroud-nozzle plasma jet test facility, figure 2-12, was used to produce the simulated flight thermal and pressure environment for testing full-scale leading edge segments. This facility was unique in that a full-scale model was able to be tested to the required test conditions with the one megawatt of power available. The initial development work of the leading edge shroud-nozzle plasma jet facility is reported under Section I of this document.

2.6.1 Plasma Arc-Chamber

A schematic of the arc chamber and shroud-nozzle is shown in Figure 2-11. The arc chamber configuration incorporated water-cooled copper electrodes formed in an oblong shape to accommodate a wide nozzle throat. Figure 2-13 shows the shape of the unique electrodes as well as their relative position with respect to each other. An external magnetic field was used to rotate the arc.

A 1-inch by 14-inch nozzle throat, figure 2-14, was featured in the arc chamber to be able to test a one foot long full-size segment of the simulated flight hardware.

The separate parts of the arc chamber received water-cooling pre-set to optimum flow rates prior to each test. Heat absorbed by the entire cooling system was calculated from the water flow rate and temperature rise of the cooling water. A quartz window and water-cooled sight tube aimed at the stagnation line of the specimen permitted sighting of the total radiation pyrometer.

2.6.2 Shroud-Nozzle (Figure 2-14)

The working fluid exhausting from the arc chamber nozzle throat was contained by a water-cooled copper shroud-nozzle. The limitations imposed by the available electrical power determined the available energy to heat a surface at incremental distances from the nozzle throat. To efficiently use the energy that was available, a shroud-nozzle was employed. The shroud contour essentially matched that of the test models with allowances made to maintain specific gaps (between model and shroud) to achieve the heating rates and pressure distributions defined by the test requirements. The passage between the shroud and nozzle forms a nozzle and thus a velocity gradient in the flow through the cross-section. By the application of Bernoulli's equation for compressible flow, pressures will vary with velocity as a function of the gap.

2.6.3 Leakage Measurement System (Figure 2-15)

For the leakage control model and the segmented double shell model, test requirements necessitated devising a method for measuring the hot gases leaking into the cavity immediately behind the leading edge. A simple set-up was made connecting the leakage collection box with the measuring instruments. A small heat exchanger was installed in the set-up to cool the gases prior to being measured to protect the instruments and to reduce the temperature of the gases to the range at which the instruments were calibrated. A photograph of the leakage rate measuring instruments are shown in figure 2-9.

2.7 TEST PROCEDURE

The check-out and calibration of the initial test facility was accomplished during the developmental phase of the facility described in Section I. The check-out and calibration procedures were repeated during this program because it was deemed necessary to establish new test condition envelopes of the facility that was updated to a more reliable configuration. Several check-out runs were made without a model installed to ensure proper arc chamber operation and control during a continuous test period.

The test philosophy was to obtain test facility calibration information in steps prior to testing the segment of the flight hardware. First, the pressure model was tested to obtain the pressure environment that the flight hardware will experience; secondly, a thermal distribution model was tested to obtain model surface temperature information; thirdly, a leakage control model was used to obtain values of tare leakage gas flow rates leaking into the leading edge cavity. Finally, the flight hardware model was tested to obtain information to establish design integrity.

All the test conditions were predetermined by engineering before the time of the run. The test conditions were translated into mass airflows (working fluid) and arc current values from arc chamber calibration data and were preplotted on the recording strip charts. The pressure distribution requirements were controlled by the mass flow rates and the heating rate requirements are controlled by both the arc current and mass flow rates. Arc chamber operating conditions to give the test environment were, thus, achieved by controlling the air flows and arc current to the prescribed values plotted on the strip charts.

2.7 Continued

Cold flow tests were conducted prior to making the test runs. These tests were conducted to ensure the proper functioning of the 48-pressure scanner system as well as to make leakage checks on the pressure pick-ups. Locations of pressure taps showing leakage were noted and data from these were considered invalid. Cold flow tests were also used to determine the proper model positioning (gap between shroud and model) has been maintained.

2.7.1 Pressure Model

The pressure model was installed with predetermined gaps between the shroud-nozzle and model. The gap setting is an important parameter for facility calibration since the relationship between the mass flow rates of the working fluid and the surface pressures on the model varies with the gap setting between the shroud-nozzle and model.

With the model installed, the arc chamber was operated at varying mass flow rates. Pressure recordings at the model surface were made at each established flow rate. Simultaneous recordings of pressures along the shroud surface were made to establish correlation with model surface pressures.

2.7.2 Thermal Distribution Model

The thermal distribution model was installed with the shroud-nozzle to model gap settings adjusted from the information obtained in the pressure model runs. An additional parameter of model surface temperatures was introduced during this portion of the program.

The arc chamber was operated at various arc current settings. In addition, under each current setting, the working fluid mass flow rate was varied. At each known condition, temperature distribution on the model surface was obtained.

2.7.3 Leakage Control Model

With the facility test conditions established to achieve the desired temperatures and pressures, the leakage control model was tested to obtain the leakage rates through the heat shield and leading edge skin interface and from the ends of the model. These leakage sources were considered to be common to any test specimen and, therefore, leakages greater than those obtained would be attributable to the particular hardware configuration.

The control of the test environment was made by controlling the arc current and the gas mass flow rates simultaneously.

2.7.3 Leakage Control Model (Continued)

Leakage rates were recorded at various stagnation temperatures and pressure values. The wet test gas meter and three rotameters connected in parallel to measure the leakage gas flow rates were monitored. Selection of the wet test gas meter as the proper instrument to measure the leakage rates was made during the test run.

2.7.4 Segmented Double Shell Model

Using data obtained from the previous calibration models, the test conditions were established to impose an environment simulating flight conditions on the segmented double shell model. Test procedures, essentially, were similar to those used on the leakage control model. The shroud-nozzle to model gap was adjusted as the calibration model runs dictate.

The leakage gas paths were increased above those in the leakage control model due to seams existing in the double shell model.

2.8 TEST RESULTS

Test data are presented as plots or tabulations and photographs. The results and purpose of each model's tests are individually included in the following paragraphs.

2.8.1 Pressure Model

Photograph -- Figure 2-17 and Figure 2-18.

Data Plots -- Figures 2-19 through 2-22

Purpose:

To obtain test facility calibration data for use in determining arc chamber conditions and proper shroud-nozzle to model gap to provide the pressure distribution requested in Reference A. Plots of required stagnation pressure and temperature are shown in Figure 2-16.

2.8.1.1 Results

The pressure data were obtained from the siliconized graphite leading edge model test runs No. 102 and No. 103. Model surface and shroud surface pressure distributions for various arc chamber conditions are shown in Figure 2-19 through 2-21. The curve of the desired pressures taken from the test requirements in Reference A are superimposed on each of the figures. The pressures obtained are based on shroud-to-model gap settings shown in Figure 2-27.

2.8.1.1 (Continued)

The shroud-to-model gaps at the upper and lower surfaces were set at approximately 0.25 and 0.18 inches respectively, 3.5 inches from the stagnation line.

Maximum model surface pressure attained with the arc chamber operating at 2000 amperes was 1.70 psig. The surface temperature measured with total radiation pyrometer was 2360°F. The minimum model surface pressure was 0.30 psig with the surface temperature below 2000°F. Results show that the stagnation line pressure on the model surface closely approximates the arc chamber total pressure.

Data for the model surface pressures at the 2500 and 3000 amperes conditions were incomplete due to leaky pressure pickups. However, there were enough valid pressure recordings to establish a trend.

Prior to run No. 102 cold flow tests indicated leakages at three pressure pickups, P_8, P_9, and P_{11} (Figure 2-5). Data Data from these pickups are therefore, not valid. Post-run cold flow tests indicated a favorable correlation between model and shroud pressures.

2.8.2 Thermal Distribution Model

Photograph -- Figures 2-23 through 2-25.

Data Plots -- Figures 2-26 through Figure 2-33

Purpose

To obtain test facility calibration data for use in determining arc chamber conditions and proper shroud-to-model gap to provide the temperature and pressure distribution requested in the test requirements. Figure 2-16 shows the required test conditions to be achieved.

2.8.2.1 Results

The plots of the leading edge skin temperatures were separately plotted to show the temperature distribution with respect to the location of the thermocouple within the model. (Figures 2-27 through 2-30) Dimensional locations of the thermocouples are shown in Figure 2-7.

The average maximum stagnation temperature of 2715°F occurred shortly after six minutes of run time with the maximum recorded temperature of 2995°F on one of the thermocouples.

2.8.2.1 (Continued)

The distribution of skin temperatures at the centerline of the model at different intervals of time are shown in Figure 2-26.

Gap measurements between shroud and model are shown in Figure 2-31. The gap at 3.5 inches from the stagnation line at both the upper and lower surfaces was 0.22 inches. Significant variances in the gap occurred further away from the stagnation line on the lower surface.

The maximum recorded temperature (Figure 2-32) for the instrumented skin stiffener was 2850°F. The thermocouple was located near the stagnation line.

Two thermocouples recorded the temperatures on the beam assembly located behind the leading edge skin. The maximum temperature recorded, Figure 2-33, was 1610°F.

The temperature recording of the lower heat shield, Figure 2-33, was lost after 3 minutes of run time.

Overheating of the model resulting in an abort during the run precluded the full achievement of the planned evaluation of the thermal distribution.

2.8.3 Leakage Control Model

Photograph -- Figure 2-34

Data Plots -- Run No. 105 -- Figures 2-35 through 2-48

Run No. 107 -- Figures 2-49 through 2-60

Purpose

To obtain tare leakage rate profile at various test environments. Tare leakage for purposes of this program is defined as those leakages attributable to test set-up, i.e., leading edge skin and heat shield interface, around end blocks, etc.

2.8.3.1 Results

Two test runs were made on the leakage control model. The first, Run No. 105, was stopped due to arc chamber malfunction after 14-1/2 minutes of the planned 26 minutes run. The second, Run No. 107, was completed as planned.

Run No. 105

A total of six test conditions were achieved during this run. Maximum leakage of 0.497 ft^3 per minute occurred at the

2,8,3.1 (Continued)

start of test. The leakage rates are shown in Figure 2.35 along with the model stagnation pressures and temperatures. The required test environment, stagnation pressures and temperatures, is shown in Figure 2-36. The shroud pressure distribution at each of the six test conditions are shown in Figures 2-37 through 2-42. The stagnation line temperatures versus time are shown in Figures 2-43 and 2-44. The temperature data from thermocouple Number 3, Figure 2-43 was used to control the arc chamber conditions. The maximum stagnation temperature on the skin surface was 2850°F.

The skin temperatures versus time at one location above the stagnation line and one location below the stagnation line are shown in Figure 2-45.

Temperatures on the beam assembly simulating the front spar web were plotted on Figure 2-46. The maximum temperature, occurring behind the stagnation line was 1290°F.

Leakage gas temperatures on both sides of the beam assembly are shown in Figure 2-47. The gas temperature behind the beam assembly reached a maximum of 1210°F.

Shroud-to-model gap settings are shown in Figure 2-48 and show that a gap of 0.22 inch existed 3.5 inches above the stagnation line and 0.17 inch measured 3.5 inches below the stagnation line.

Run No. 107

Leakage air volumetric flow versus time is plotted on Figure 2-49. Plots of stagnation temperatures and stagnation pressures achieved during the test as well as the required test conditions are also included. A maximum leakage of 0.43 $ft^3/min.$ (at 70°F) occurred after 9.4 minutes of run time. A stagnation temperature of 2625°F and stagnation pressure of 0.53 psig was recorded at the same time.

The maximum stagnation temperature was 2805°F with an instantaneous peak of 2850°F. The maximum stagnation pressure of 0.60 psig was below the maximum of 0.80 desired.

The shroud pressure distributions are recorded on Figures 2-50 through 2-54. Each figure corresponds to the pressure step identified on Figure 2-49. The shroud-to-model gaps associated with the pressures are shown on Figure 2-55. A gap of approximately 0.30 occurred 3.5 inches from stagnation line.

2.8.3.1 (Continued)

Leakage air temperatures behind the web assembly in the back-up structure are shown in Figure 2-56. The thermocouple to measure temperatures in front of the web failed to give valid data. The maximum air temperature behind the web was 1130°F occurring approximately the same time as the peak stagnation temperature.

Temperatures in the area of the lower heat shield are also shown in Figure 2-56 with the maximum temperature recorded of 1965°F. Skin temperatures 15° below and 30° above the stagnation line are plotted on Figure 2-57 with maximums of 2800°F and 2595°F respectively.

The temperatures on the beam web of the leakage collector box are shown on Figures 2-58 and 2-59. Maximum temperatures of all the recorded thermocouples ranged from 1210°F to 1320°F.

The stagnation temperature recorded by the thermocouples were substantiated by a total radiation pyrometer. Plots of temperature versus time are shown on Figure 2-60.

2.8.4 Segmented Double Shell Model

Photograph -- Figure 2-61.

Data Plots -- Figures 2-62 through 2-67.

Purpose

To obtain leakage rate profile at various test environments attributable to the simulated flight hardware configuration and to determine the temperature effect of the leakage gases on the beam assembly behind the leading edge.

2.8.4.1 Results

Plots of stagnation conditions, temperatures and pressures, achieved during the test shown in Figure 2-62 indicated that the desired test conditions were achieved. Three significant data points showed the following:

2.8.4.1 (Continued)

Stagnation Pressure psig		Stagnation Temperature °F		Leakage Flow ft^3/min @ 70°F
Desired	Actual	Desired	Actual (Avg)	
0.275	0.290	2,750	2,750	0.075
0.363	0.375	2,690	2,700	0.23
0.775	0.770	2,640	2,670	0.36

The average pressure distribution along the shroud is shown in Figure 2-63. Shroud-to-model gaps, Figure 2-64 of 0.27 occurred 3.5 inches above and below the stagnation line.

Temperatures recorded on the beam assembly behind the leading edge is shown on Figures 2-65 and 2-66. The maximum temperature was 1750°F occurring at approximately the same time as the maximum leakage.

The stagnation temperature recorded by the total radiation pyrometer is shown in Figure 2-67. Good correlation existed between thermocouple and pyrometer temperature readouts.

No inner skin temperatures were obtained because of instrumentation problems encountered.

2.9 TEST OBSERVATION

2.9.1 Pressure Model

The first test run was aborted after 10 minutes because of sparks or glowing material appearing at the exit of the shroud-nozzle. Inspection of the model after the test, Figure 2-16, indicated that the "glasrock" end blocks reacted with the coated molybdenum-0.5 titanium straps. The sparks were most likely caused by the rapidly oxidizing and glowing pieces of the straps.

The second test run lasted approximately 17 minutes. A major portion of both molybdenum end straps were destroyed by oxidation apparently precipitated by a coating reaction with the "glasrock" end blocks (Alumina end blocks used on later tests did not cause strap failures).

The "water glass," used to seal the ceramic tubing to the stainless steel connection in the pressure pick-up system, frothed in the back of the model. A small amount also melted and spilled over onto the front section of the model possibly causing occlusion of some pressure ports.

2.9.1 (Continued)

No apparent damage to the siliconized graphite model was noted.

2.9.2 Thermal Distribution Model

A run duration of 875 seconds was originally planned, but a coating failure on a portion of the molybdenum straps and the resultant overheating caused premature shutdown. After 360 seconds, a fire was started in the thermocouple insulation sheaths which protruded from the back-up structure, Figure 2-25. The test was terminated after 408 seconds of run time.

During the test, the stagnation thermocouple being used to follow a preprogrammed trace on a strip chart failed due to instrumentation problems. Another stagnation thermocouple and the total radiation pyrometer were used to continue the test.

Post-test inspection revealed that both coated molybdenum end straps were severely damaged and partially destroyed by oxidation because of the coating reaction with the "glasrock" end blocks. Both edges of the model were also severely damaged because of this coating reaction followed by continuous exposure to the intense heat resulting from plasma penetration through the shell. This penetration through the shell resulted in melting and permanent warpage of the super alloy supporting structure, Figure 2-24.

2.9.3 Leakage Control Model

One of the main problems in the leakage rate study was the proper allowance for thermal expansion caused by large temperature differences between the shroud-nozzle and the model. This expansion could create undue thermal stresses in the shell of the one piece model or the back-up structure. Distortions caused by these thermal stresses could permit an undesirable amount of overheated air to leak inside the leading edge structure.

In Test No. 105, no leakage flow rate was registered on the rotameters after 5 minutes of testing. This was caused mainly by a lowering of the pressure in the leakage collector box. This decrease in pressure was attributed to thermal growth of the model. Since the model assembly was restrained at the back-up structure, the thermal growth would be forward resulting in a venturi effect at the leading edge skin and heat shield joint. The venturi effect would tend to cause air flow out of

2.9.3 (Continued)

the cavity behind the leading-edge skin into the stream flow of the working fluid. The longitudinal expansion of the model created a better lateral seal against the shroud side plates, thereby contributing to a more perfect seal for the tested configuration.

In the above test, a run duration of 26 minutes, 40 seconds was originally planned, but because of arc chamber malfunction, the test was stopped after approximately 14 minutes of run time. A post-test inspection of the model showed no visible damage.

Results of Run No. 107, Figure 2-35, showed that the leakage rate could be directly correlated with the model stagnation pressure for a constant model temperature. Test data also showed that the leakage rate was dependent upon changes in model temperature.

The model-to-shroud gap was increased prior to this run to allow greater pressures to act on leakage paths inherent in the test specimen. Leakage rates notably increased but because of the larger gap the test condition of 0.80 stagnation pressure could not be attained.

Inspection of the model after the test showed the heat shields oxidation damage at the edges, Figure 2-61. Contact points of the heat shields with the end straps were also damaged by oxidation. Figure 2-61 shows minor surface pitting in the stagnation region on both the leading edge shell and the end straps.

Comparison of stagnation thermocouple data with the total radiation pyrometer data indicated close correlation.

2.9.4 Segmented Double Shell Model

As in the leakage control model, the leakage flow rate could be correlated qualitatively with the model stagnation pressures. There was evidence of oxidation failures on the model skin and it is likely that a portion of the increase in leakage rate could be attributed to plasma penetration through the skin at these locations.

Four of the six leading edge skin surface temperatures being obtained from thermocouples were lost due to faulty oscillograph paper. Fortunately, two of four thermocouples located at the stagnation line were being recorded on separate recorders and appears as valid data in the results.

2.9.4 (Continued)

Post-test inspection of the model showed that small areas of pitting had pierced the outer shell of the model. This pitting was attributed to extensive coating breakdown caused by long surface exposure time to very high temperatures.

Approximately two-thirds of the leading edge surface area showed signs of molybdenum disilicide protective coating melting. In addition, small portions of the heat shield showed the same signs of the coating melting.

The coated molybdenum straps, Figure 2-61, showed incipient coating failures in the stagnation area with possible cracks in some areas.

Heat shields were buckled and cracked in two areas opposite to each other because of severe thermal gradients across the width of the shields.

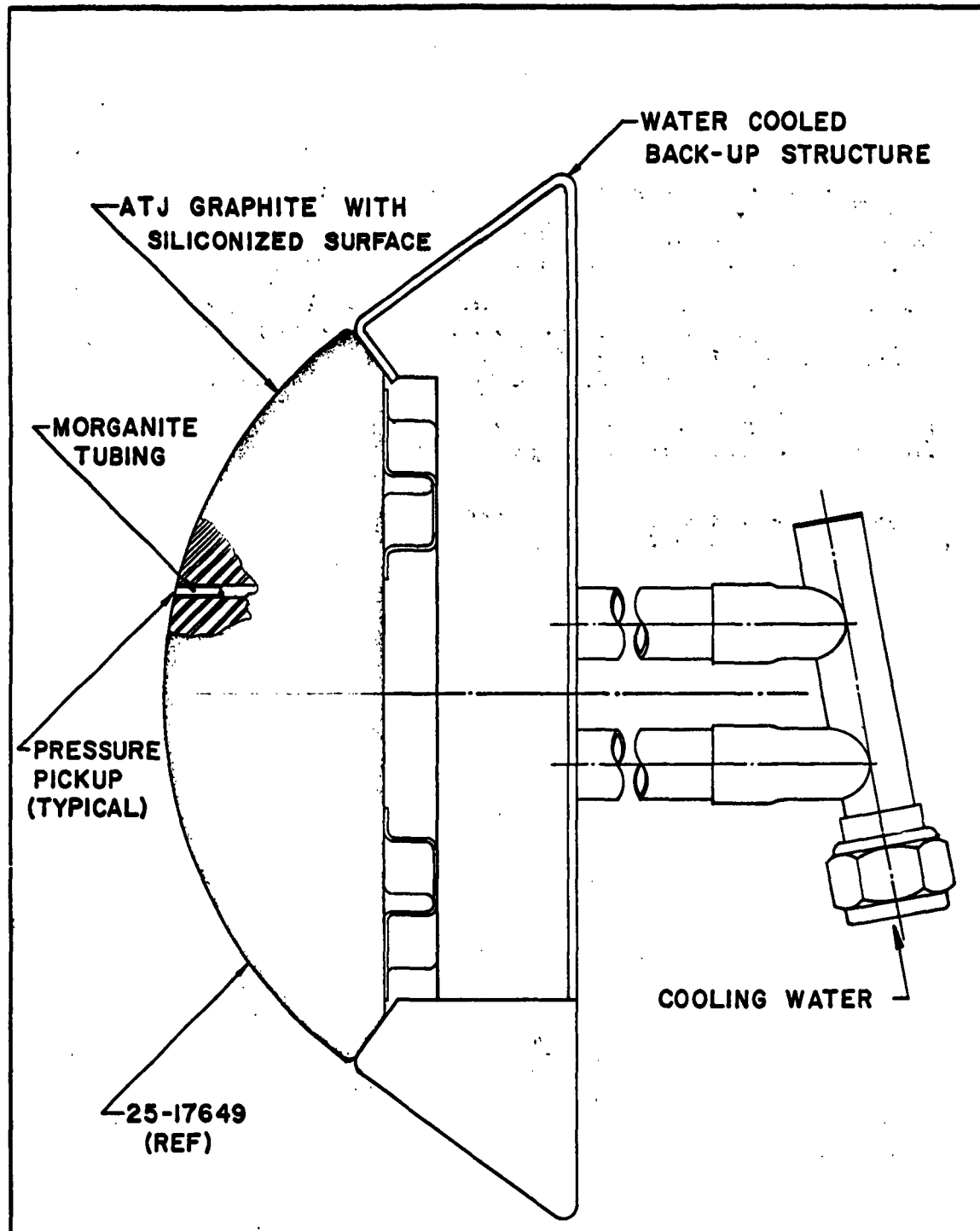

PRESSURE MODEL

FIGURE 2-1

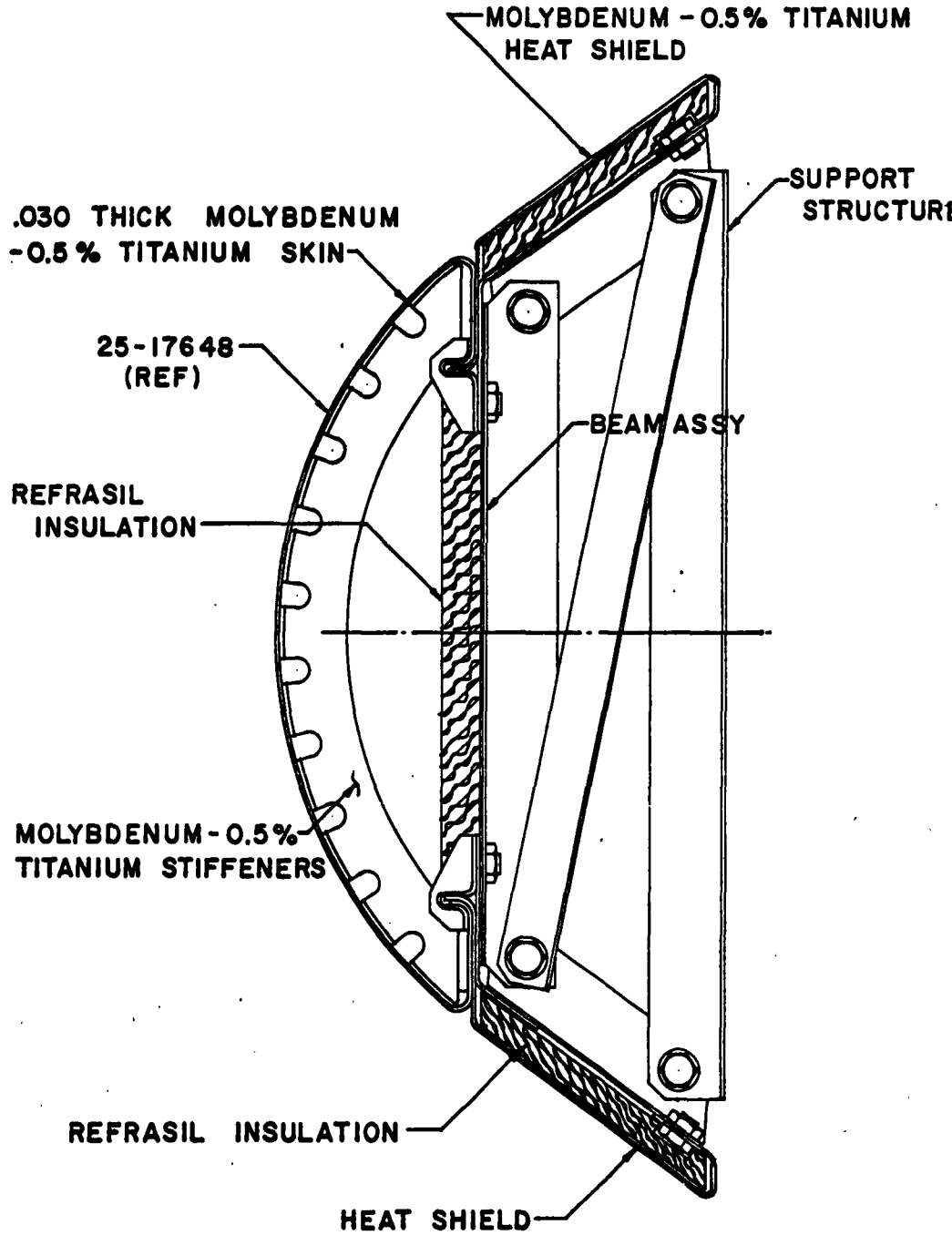

THERMAL DISTRIBUTION MODEL

FIGURE 2-2

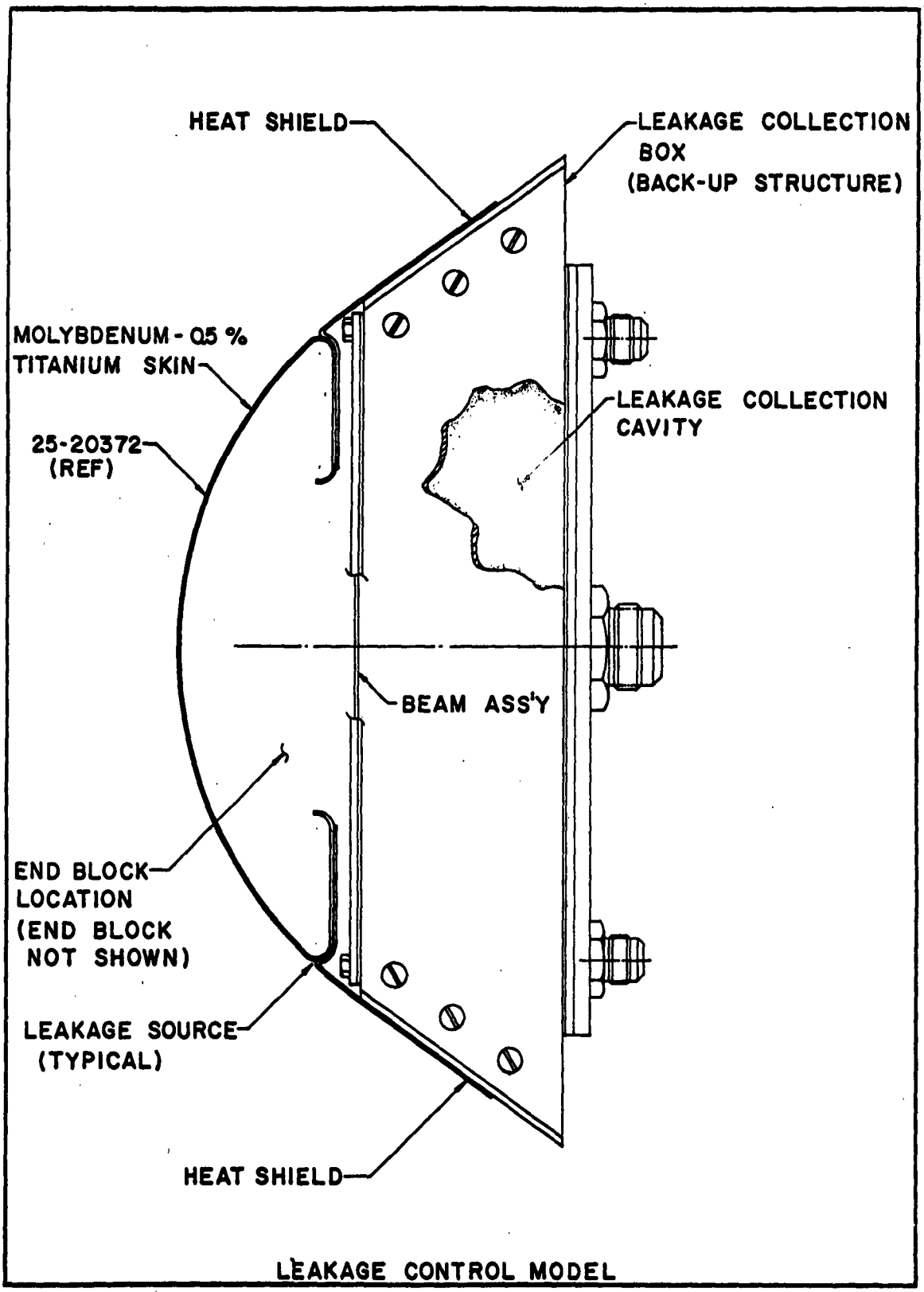

LEAKAGE CONTROL MODEL

FIGURE 2-3

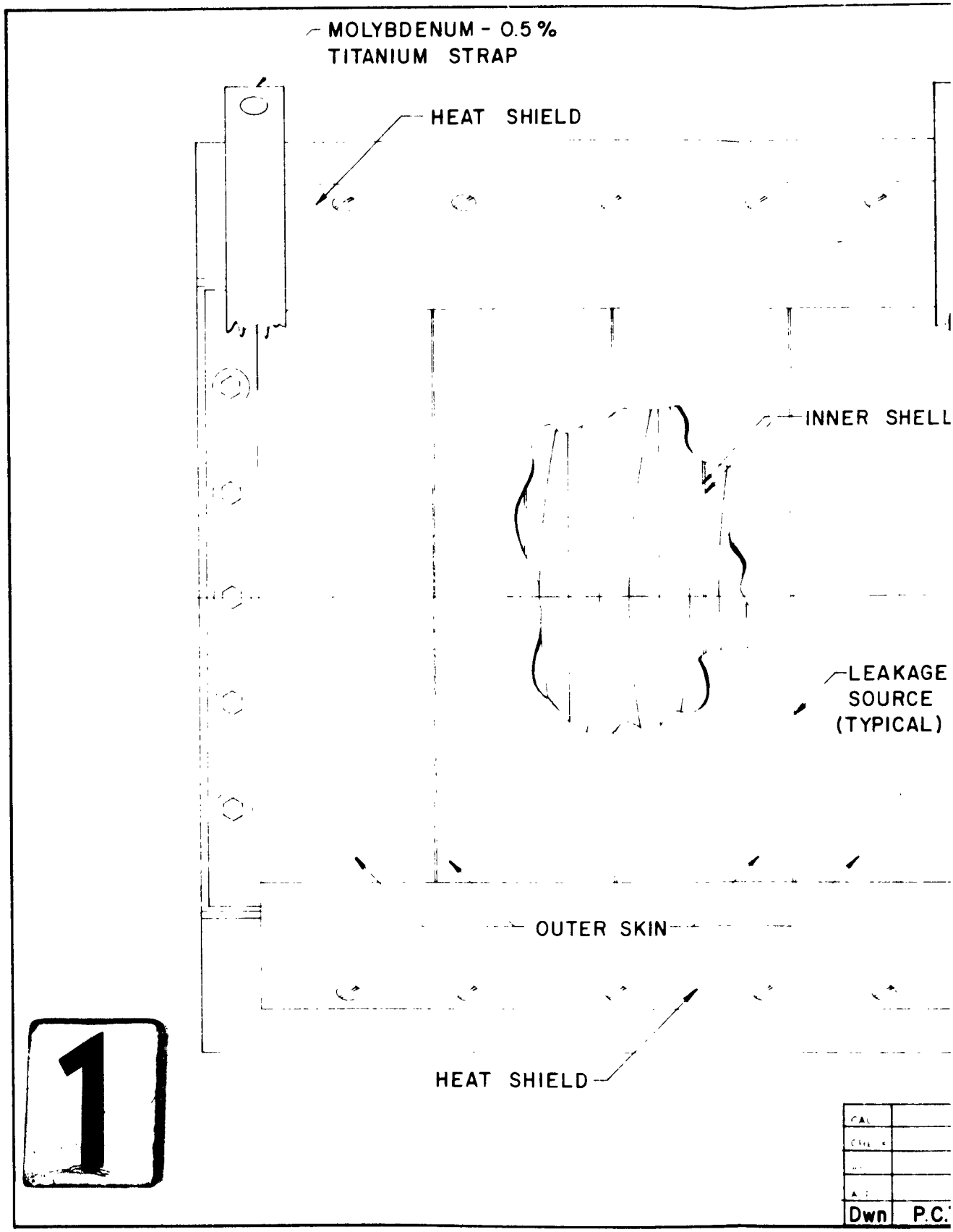

CAL	
CHK	
...	
APP	
Dwn	P.C.

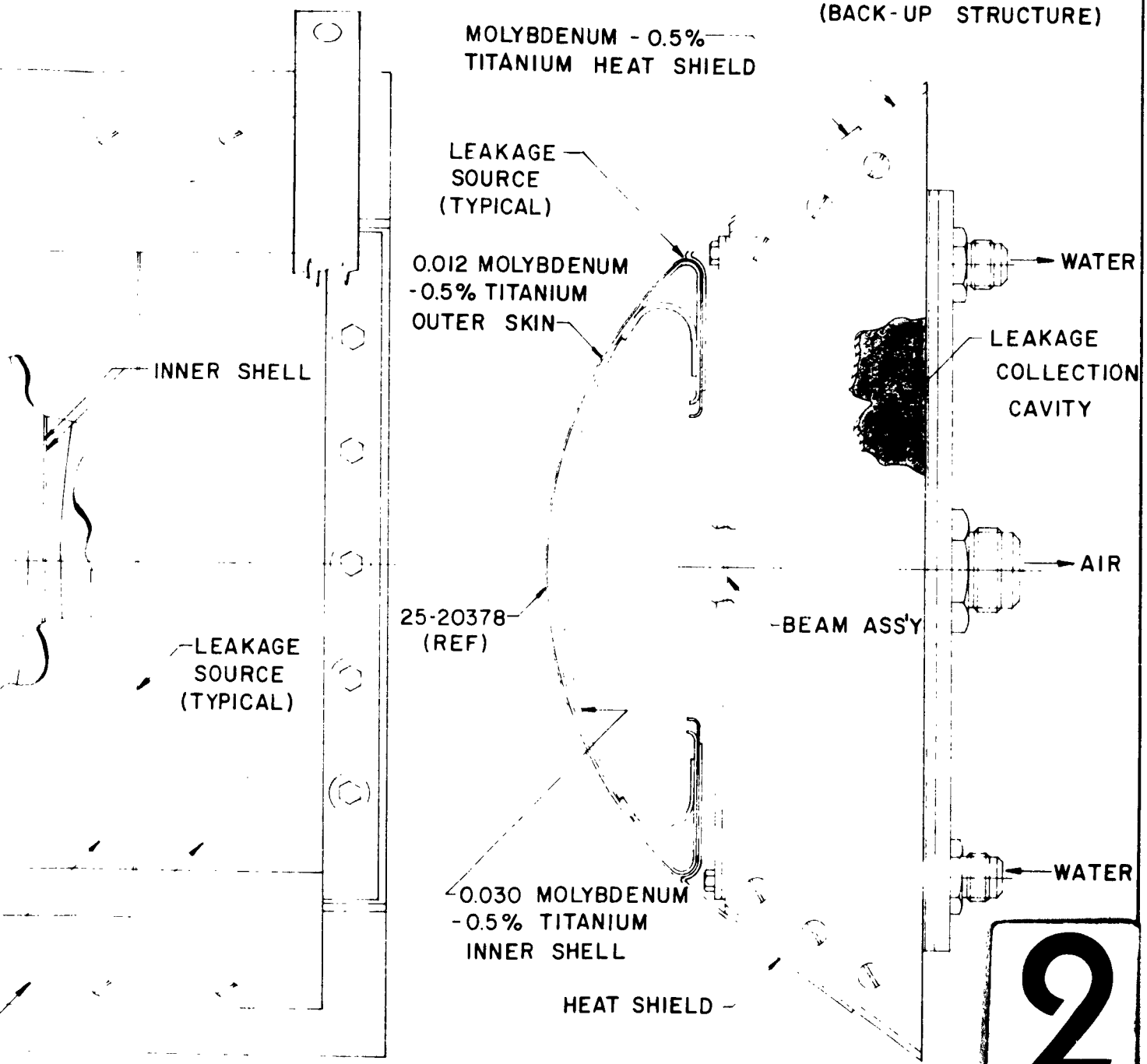

FIGURE 2-4

				DATE	SEGMENTED DOUBLE SHELL MODEL	D2-80085
					EWA 5-609 TEST 2224	
Dwn	P.C.T.	4-2-63			AIRPLANE COMPANY	PAGE 2-29

2

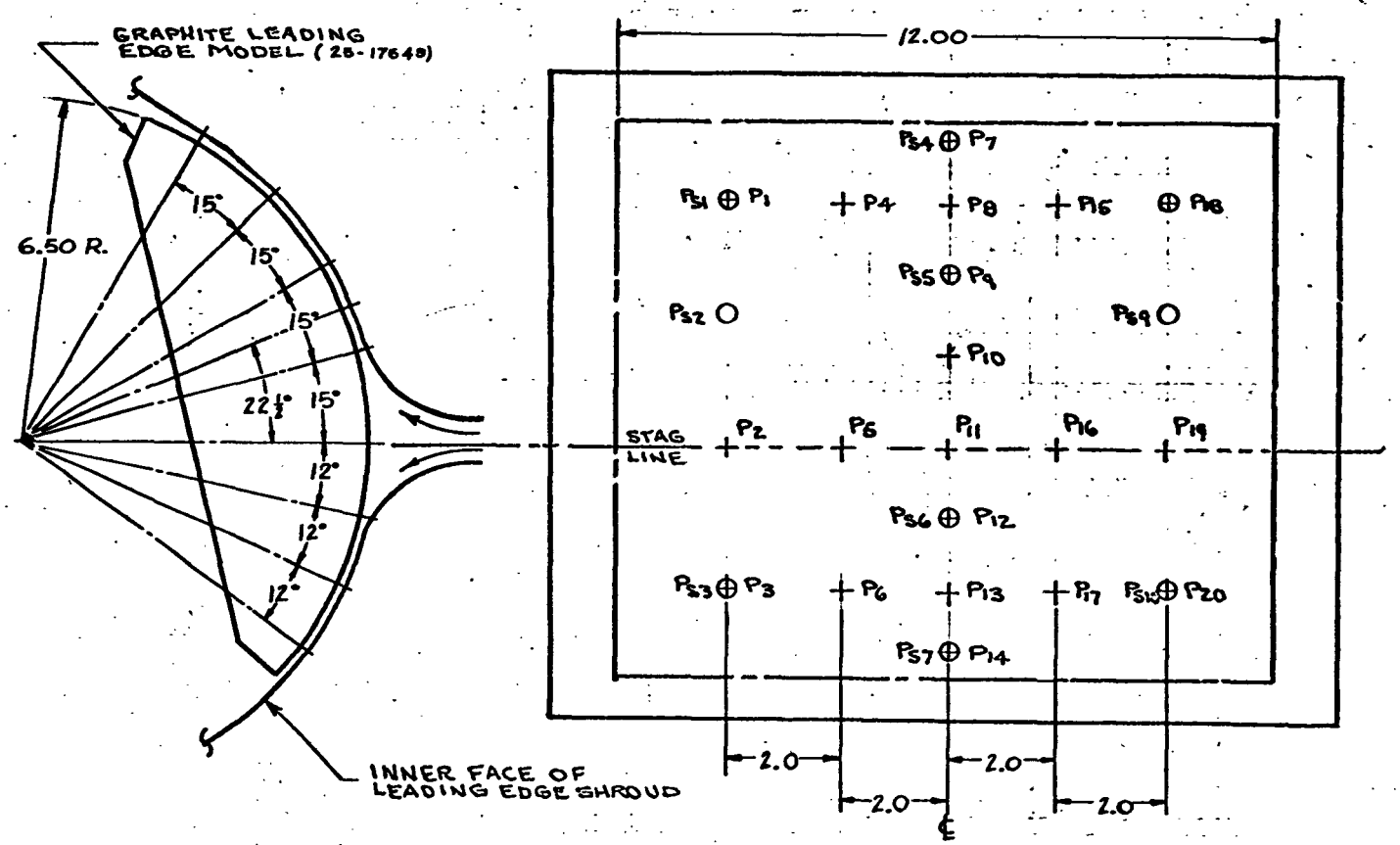

CALC	CHECK	APP	APP	APP
CAW	W.M.G.			
11/8/62	11/8/62			

REVISED	DATE

LEADING EDGE SHROUD AND MODEL PRESSURE PORT LOCATIONS

EWA #1409 TEST 2224

THE BOEING COMPANY

D2-80085

Figure 2-5

PAGE 50

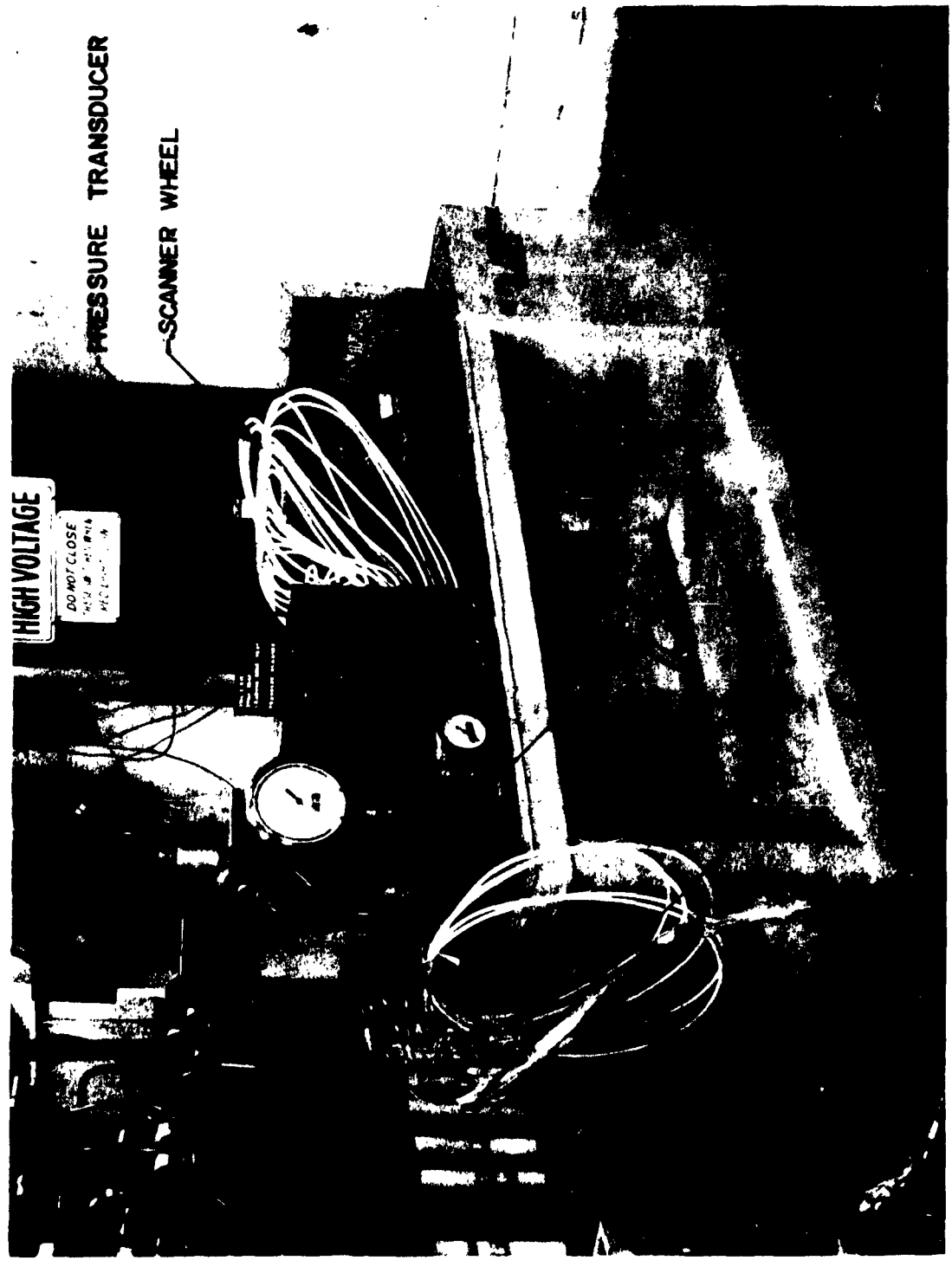

PRESSURE SCANNER

U3-4071-1000 (was BAC 1546-L-R3)

FIGURE 2-6

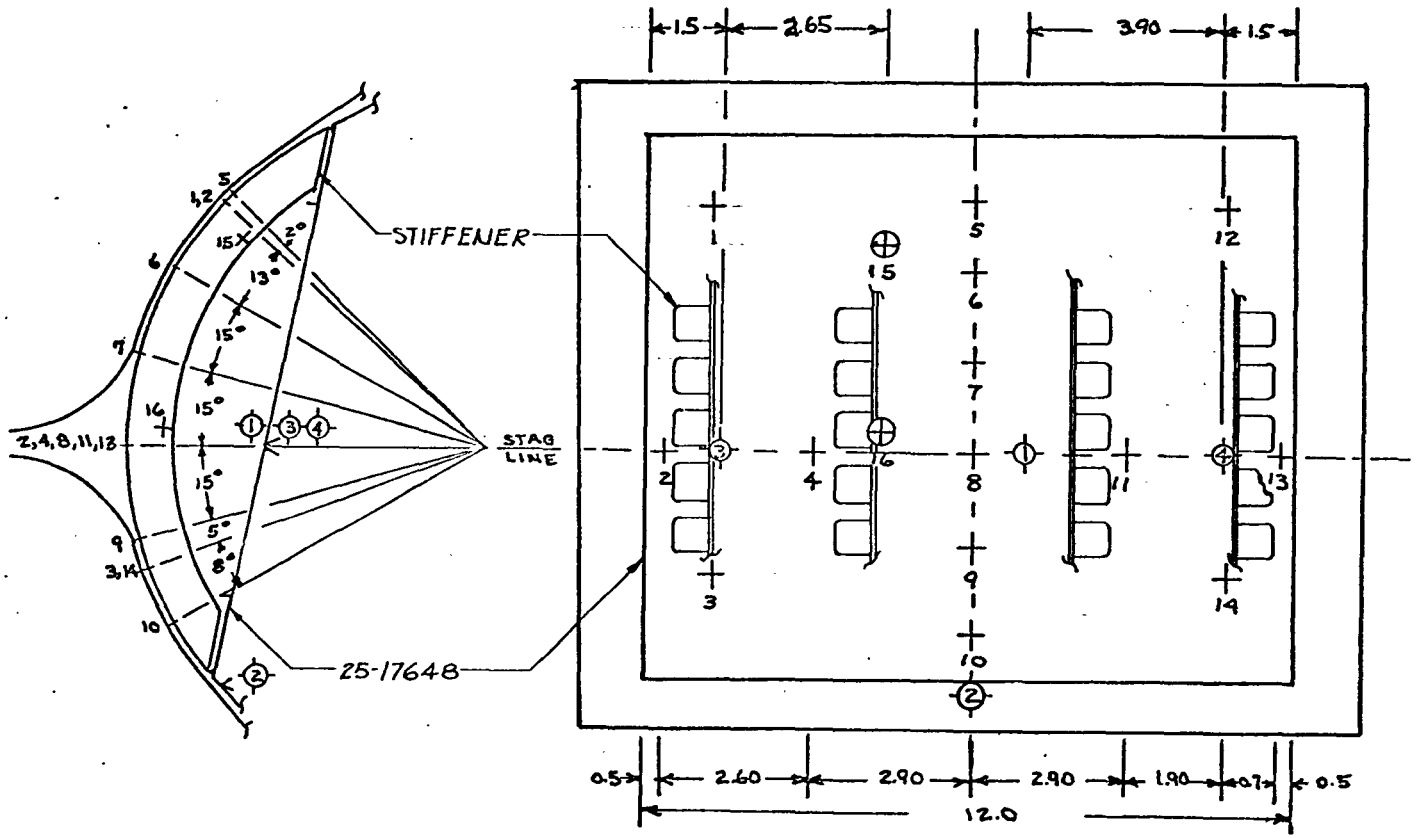

+ LOCATED ON INNER FACE OF LEADING EDGE PLT/PLT 13% RH T/C'S

⊕ LOCATED ON STIFFENER PLT/PLT 13% RH T/C'S

⊙ LOCATED ON BEAM ASS'Y. #2 LOCATED ON LOWER HEAT SHIELD T/C'S ARE ALL C/A'S EXCEPT #2 (PLT/PLT 10% RH T/C

CALC	pak	5/14/82			
CHECK	V.M.G.				
APR					
APR					

US 4038 8000

THERMAL DISTRIBUTION MODEL
T/C LOCATION
SWA 5-1998 TEST 2224
THE BOEING COMPANY

D2-20005
Figure 2-7
PAGE 2-32

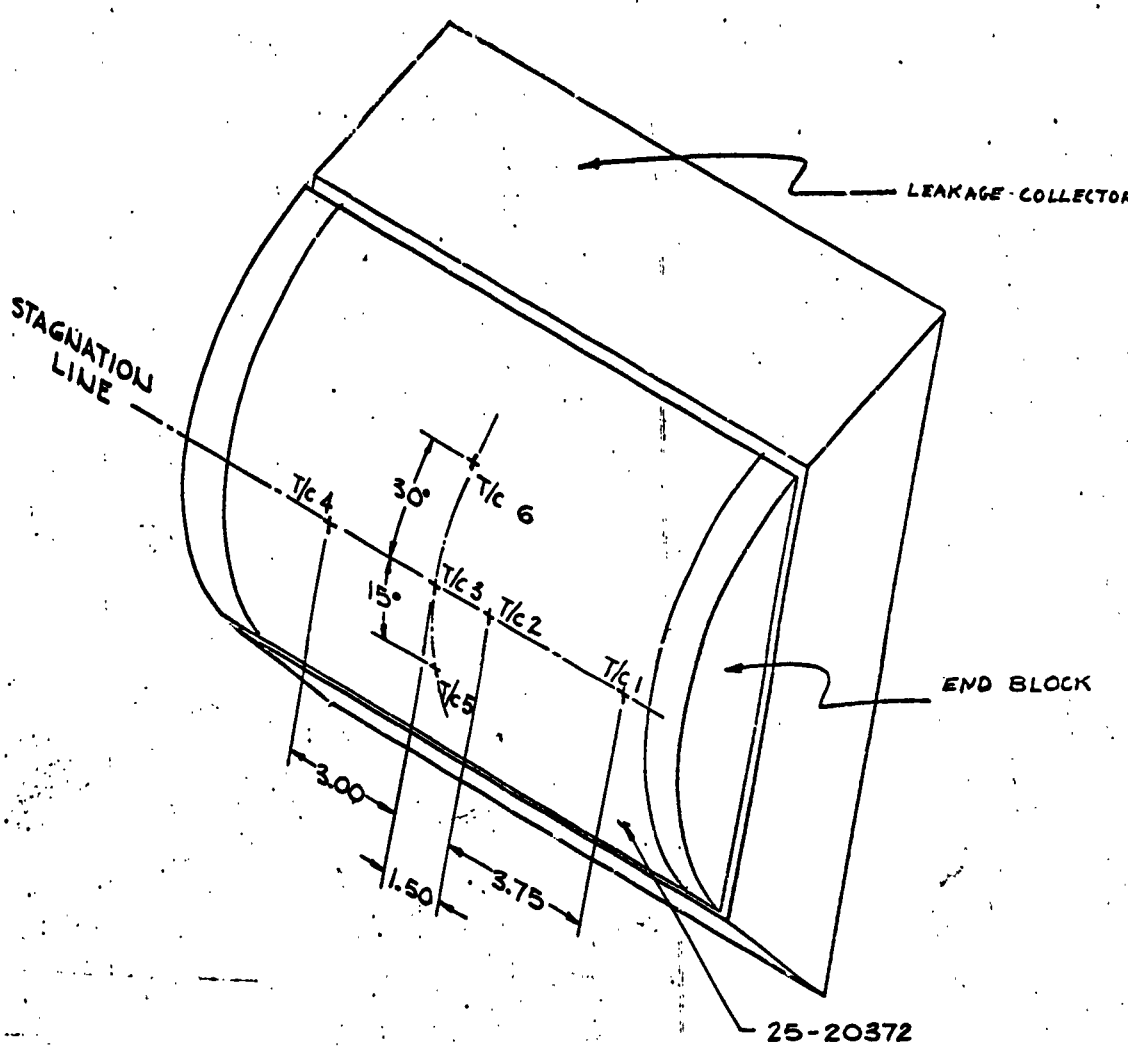

CALC	C.A.K.	5/15/62	REVISED	DATE	LEAKAGE CONTROL MODEL T/C LOCATIONS	D2-80085
CHECK	V.M.G.	5/16/62				
APPD					EWA 6-609 TEST 2224	Figure 2-8
APPD					BOEING AIRPLANE COMPANY	PAGE 33

US 4086 3000 (WAS BAC 9730-112) BSD 10000

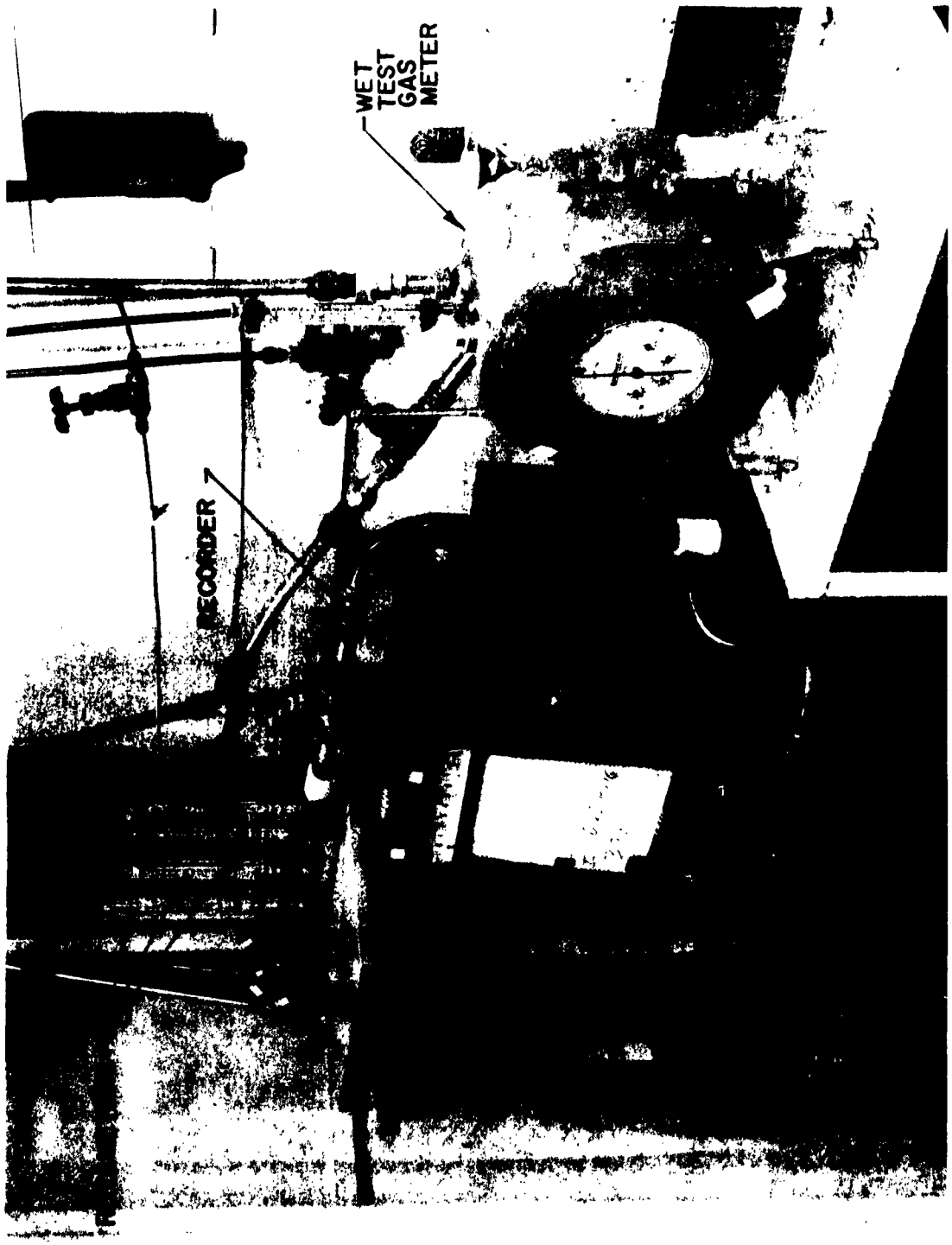

LEAKAGE RATE MEASURING INSTRUMENTS

U3-4071-1000 (was BAC 1546-L-R3)

FIGURE 2-9

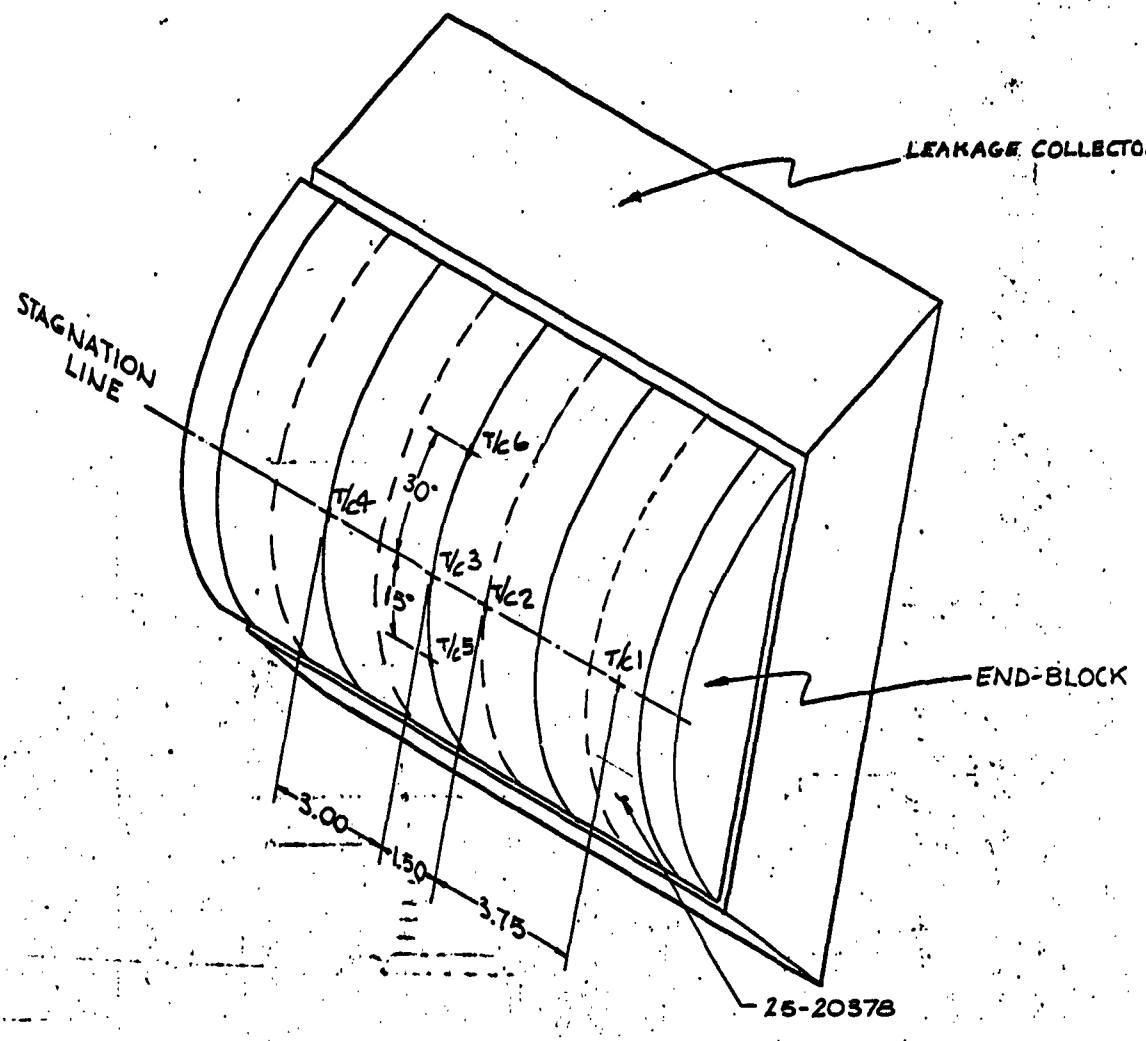

CALC	C.A.K	5/15/62	REVISED	DATE	SEGMENTED DOUBLE SHELL MODEL T/C LOCATION	D2-80085
CHECK	U.M.C.	5/15/62				Figure 2-11
APPD						
APPD					EWA 5-609 TEST 2224	
					BOEING AIRPLANE COMPANY	PAGE 2-35

US 4034 2000 (WAS BAC 9730-52) REQ 16088

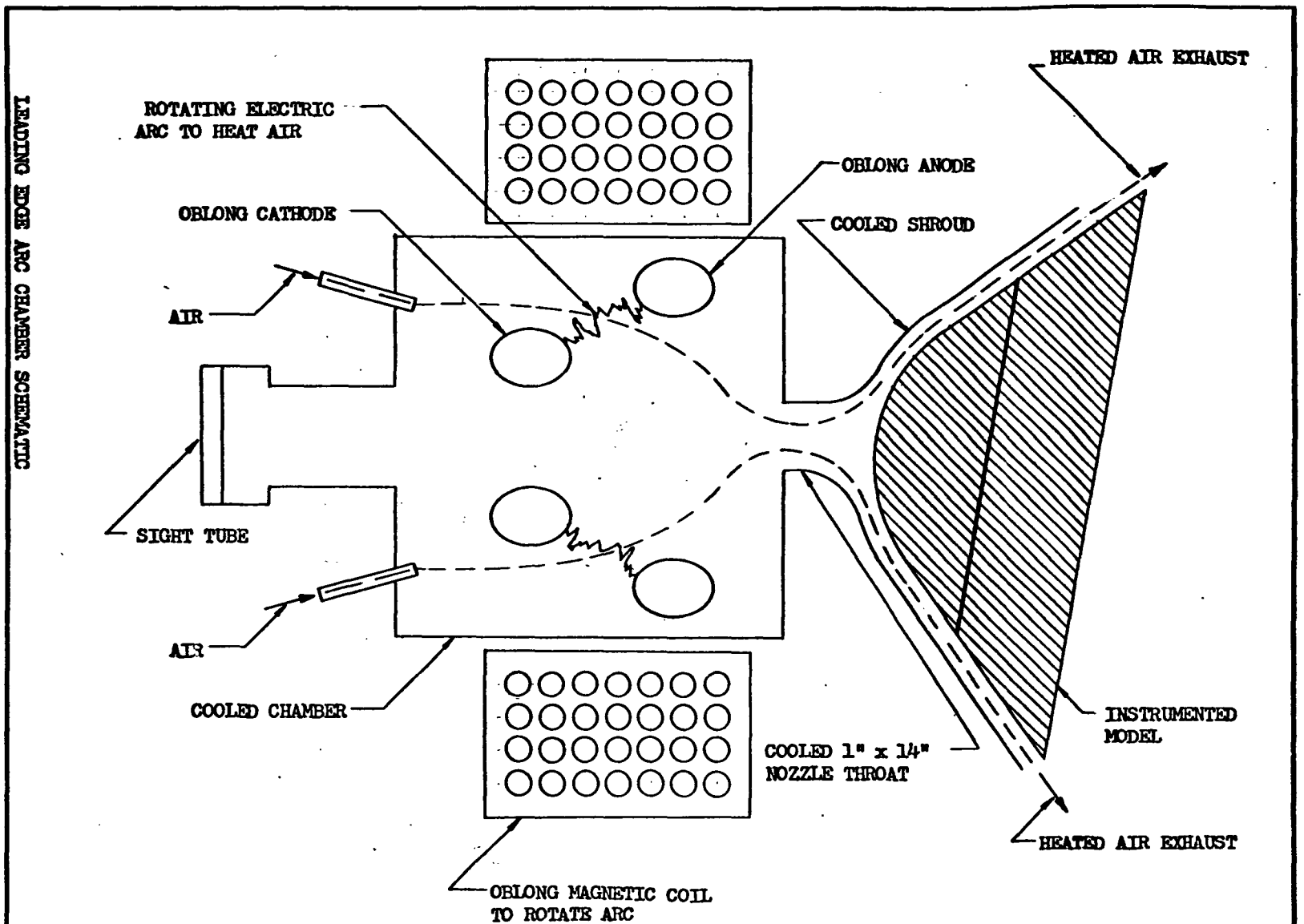

FIGURE 2-11 LEADING EDGE ARC CHAMBER SCHEMATIC

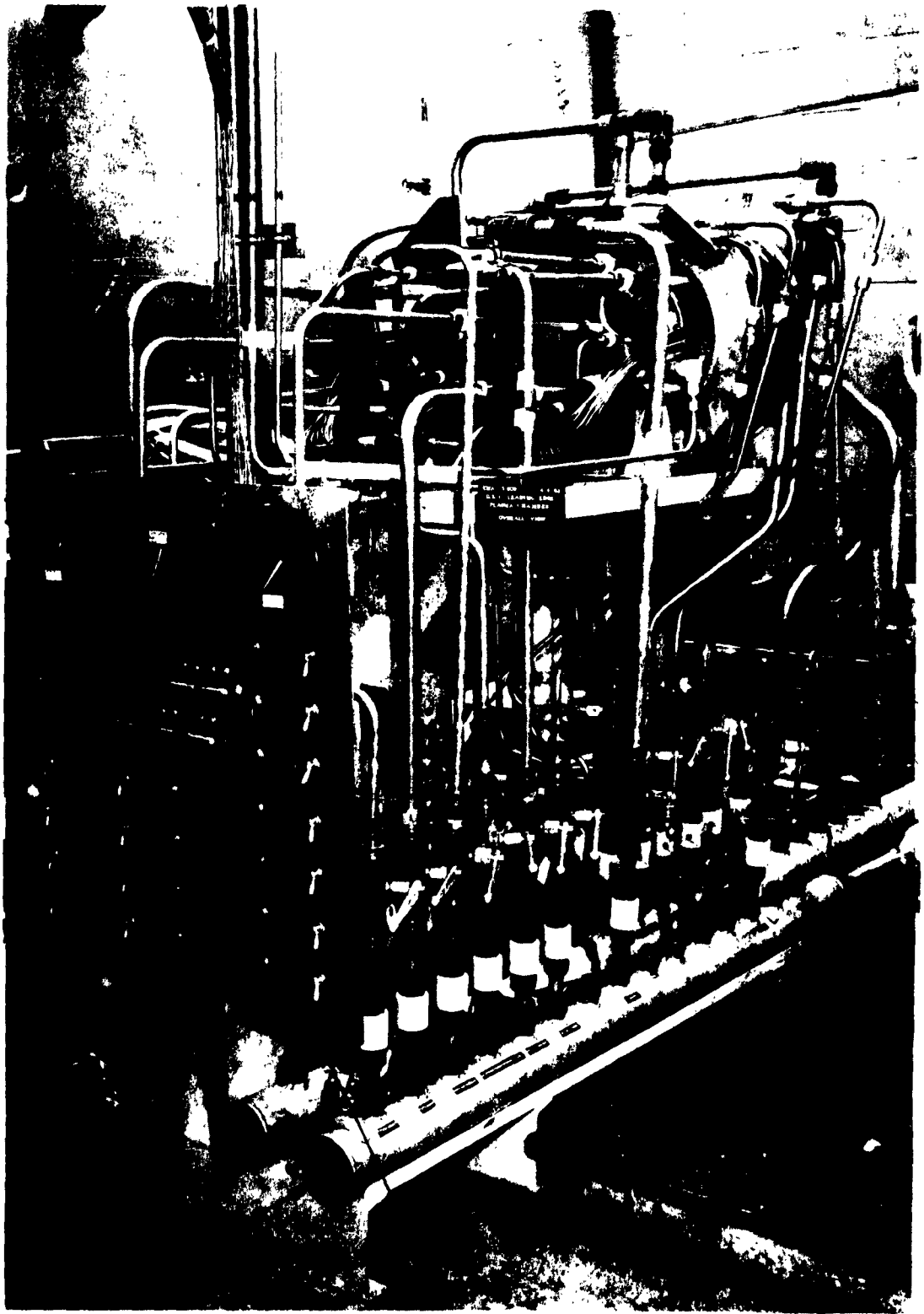

LEADING EDGE PLASMA JET FACILITY

U3-4071-1000 (was BAC 1546-L-R3)

FIGURE 2-12

BASIC ARC CHAMBER WITH ELECTRODES AND MODEL IN RELATIVE POSITIONS

U3-4071-1000 (was BAC 1546-L-R3)

FIGURE 2-13

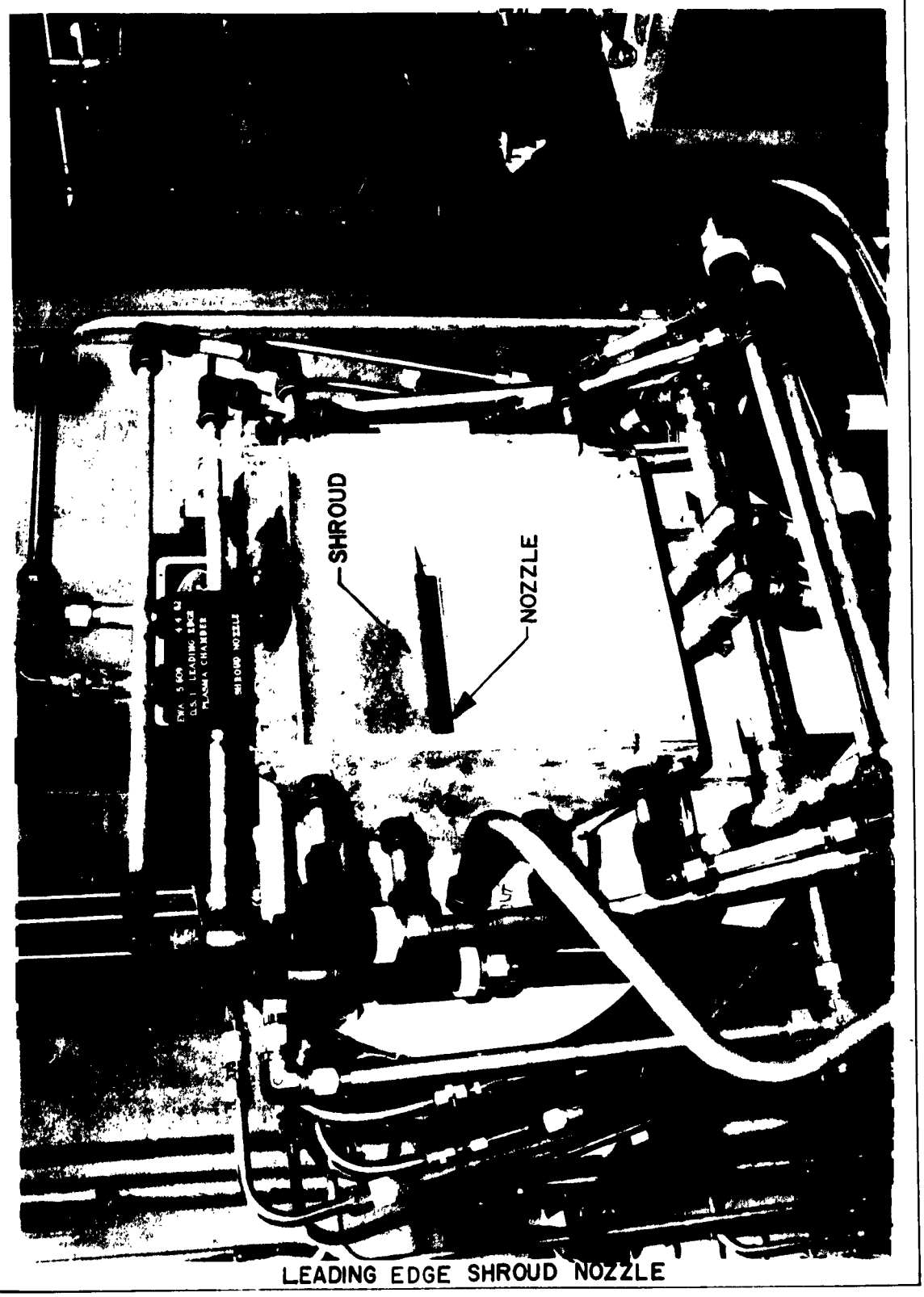

LEADING EDGE SHROUD NOZZLE

U3-4071-1000 (was BAC 1546-L-R3)

FIGURE 2-14

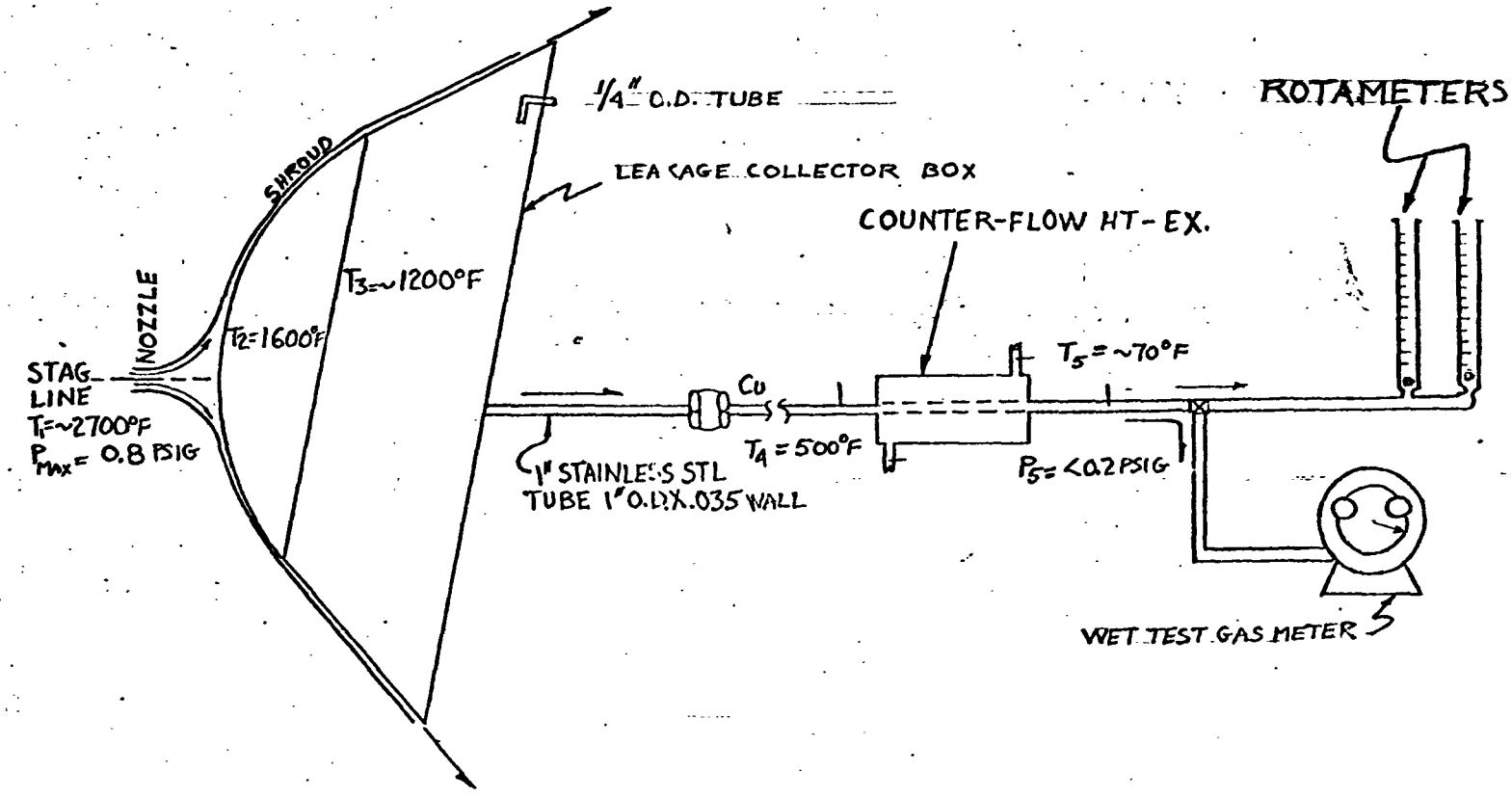

LEAKAGE AIR FLOW SYSTEM SCHEMATIC

Figure 2-15

CALC			REVISED	DATE
CHECK	V. M. Glanton	4/8/62	<	
APR				
APR				

REQUIRED PLASMA JET TEST ENVIRONMENT FOR PRESSURE AND THERMAL DISTRIBUTION TEST RUNS

EWA 5-609 TEST 2224

THE BOEING COMPANY

D2-80085

Figure 2-16

PAGE 2-41

US 4018 8000

K+E ALBANENE 1000 68587

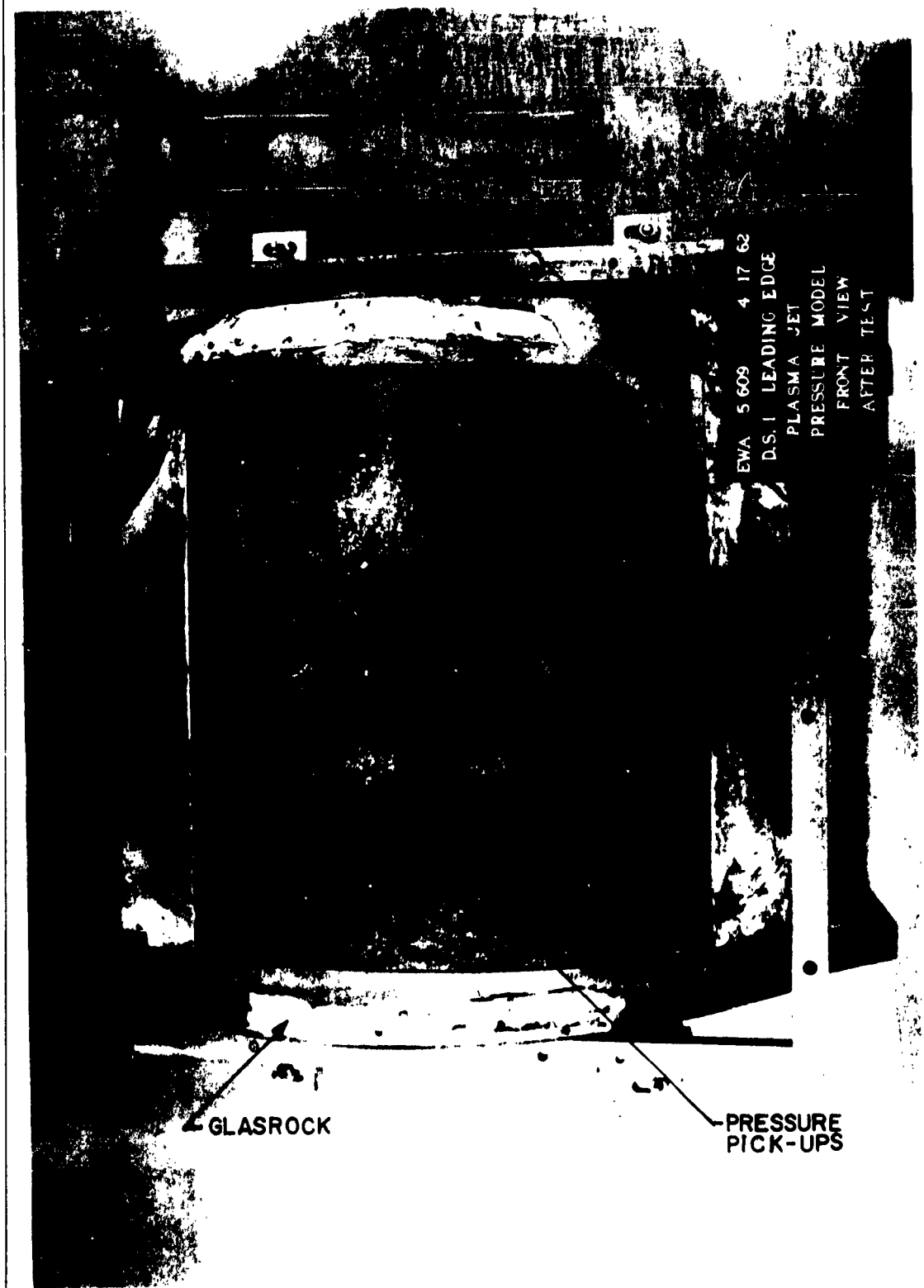

SILICONIZED GRAPHITE PRESSURE MODEL

U3-4071-1000 (was BAC 1546-L-R3)

FIGURE 2-17

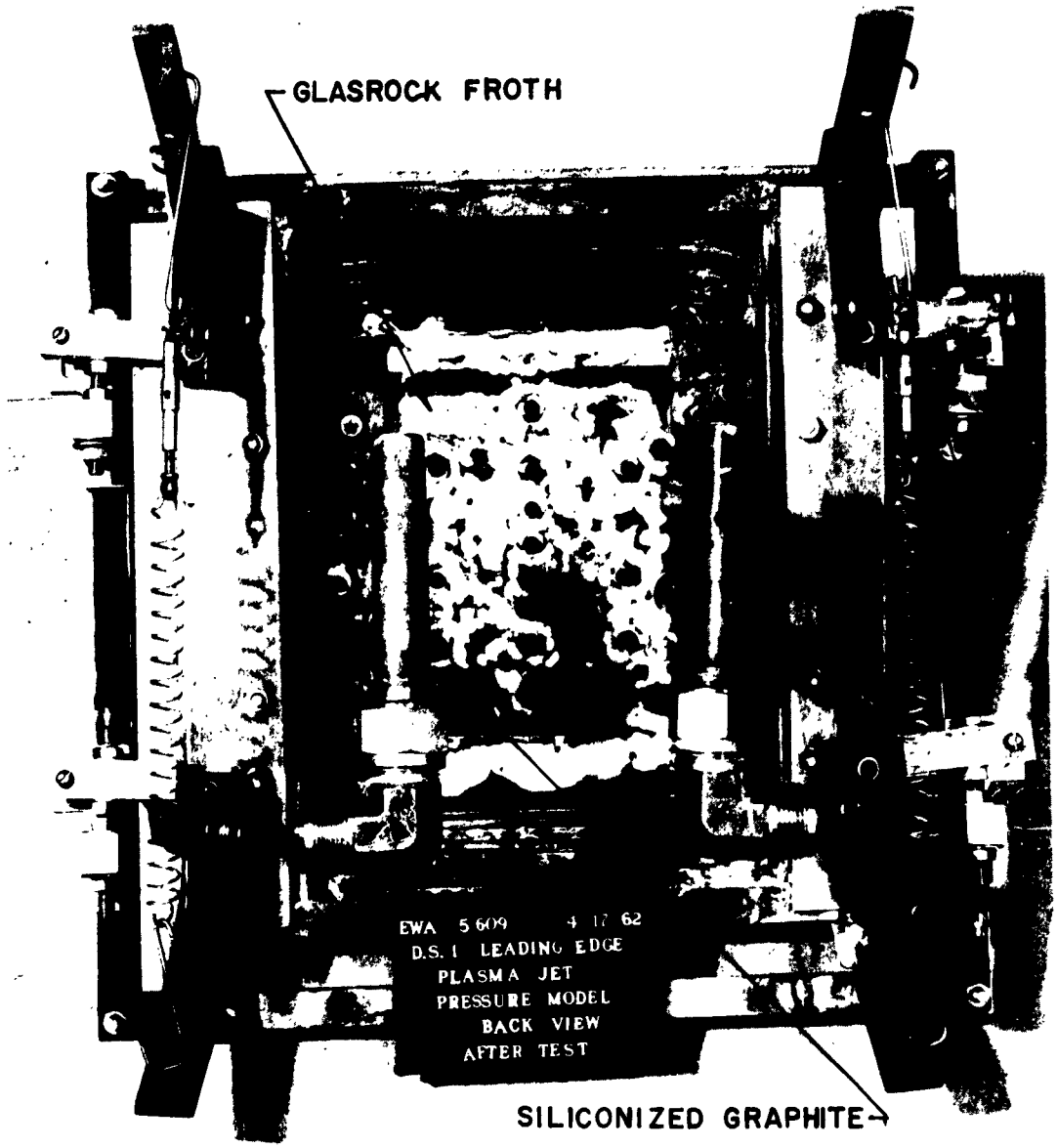

PRESSURE MODEL - BACK VIEW

U3-4071-1000 (was BAC 1546-L-R3)

FIGURE 2-18

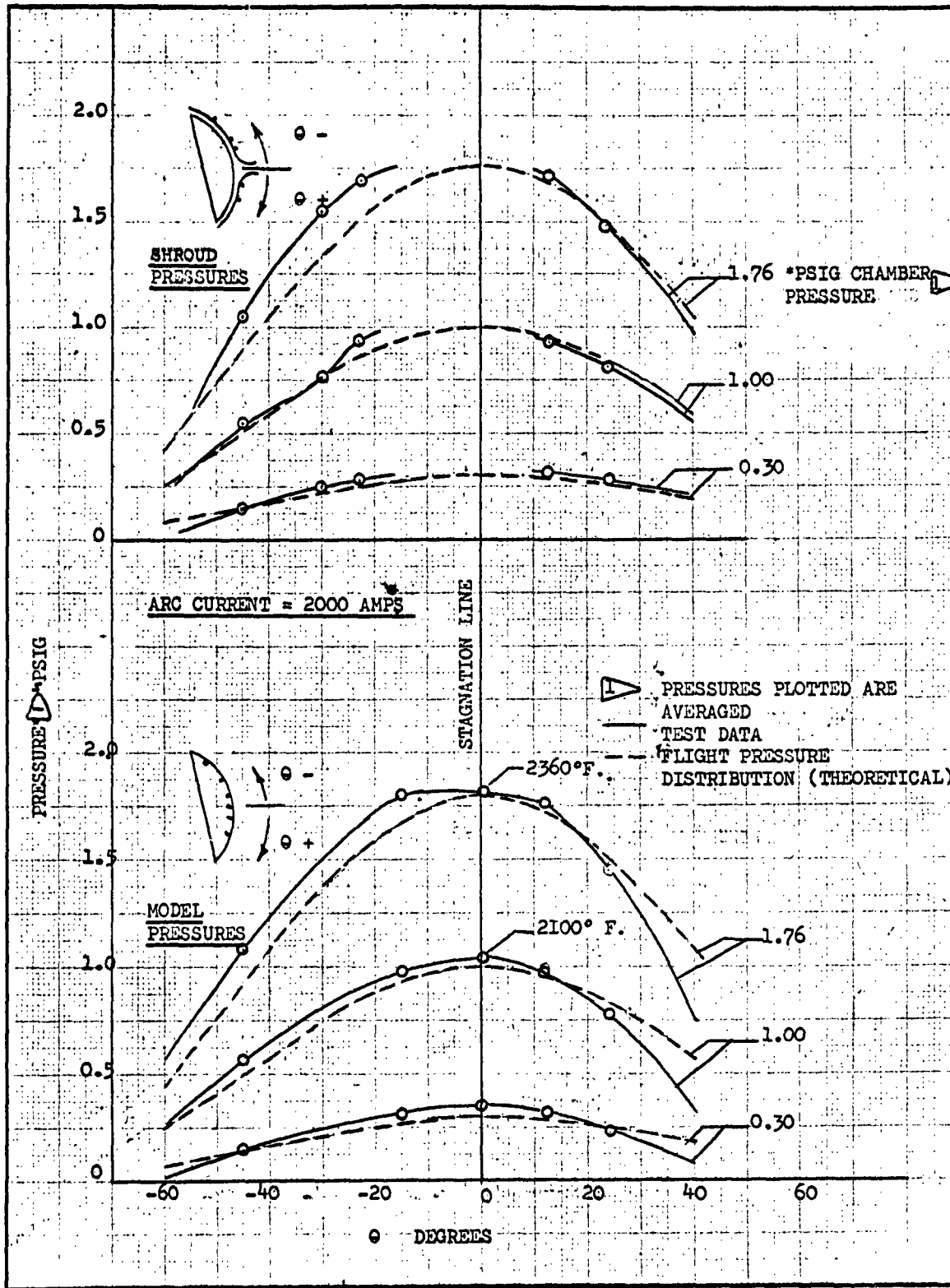

CALC			REVISED	DATE	LEADING EDGE PRESSURE MODEL, P_{static} PLASMA JET TEST EWA 5-609 TEST 2224	D2-80085
CHECK						Fig. 2-19
APR						
APR					THE BOEING COMPANY	PAGE 2-44
Plot	P.C.T.	4-12-3				

US 4018 8000

K•E ALBANENE 70737

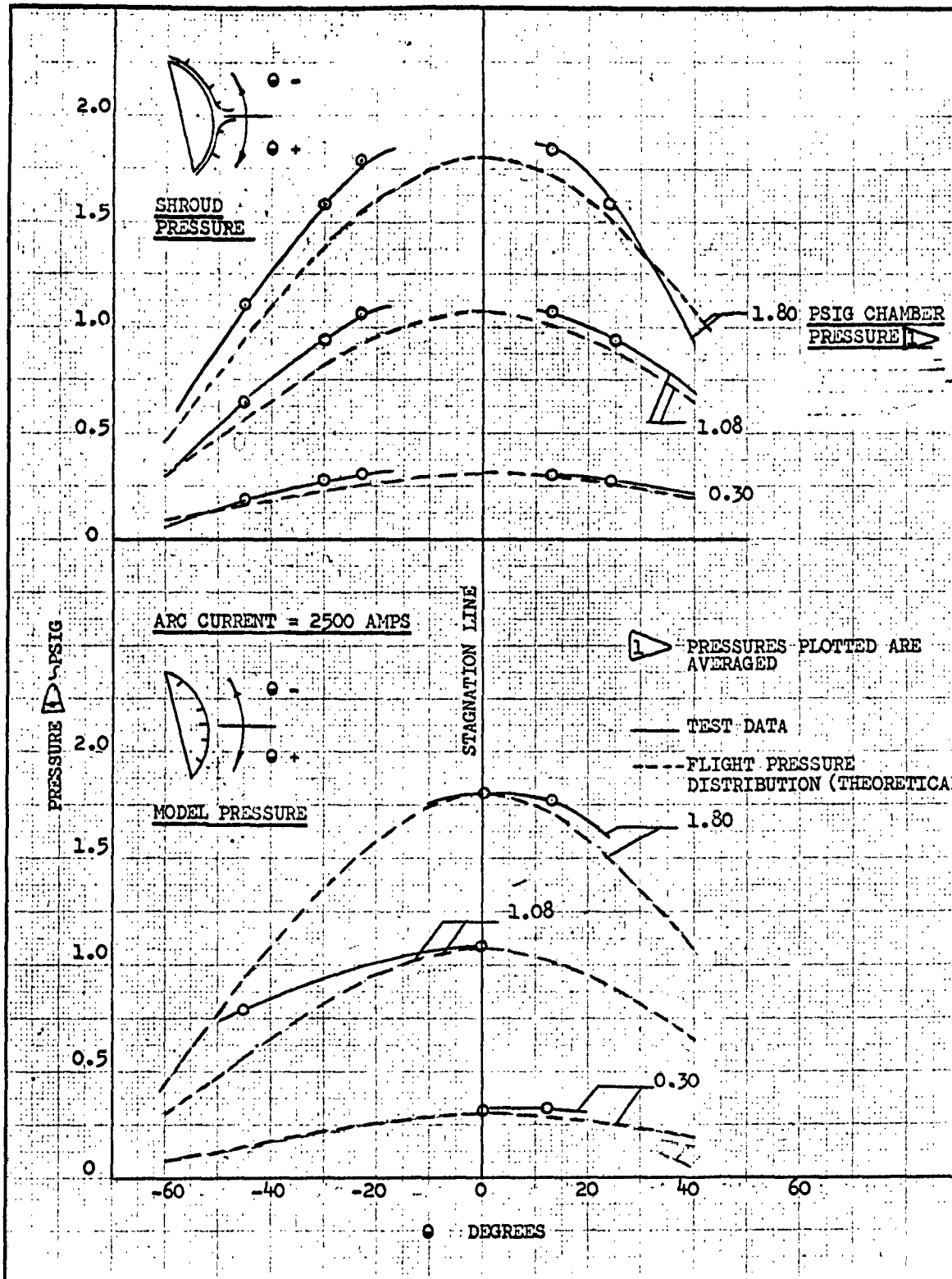

CALC			REVISED	DATE	LEADING EDGE PRESSURE MODEL, P_{static} PLASMA JET TEST EWA 5-609 TEST 2224	D2-80085
CHECK						Fig. 2-20
APR						
APR					THE BOEING COMPANY	PAGE 2-45
Plot	P.C.T.	4-12-3				

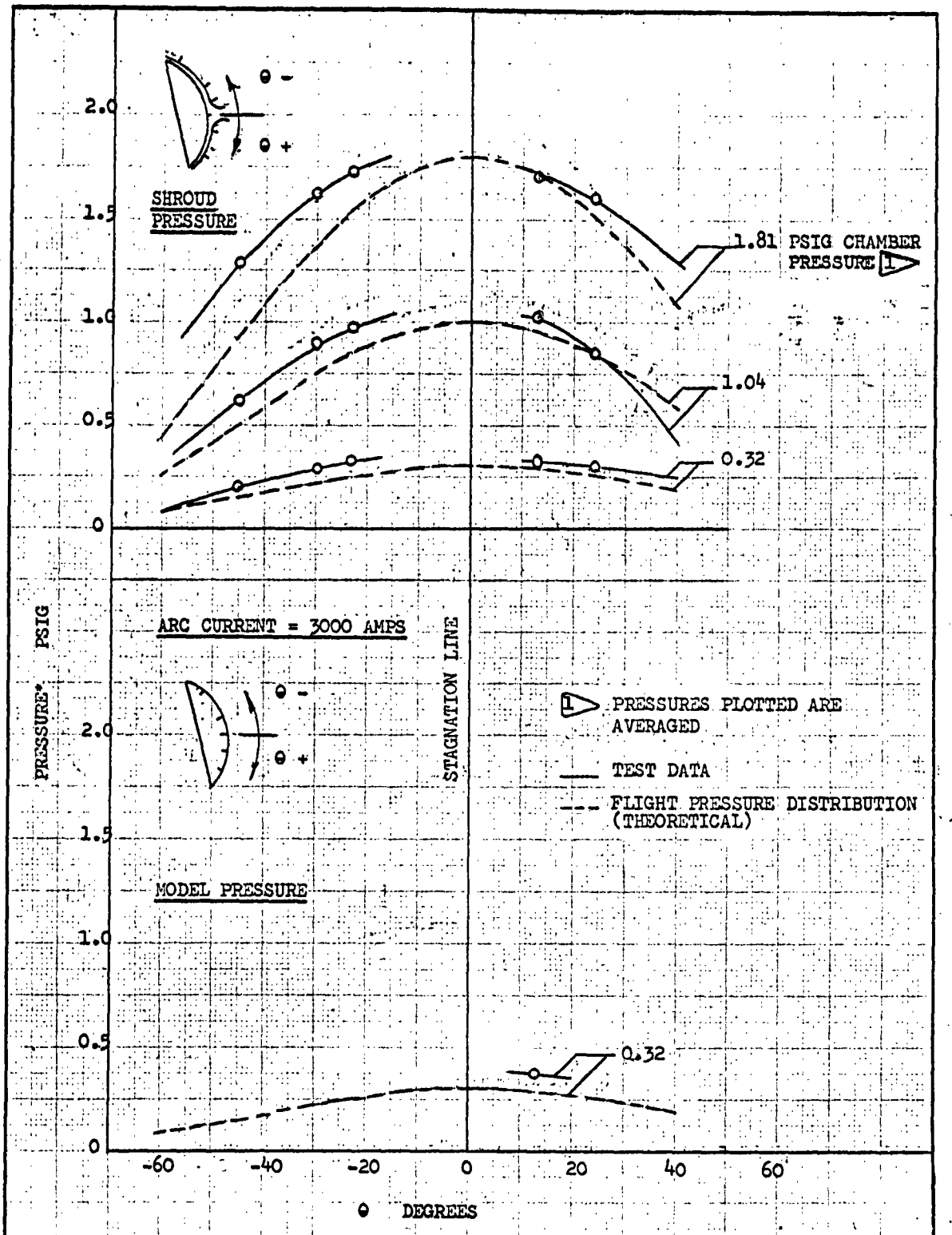

CALC			REVISED	DATE	LEADING EDGE PRESSURE MODEL, P_{static}	D2-80085
CHECK					PLASMA JET TEST	
APR					EWA 5-609 TEST 2224	Fig. 2-21
APR						
Plot	P.C.T.	4-12-			THE BOEING COMPANY	PAGE 2-46

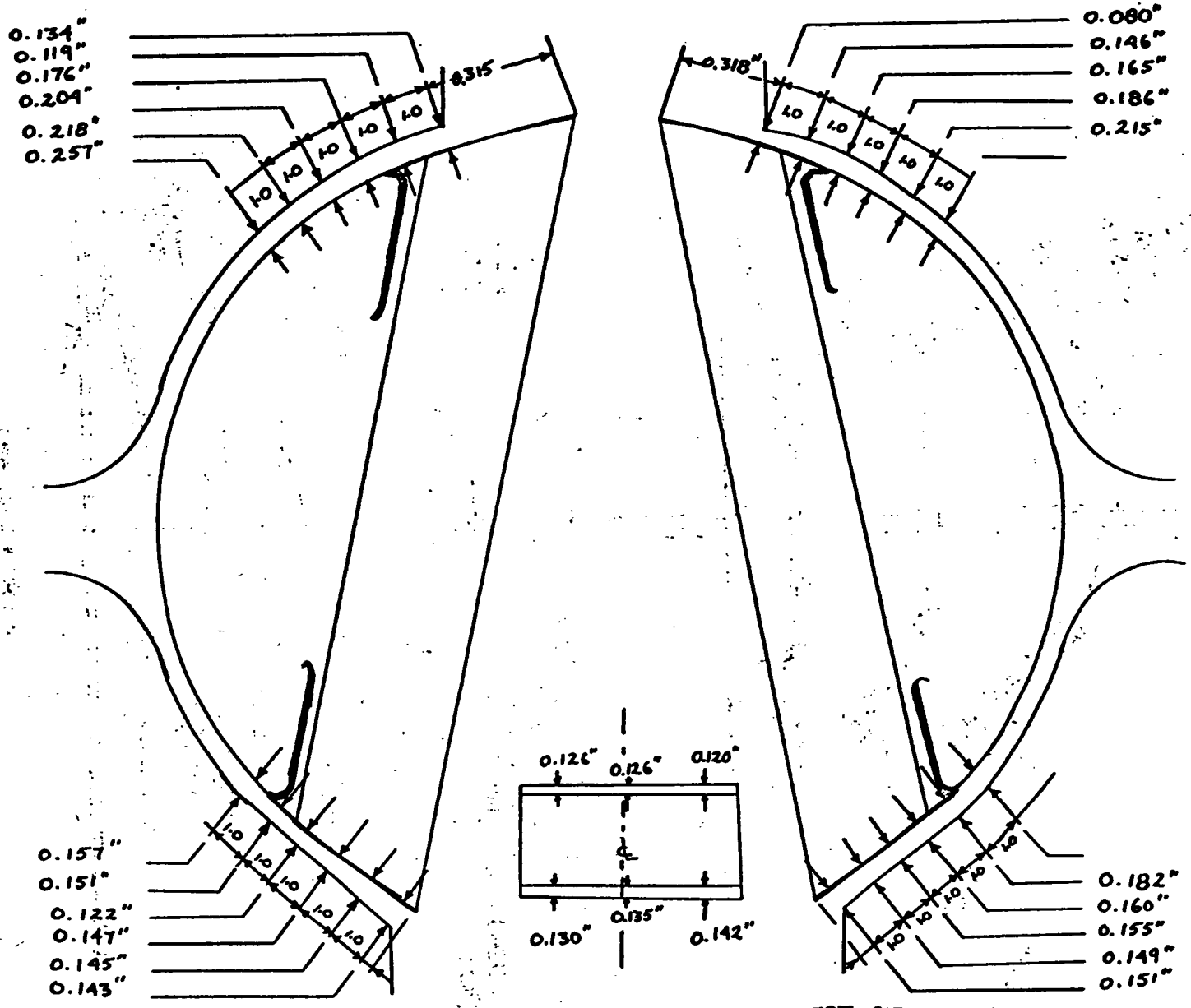

CALC	V.M.G. 4/15/62	REVISED	DATE
CHECK			
APPR			
APPR			

THE BOEING COMPANY
SEATTLE 24, WASHINGTON

PRESSURE MODEL
GAP MEASUREMENTS
TEST 2224 RUN No. 102 & 103 EWA 5-609

D2-80085
FIG. 2-22
2-47

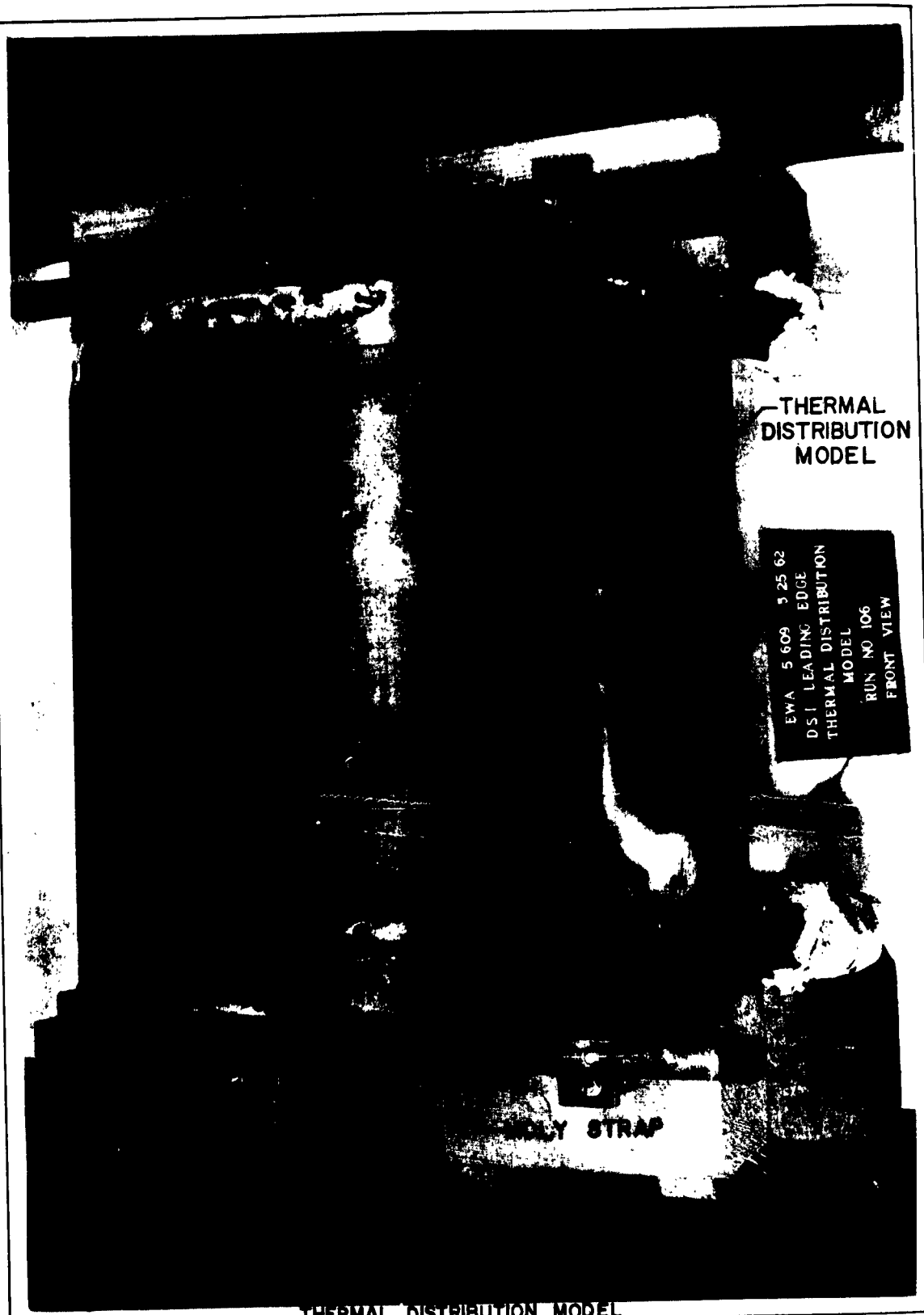

THERMAL DISTRIBUTION MODEL

FIGURE 2-23

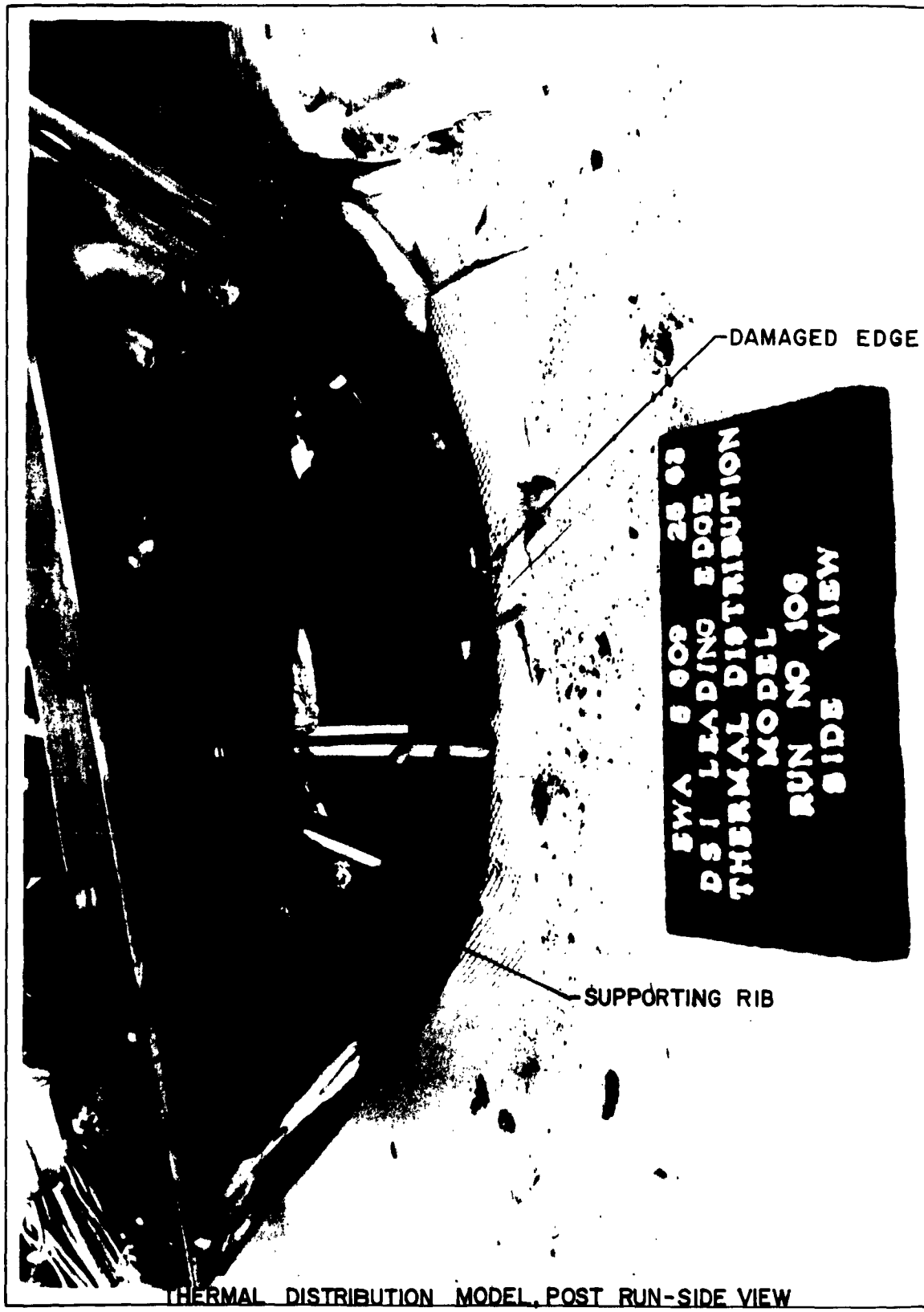

THERMAL DISTRIBUTION MODEL, POST RUN-SIDE VIEW

U3-4871-1000 (was BAC 1546-L-R3)

FIGURE 2-24

THERMAL DISTRIBUTION MODEL - REAR VIEW

U3-4071-1000 (was BAC 1546-L-R3)

FIGURE 2-25

			REVISED	DATE	THERMAL DISTRIBUTION MODEL CENTERLINE TEMPERATURE DISTRIBUTION	D2-80085
CALC						
CHECK					TEST 2224 RUN 106 EWA 5-609	FIGURE 2-
APR						
APR					THE BOEING COMPANY	PAGE 2-51
Plot	P.C.T.	4/19/63				

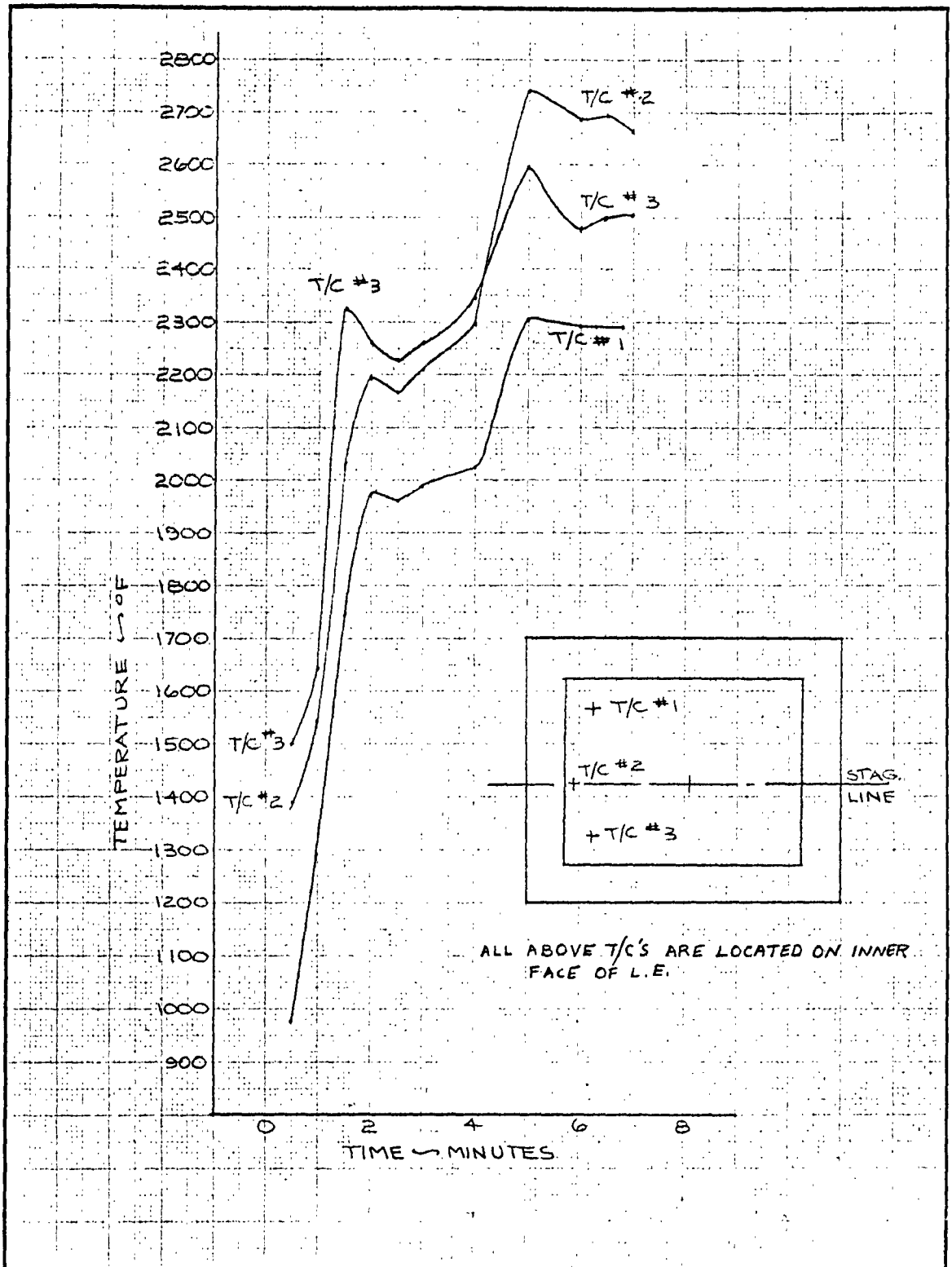

CALC	NP	6/20/62	REVISED	DATE	THERMAL DISTRIBUTION MODEL T/C's 1, 2, & 3	D2-80085
CHECK	V.M.G.	6/20/62				
APR					TEST 2224 RUN 106 5-25-62	Figure 2-27
APR					THE BOEING COMPANY	PAGE 52

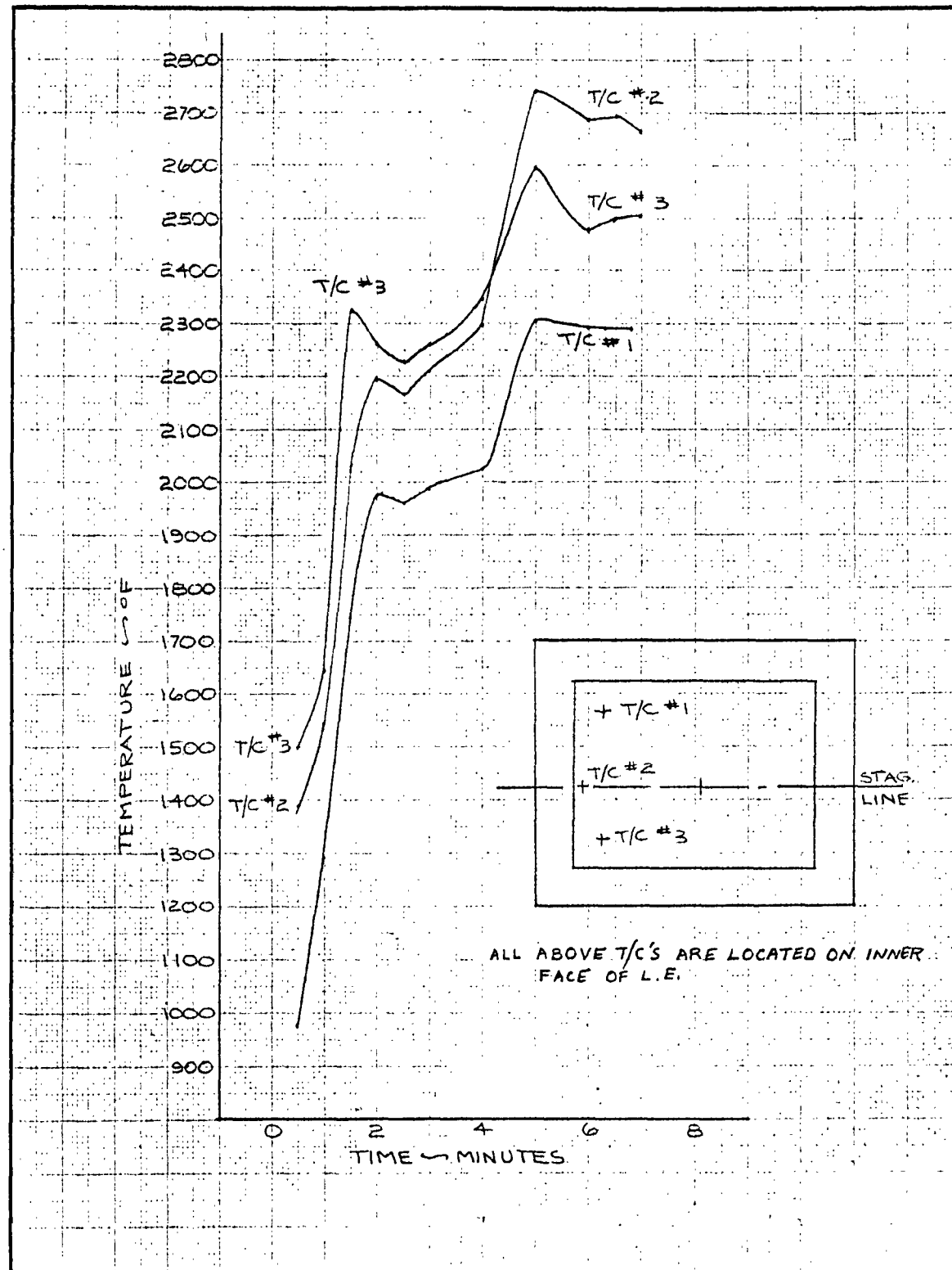

CALC	NP	6/20/62	REVISED	DATE	THERMAL DISTRIBUTION MODEL T/C's 1, 2, & 3	D2-80085
CHECK	V.M.G.	6/20/62				
APR					TEST 2224 RUN 106 5-25-62	Figure 2-27
APR					THE BOEING COMPANY	PAGE 52

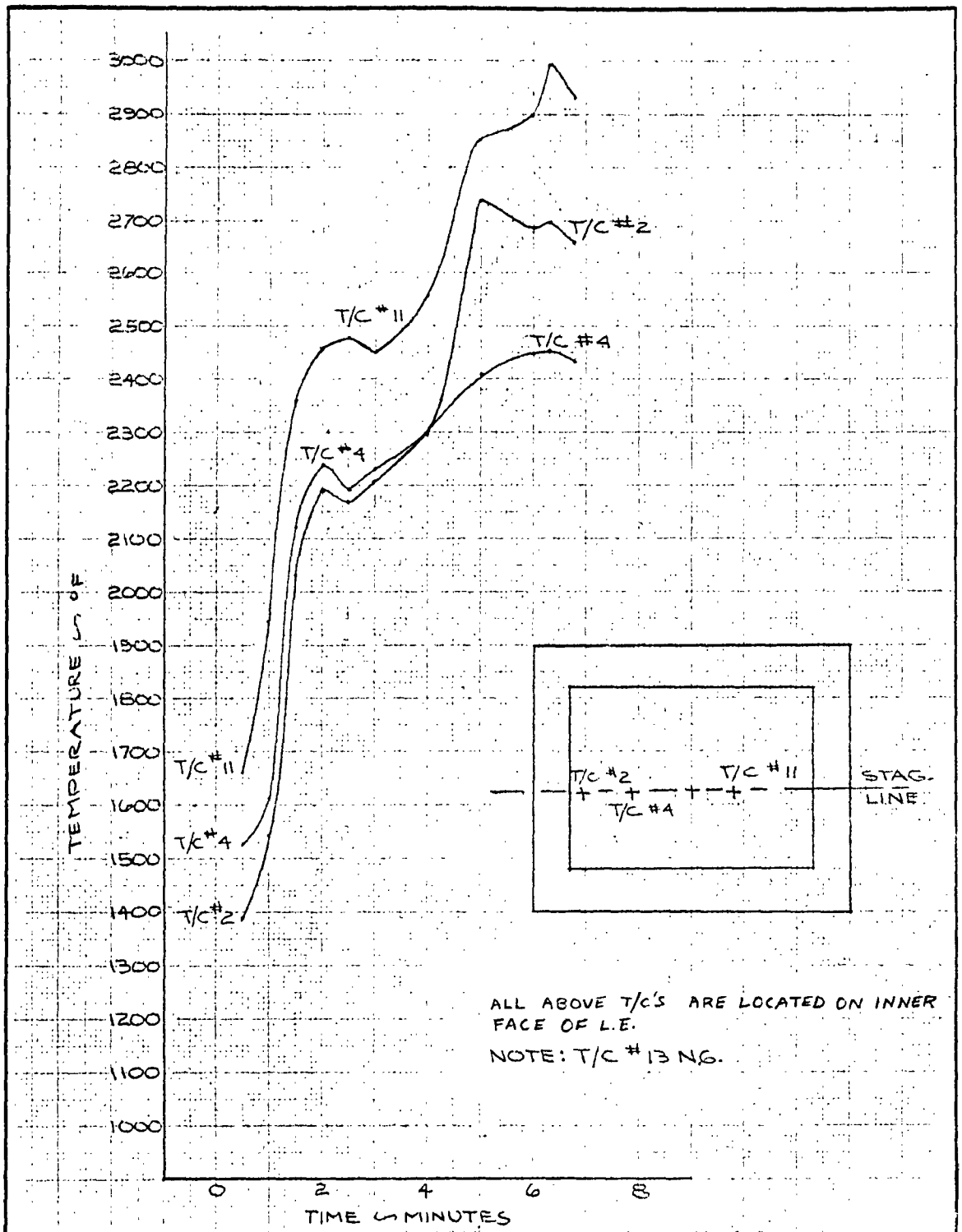

CALC	NP	6/22/62	REVISED	DATE	THERMAL DISTRIBUTION MODEL T/C's #2, 4, & 11	D2-80085
CHECK	V.M.G.	6/22/62			TEST 2224 RUN 106 5-25-62	Figure 2-2
APR					THE BOEING COMPANY	PAGE 2-53
APR						

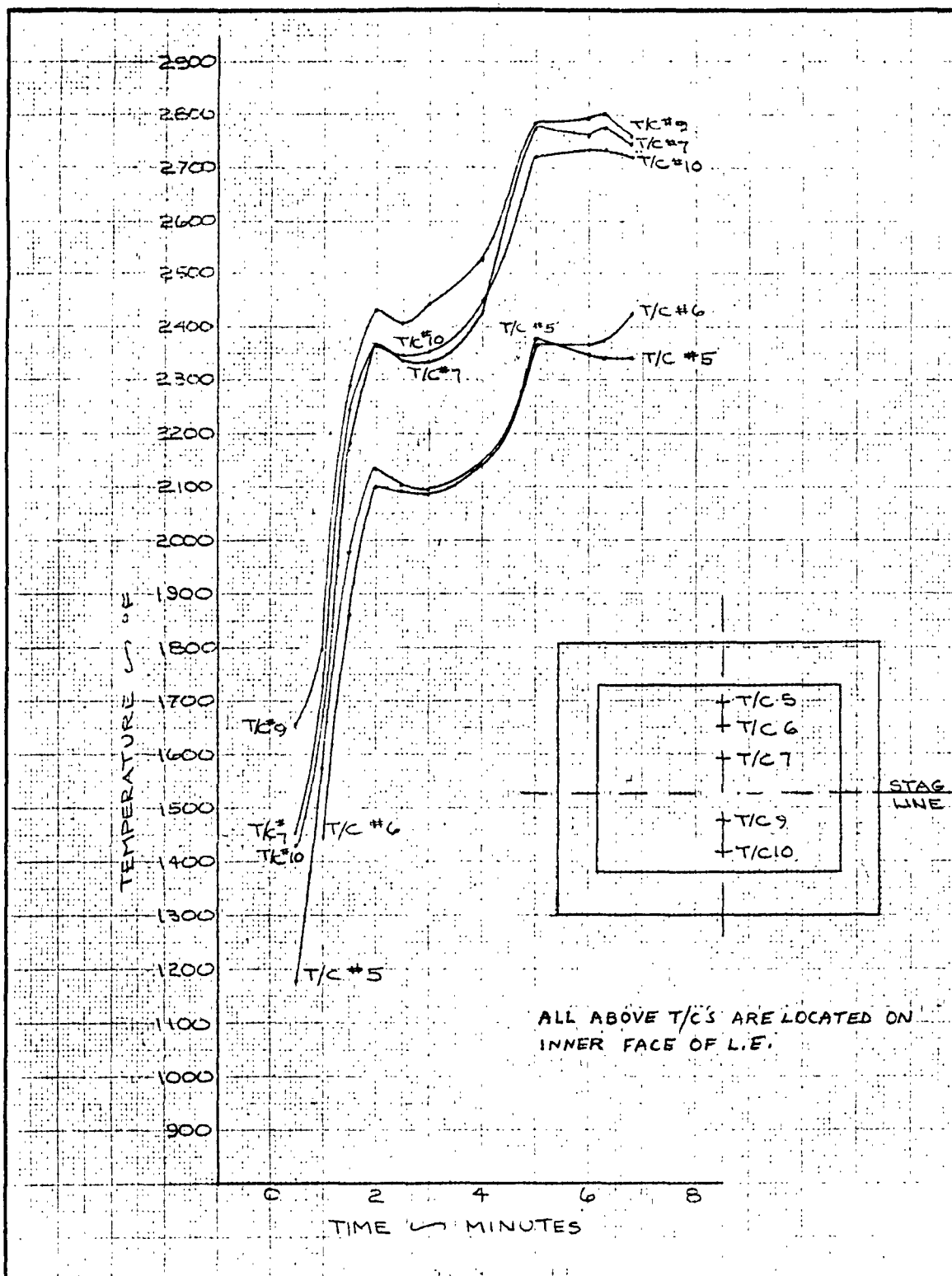

CALC	NP	6/20/62	REVISED	DATE	L THERMAL DISTRIBUTION MODEL T/C's 5, 6, 7, 9, & 10 TEST 2224 RUN 106 5-25-62
CHECK	K.A.G.	6/20/62			
APR					
APR					
					THE BOEING COMPANY

D2-80085

Figure 2-29

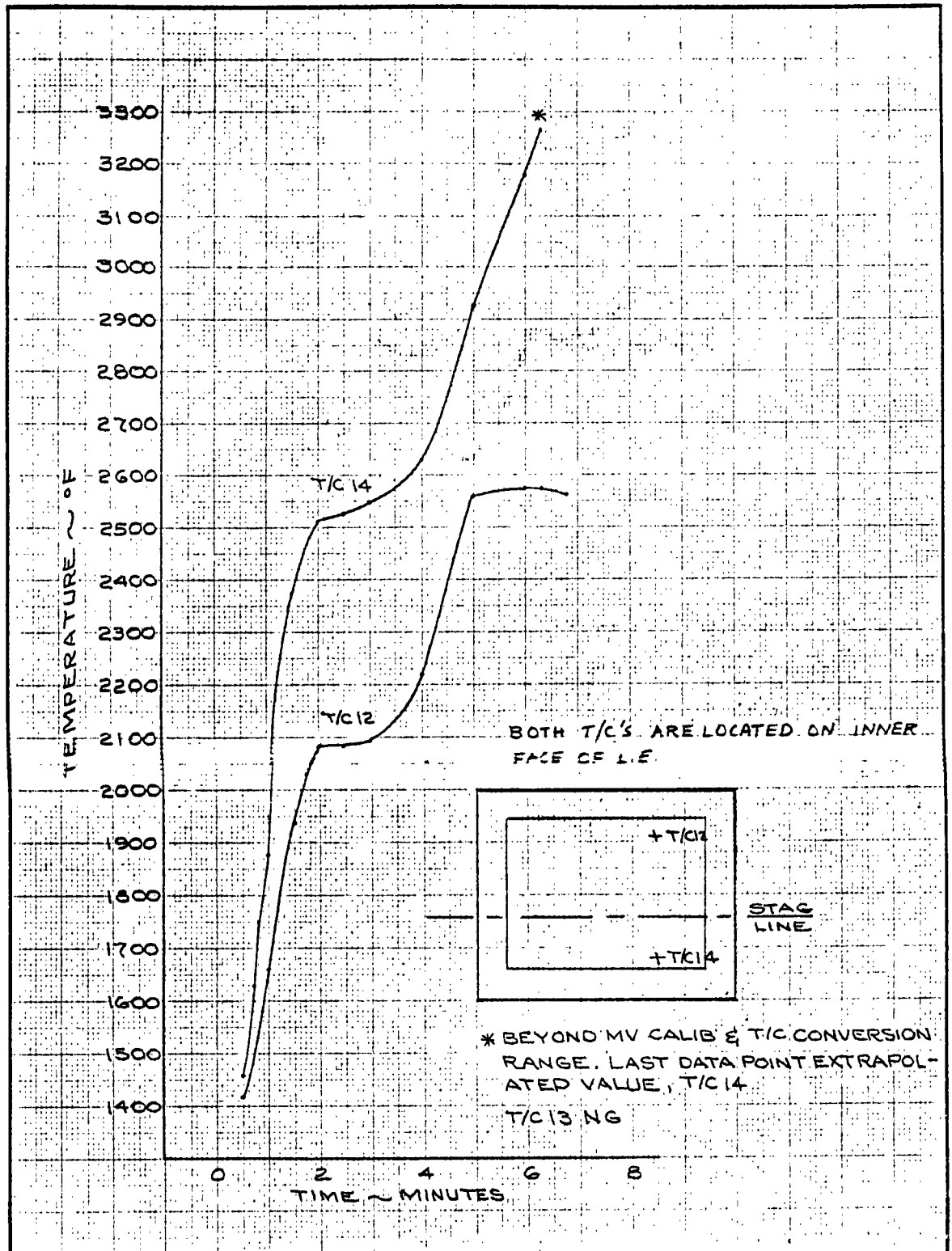

CALC	LMR-DD NB-LM	6-20-62	REVISED	DATE	THERMAL DISTRIBUTION MODEL T/C'S 12 & 14
CHECK	V.M.G.	6-20-62			
APR					TEST 2224 RUN 106 5-25-62
APR					THE BOEING COMPANY
PLOT	LM	6-26-62			

D2-80085

Figure 2-39

PAGE 2-55

US 4013 6000

K&E ALBANENE TOOL TRACING PAPER 68587

CALC	U.M.G	5/25/62	REVISED	DATE	THERMAL DISTRIBUTION MODEL GAP MEASUREMENTS	D2-80085
CHECK						
APPR					TEST 2224 RUN # 106 EWA 5-609	Fig. 2-31
APPR					THE BOEING COMPANY SEATTLE 24, WASHINGTON	PAGE 2-56

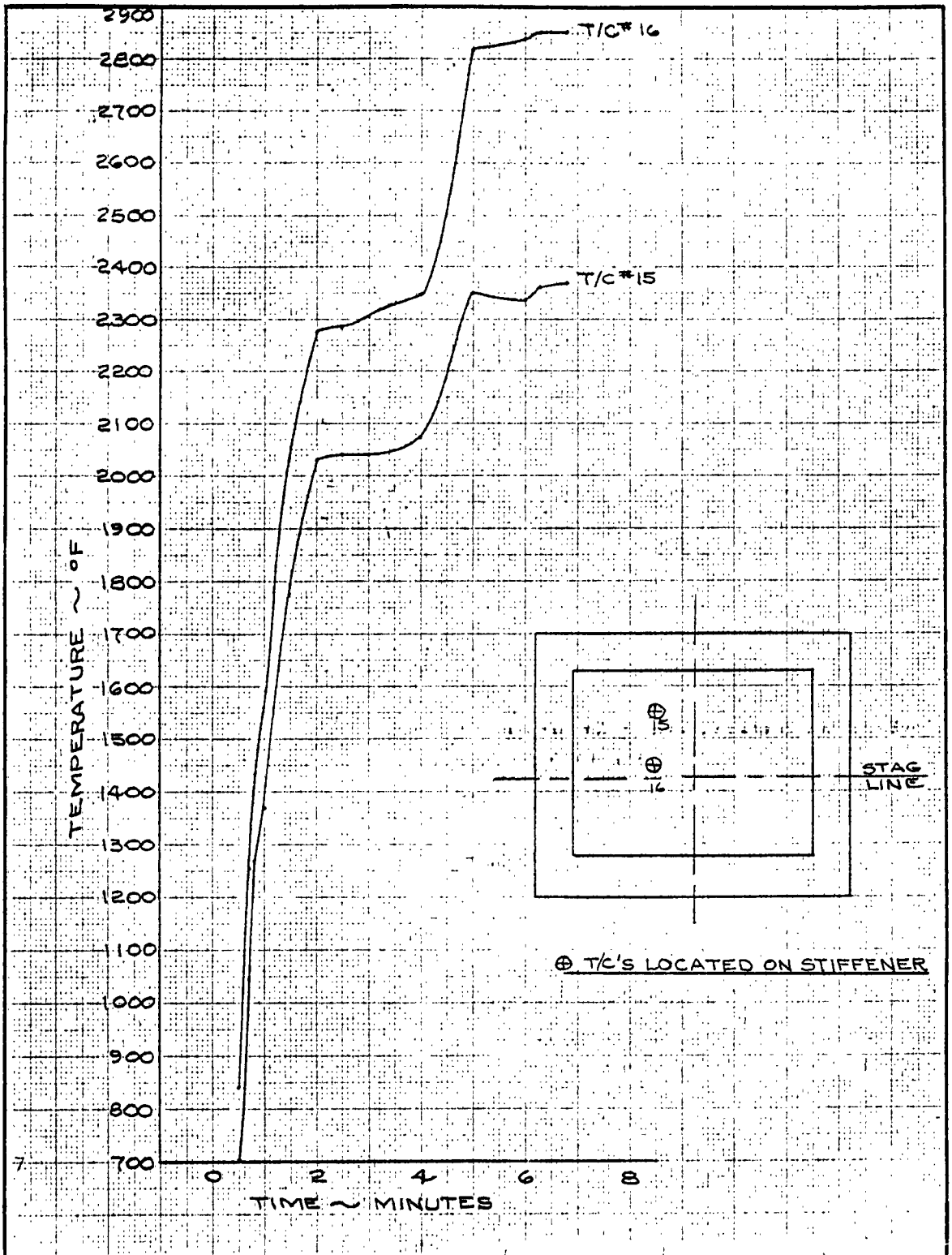

CALC	LMR - NP	5-29-62 6-15-62	REVISED	DATE	THERMAL DISTRIBUTION MODEL T/C'S #15 & #16
CHECK	V.N.G.	6/15/62			
APR					TEST 2224 RUN 106 5-25-62
APR					THE BOEING COMPANY
PLOT	LM	6-21-62			

D2-80085

Figure 2-32

PAGE 2-57

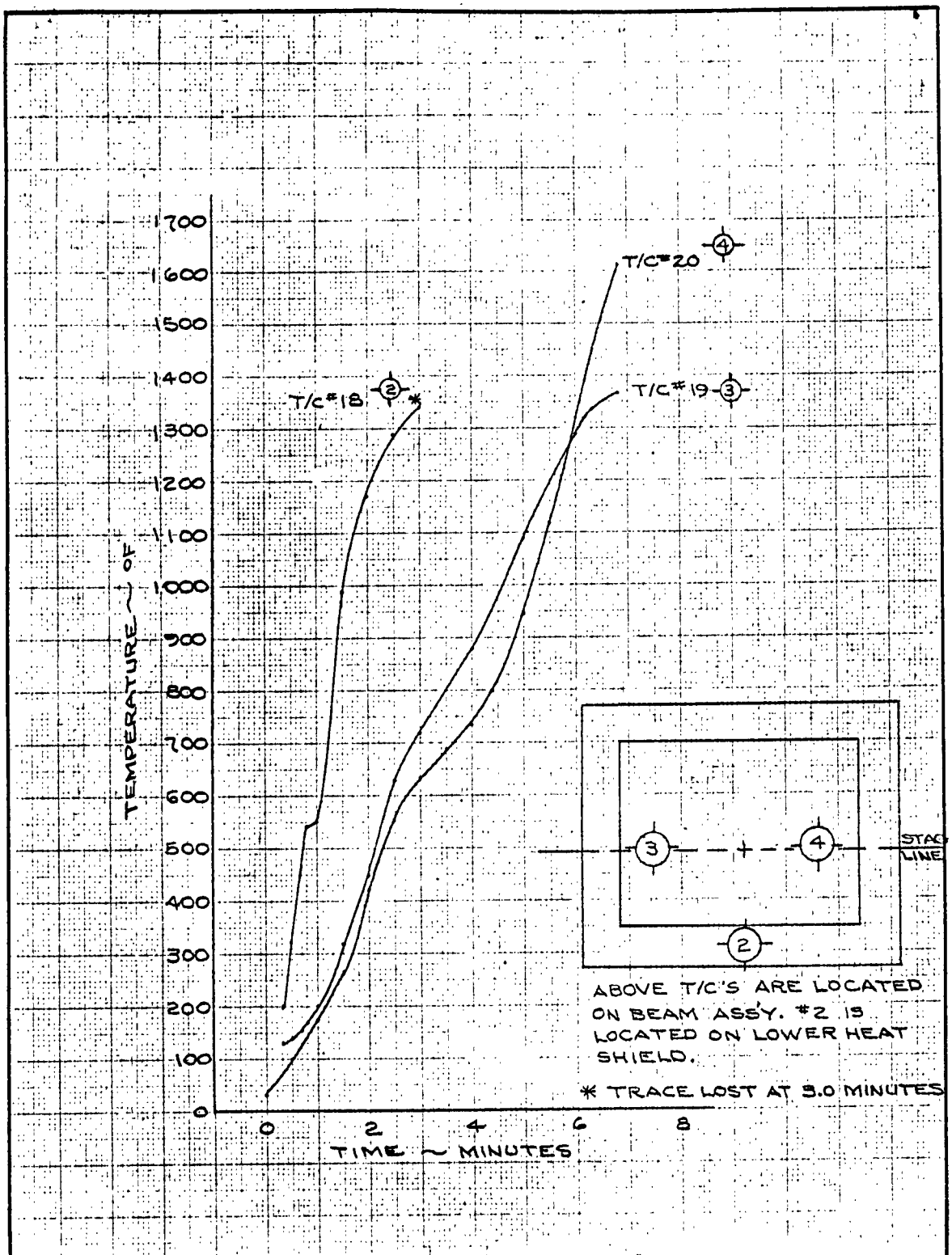

CALC	MA-LMR	6-18-62 6-29-62	REVISED	DATE
CHECK	V.M.G.	6/18/62		
APR				
APR				
PLOT	LM	6-21-62		

THERMAL DISTRIBUTION MODEL T/C'S (2), (3), (4)

TEST 2224 RUN 106 5-25-62

THE BOEING COMPANY

D2-80085

Figure 2-33

PAGE 2-58

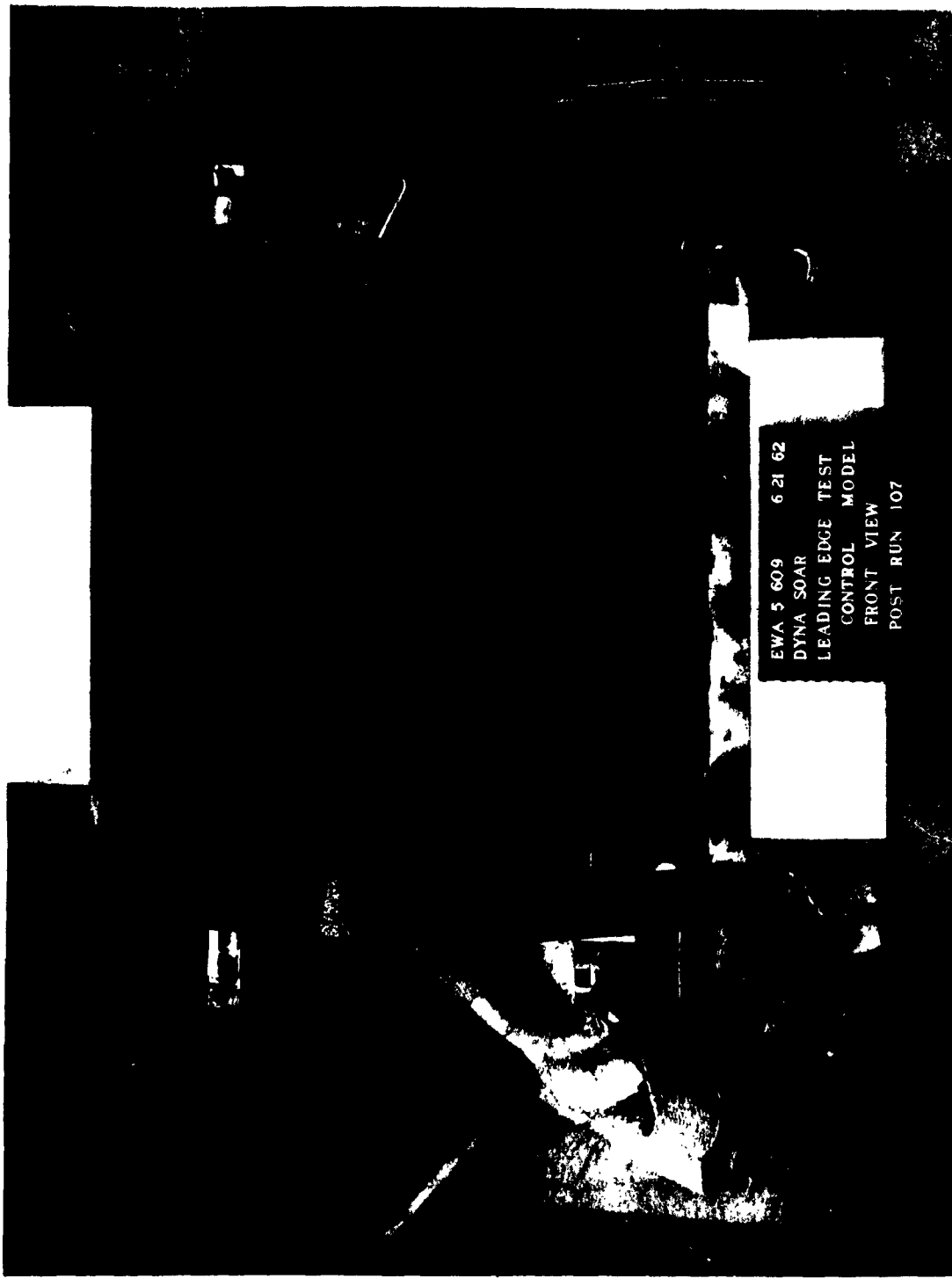

LEAKAGE CONTROL MODEL

CONTROL MODEL POST-RUN LEADING EDGE
6-26-62

U3-4071-1000 (was BAC 1546-L-R3)

FIGURE 2-34

CALC			REVISED	DATE	LEAKAGE CONTROL MODEL LEAKAGE RATE, STAG. PRESS & TEMP	D2-80085
CHECK						
APR					Test 2224 RUN 105 EWA 5-609	FIGURE 2-
APR					THE BOEING COMPANY	PAGE 2-60
PLOT	PS	4-19-65				

US 4013 8000

K·E ALBANENE 1951 68587

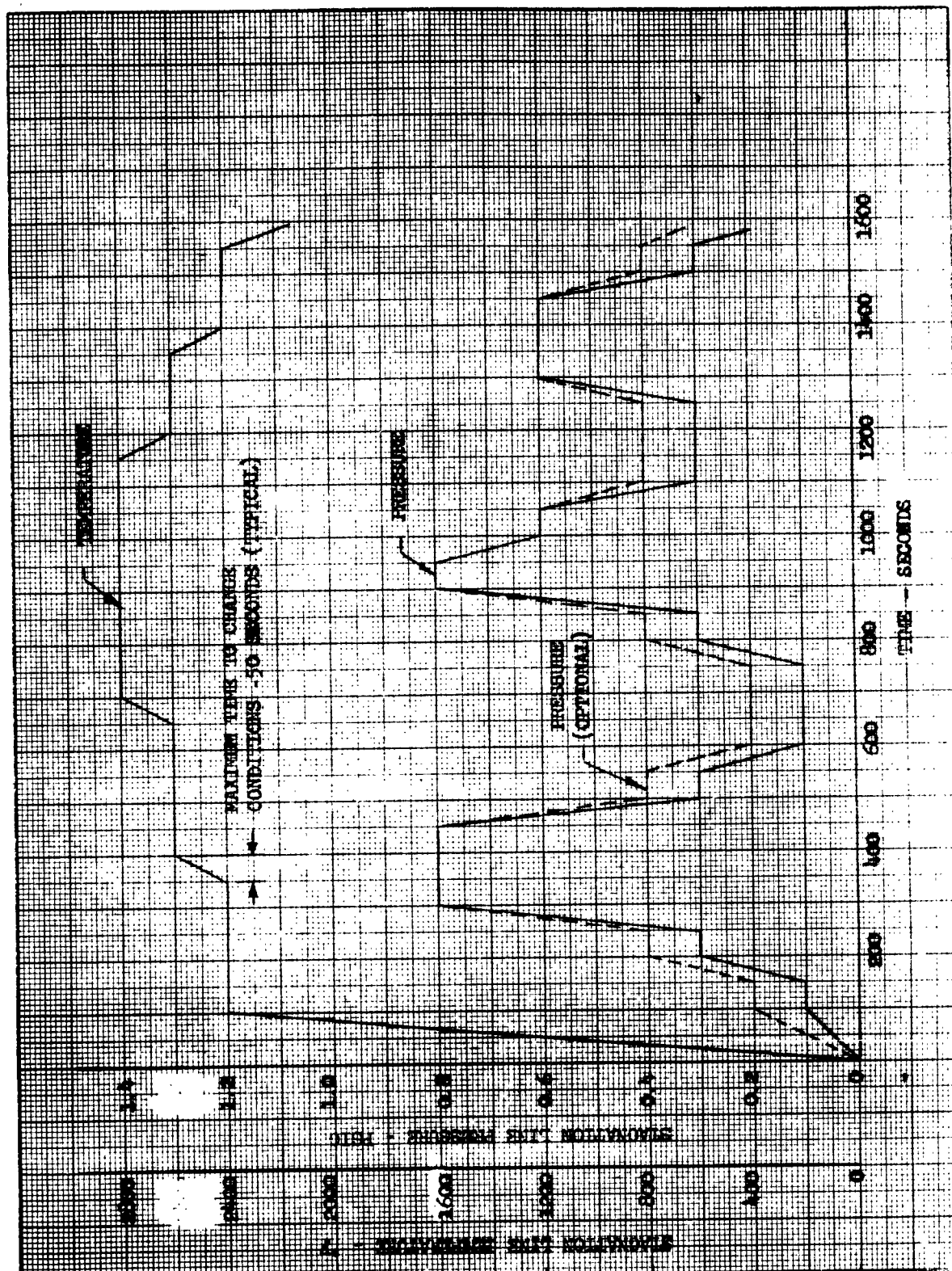

CALC	D B.		REVISED	DATE	PLASMA JET TEST ENVIRONMENT LEADING EDGE SEAL REQUIREMENTS EVALUATION Test 2224 EWA 5-609	D2-80085 Fig. 2-36
CHECK	V.M.G.					
APR					BOEING AIRPLANE COMPANY	PAGE 2-61
APR						

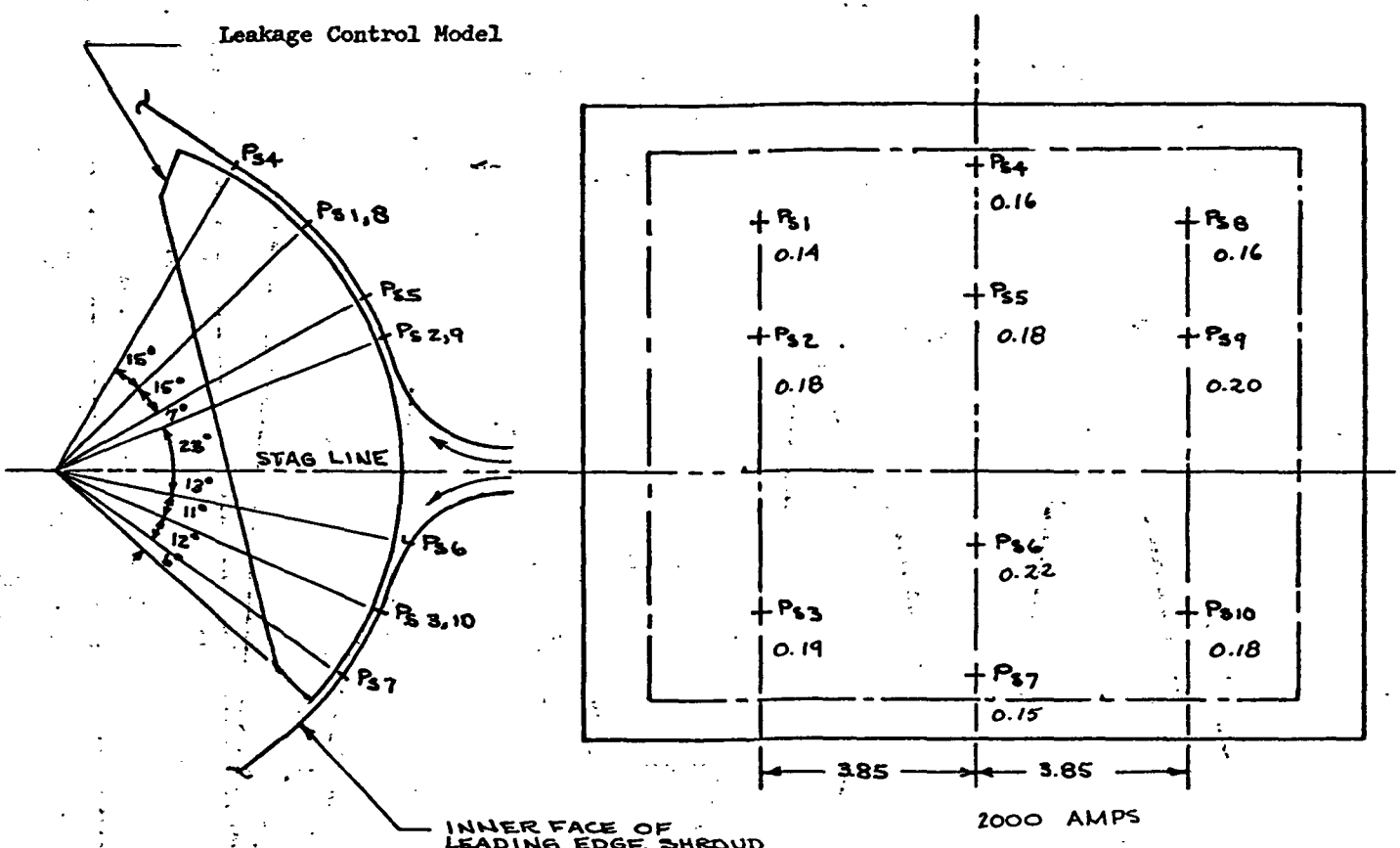

	CALC	CHECK	APP	APP	APP
	CAK	W.M.G.			
	5/11/62	5/11/62			
REVISED					
DATE					

US 4038 8000

LEADING EDGE SHROUD PRESSURE
LEAKAGE CONTROL MODEL
EWA 5-609 TEST 222.4

THE BOEING COMPANY

D2-80085

Figure 2-

PAGE 2-62

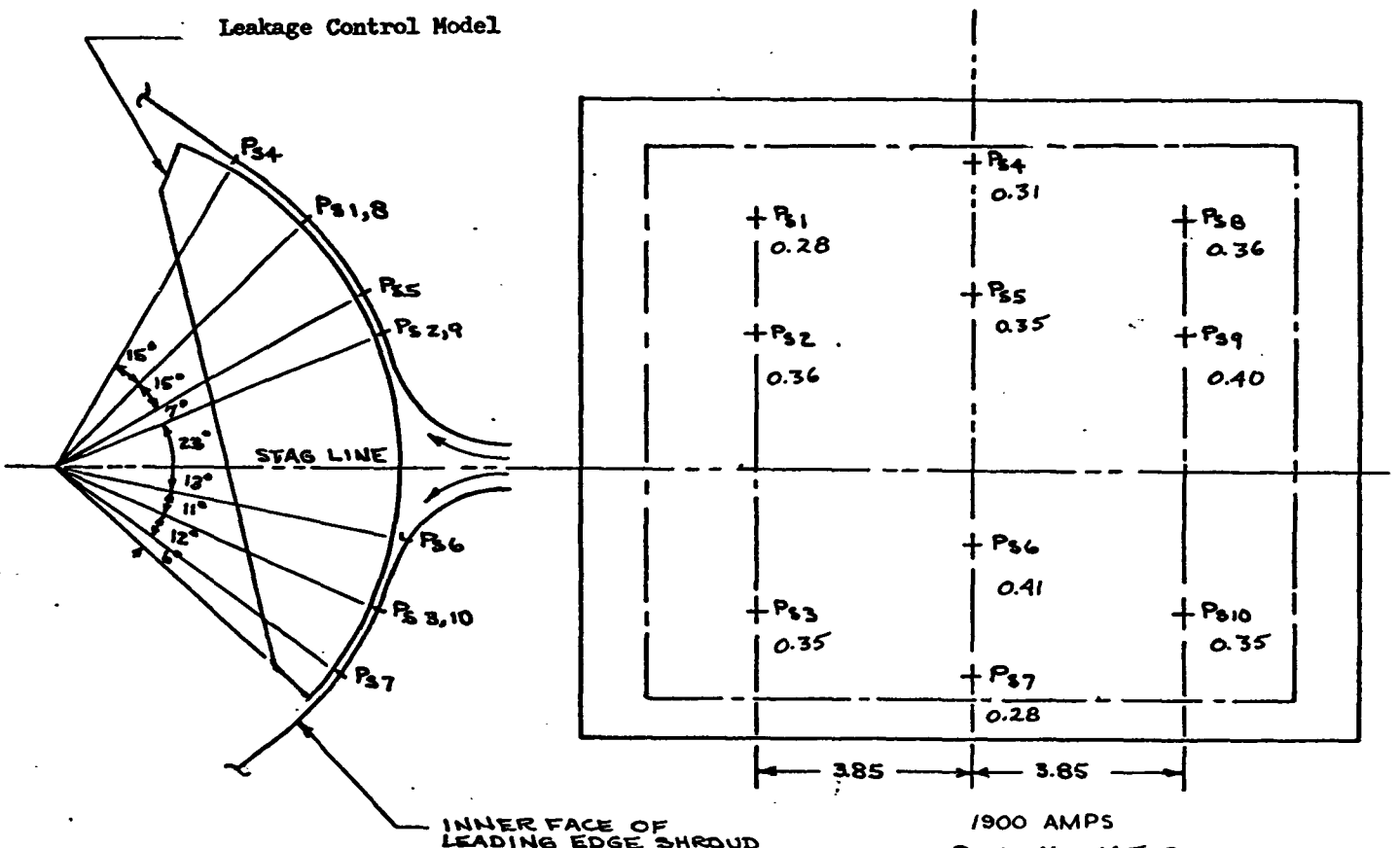

CALC	CAK	5/7/62		
CHECK	WM.G.	5/11/62		
APP				
APP				
			REVISED	DATE

LEADING EDGE SHROUD PRESSURES
LEAKAGE CONTROL MODEL
EWA 6-609 TEST 222.4
THE BOEING COMPANY

D2-[illegible]

Figure 2

PAGE 2-62

US 4038 8000

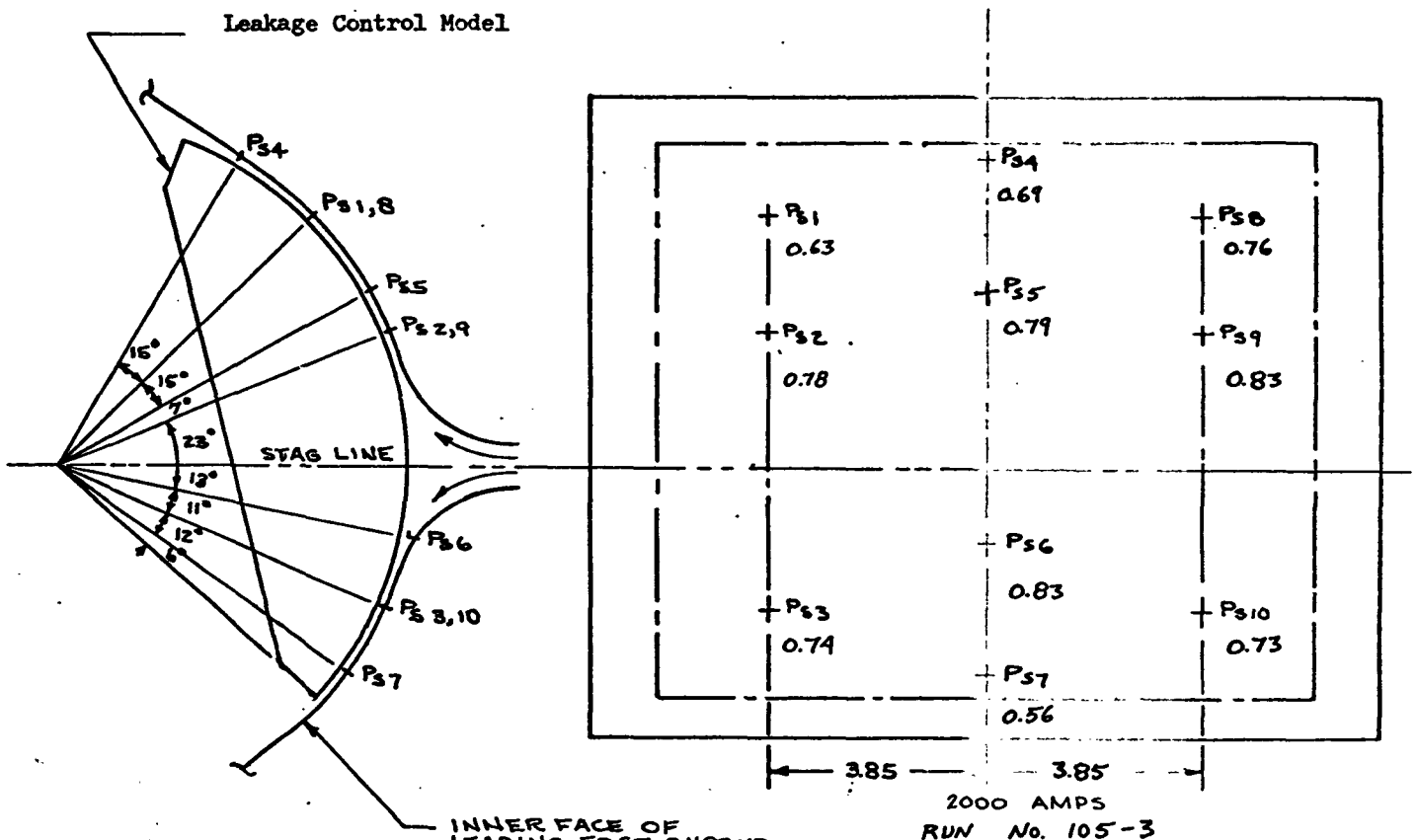

CALC	CAK	5/17/62		
CHECK	U.M.G.	5/17/62		
APP				
APP				
			REVISED	DATE

LEADING EDGE SHROUD PRESSURES
LEAKAGE CONTROL MODEL
EWA 6-609 TEST 222.4
THE BOEING COMPANY

D2-80085

Figure 2-43

US 4038 8000

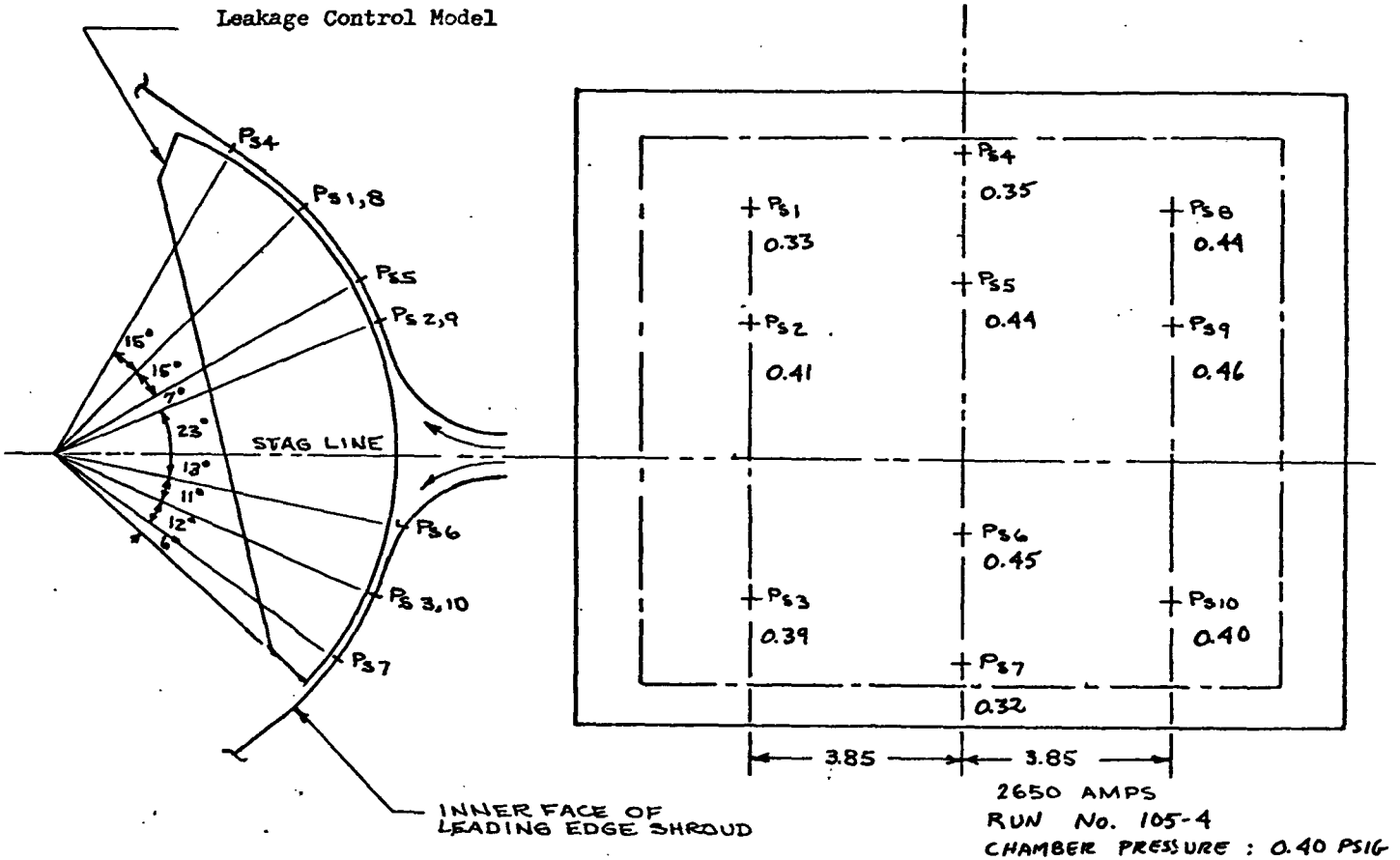

CALC	CAK	5/7/62	REVISED	DATE
CHECK	W.M.G.	5/7/62		
APP				
APP				

LEADING EDGE SHROUD PRESSURES
LEAKAGE CONTROL MODEL
EWA 5-609
TEST 2.2.2.4
THE BOEING COMPANY

D2-80085

Figure 2-65

PAGE 2-65

US 4038 8000

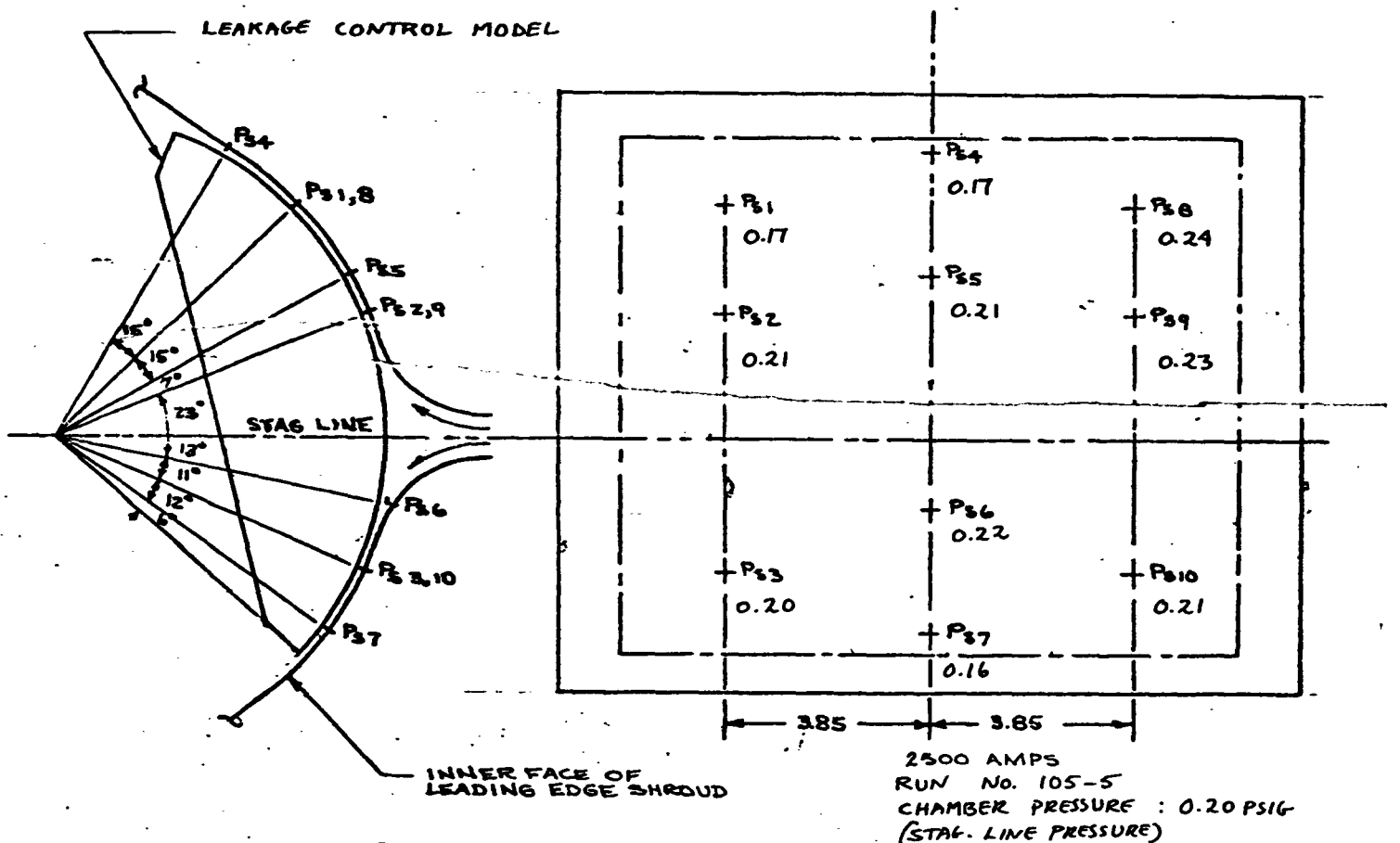

CALC	CAK	5/11/62	REVISED	DATE
CHECK	U.M.L.	5/11/62		
APP.				
APP.				

LEADING EDGE SHROUD PRESSURE

LEAKAGE CONTROL MODEL

EWA 5-609 TEST 222.4

THE BOEING COMPANY

D2-80085

PAGE 2-66

Figure 2-41

CALC	CHECK	APP	APP	APP
CAK	W.M.G.			
5/7/62	5/7/62			

REVISED	DATE

LEADING EDGE SHROUD PRESSURE
LEAKAGE CONTROL MODEL

EWA 5-609

THE BOEING COMPANY

TEST 2224

D2-80085

PAGE 2-67

Figure 2-42

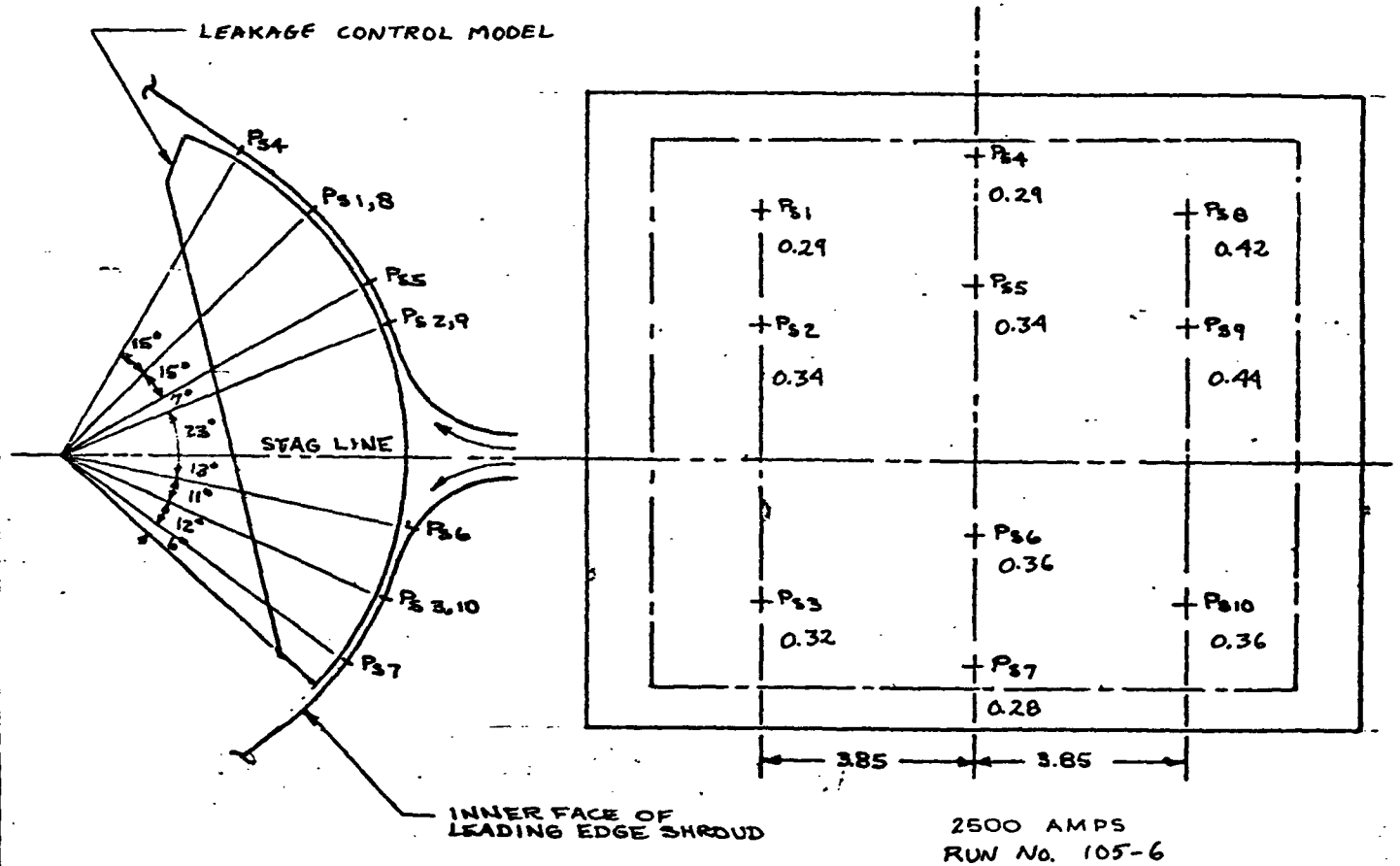

2500 AMPS
RUN No. 105-6
CHAMBER PRESSURE : 0.43 PSIG
(STAG. LINE PRESSURE)

CALC	DD	5-18-62	REVISED	DATE	LEAKAGE CONTROL MODEL STAG. LINE TEMP - T/C #3 TEST 2224 RUN 105 5-16-62
CHECK	V. M. G.	5-18-62			
APR					
APR					
					THE BOEING COMPANY

D2-80085

Figure 2-45

US 4018 8000

K+E ALBANENE 1068 TRACING PAPER 68587

			REVISED	DATE	LEAKAGE CONTROL MODEL T/C #1, 2 & 4 TEST 2224 5-16-62 RUN 105	D2-80085
CALC						
CHECK	V. M. C.	6/16/62				Figure 2-44
APR						
APR						
PLOT	NP	6/16/62			THE BOEING COMPANY	PAGE 2-69

US 4013 6000

K+E ALBANENE 100L TRACING PAPER 68587

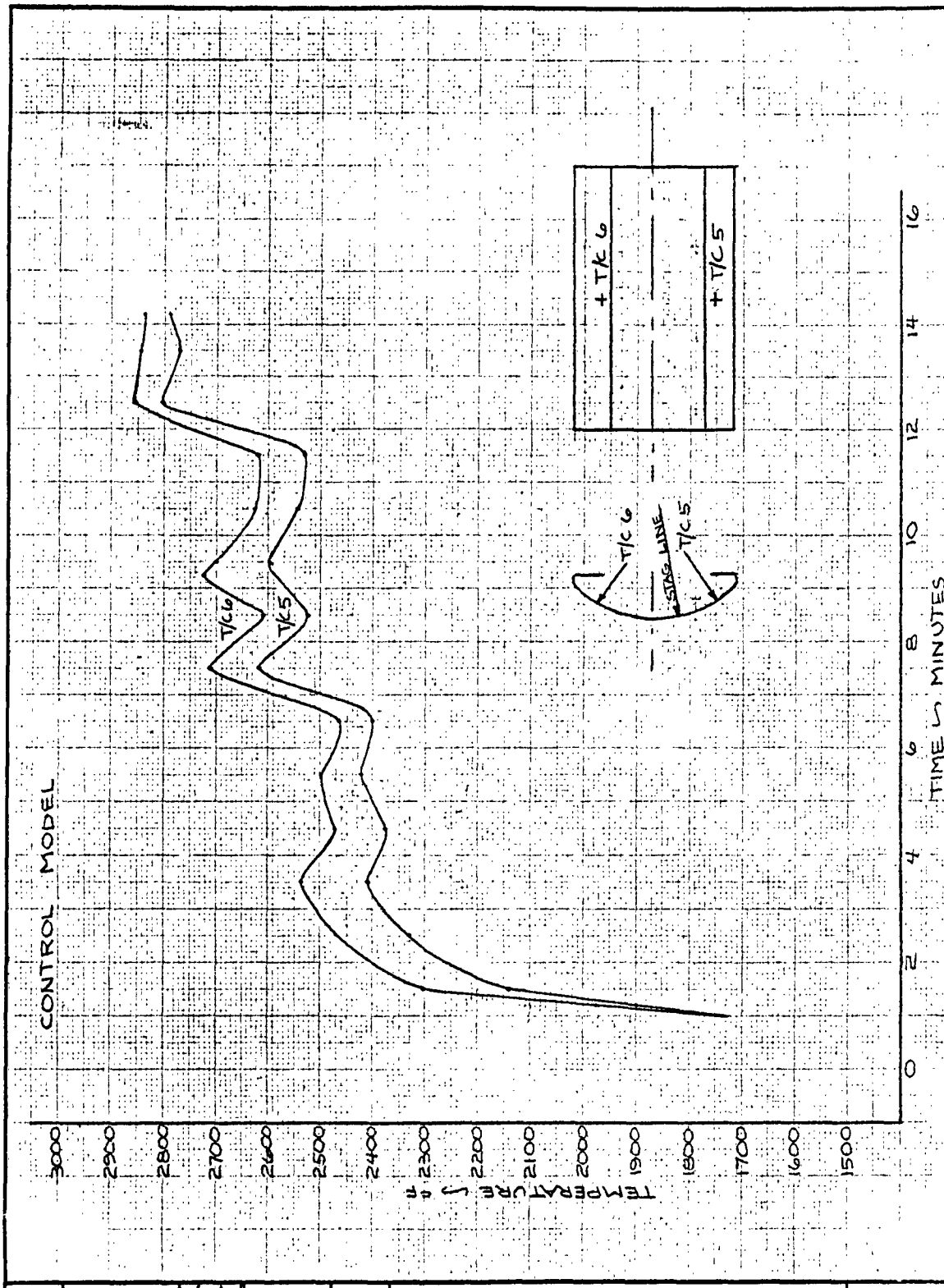

CALC	V. M. G	6/16/62	REVISED	DATE	LEAKAGE CONTROL MODEL T/C #5 & #6
CHECK	V.M.G	6/16/62			
APR					TEST 2224 5-16-62 RUN 105
APR					
PLOT	NP	6/15/62			THE BOEING COMPANY

D2-80055

Figure 2-35

PAGE 2-703

US 4018 8000

H-E ALBANENE 100L 68587

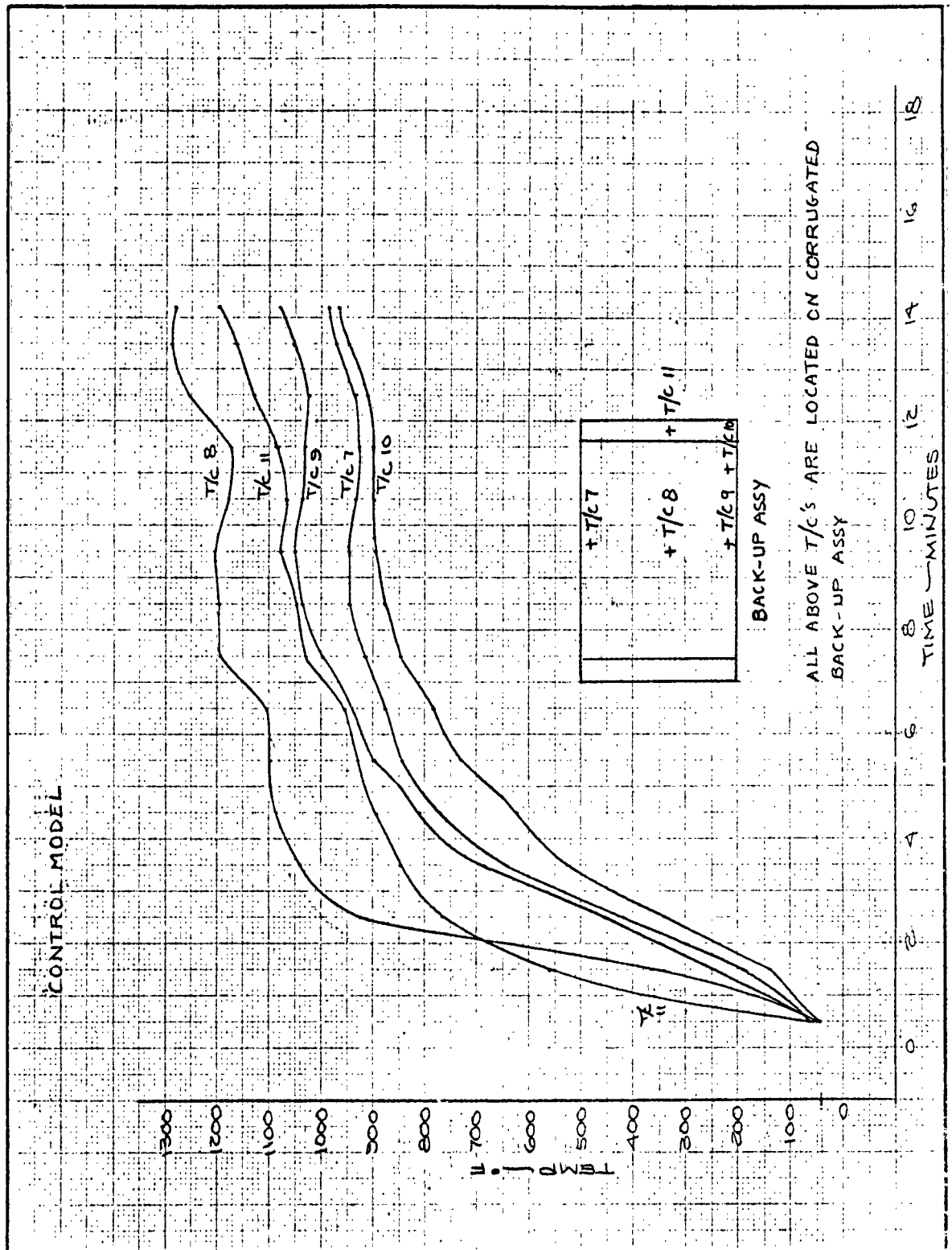

CALC	lek	5-21-62	REVISED	DATE	LEAKAGE CONTROL MODEL T/C 7, 8, 9, 10 & 11 TEST 2225 5-16-62 RUN 105
CHECK	V.M.G	5-21-62			
APR					
APR					
					THE BOEING COMPANY

D2-80085

Figure 2-46

PAGE 2-71

US 4013 8000

K+E ALBANENE 1964 60629

			REVISED	DATE
CALC	ND	6-15-62		
CHECK	V.M.G.	6-15-62		
APR				
APR				
PLOT	LM	6-27-62		

LEAKAGE CONTROL MODEL
T/C's 12, 13 & 14

TEST 2224 RUN 105 5-16-62

THE BOEING COMPANY

D2-80005

Figure 2-4

PAGE 2-72

US 4013 8000

K+E ALBANENE 10SL 68587

CALC	U.M.G.	5/16/62	REVISED	DATE	LEAKAGE CONTROL MODEL GAP MEASUREMENTS	D2-80085
CHECK					TEST 2224 RUN No. 105 EWA 5-609	Fig. 2-48
APPD					THE BOEING COMPANY SEATTLE 24, WASHINGTON	2-73
APPD						

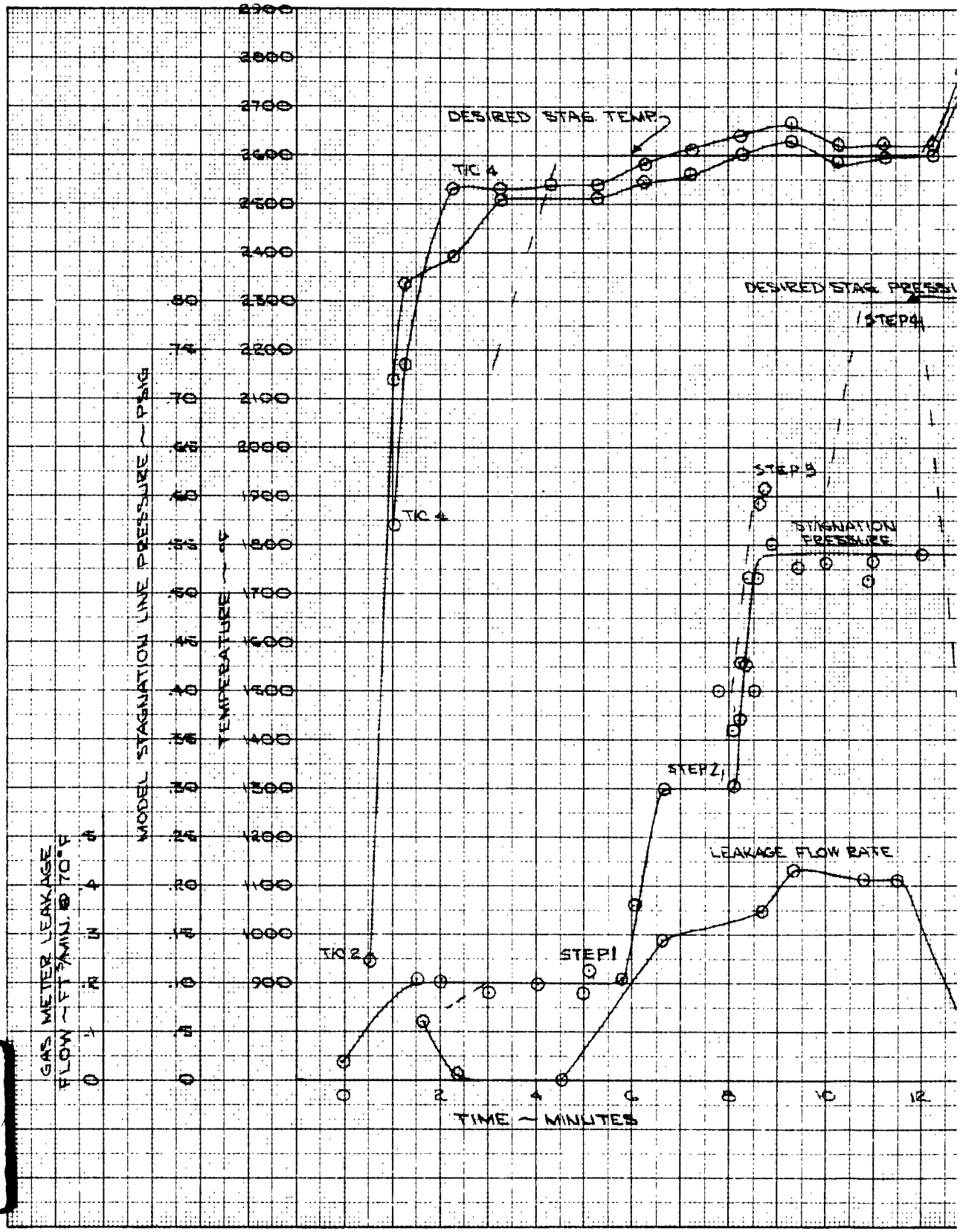
DESIRED STAG. TEMP.
TIC 4
DESIRED STAG. PRESS.
STEP 4
STEP 3
TIC 4
STAGNATION PRESSURE
STEP 2
LEAKAGE FLOW RATE
TIC 2
STEP 1
TIME ~ MINUTES
MODEL STAGNATION LINE PRESSURE ~ PSIG
TEMPERATURE ~ °F
GAS METER LEAKAGE FLOW ~ FT³/MIN @ 70° F
2900
2800
2700
2600
2500
2400
2300
2200
2100
2000
1900
1800
1700
1600
1500
1400
1300
1200
1100
1000
900
.80
.75
.70
.65
.60
.55
.50
.45
.40
.35
.30
.25
.20
.15
.10
.05
0
6
5
4
3
2
1
0
2
4
6
8
10
12

1

CALC			REVISED	DATE	LEAKAGE CONTROL MODEL
CHECK					LEAKAGE RATE, STAG. PRESS. & TEMP.
APPD					TEST 2224 RUN 107 6-22-62
APPD					PLASMA JET TEST
PILOT LEK		4-19-63			

D2-80085

Fig. 2-49

PAGE 2-74

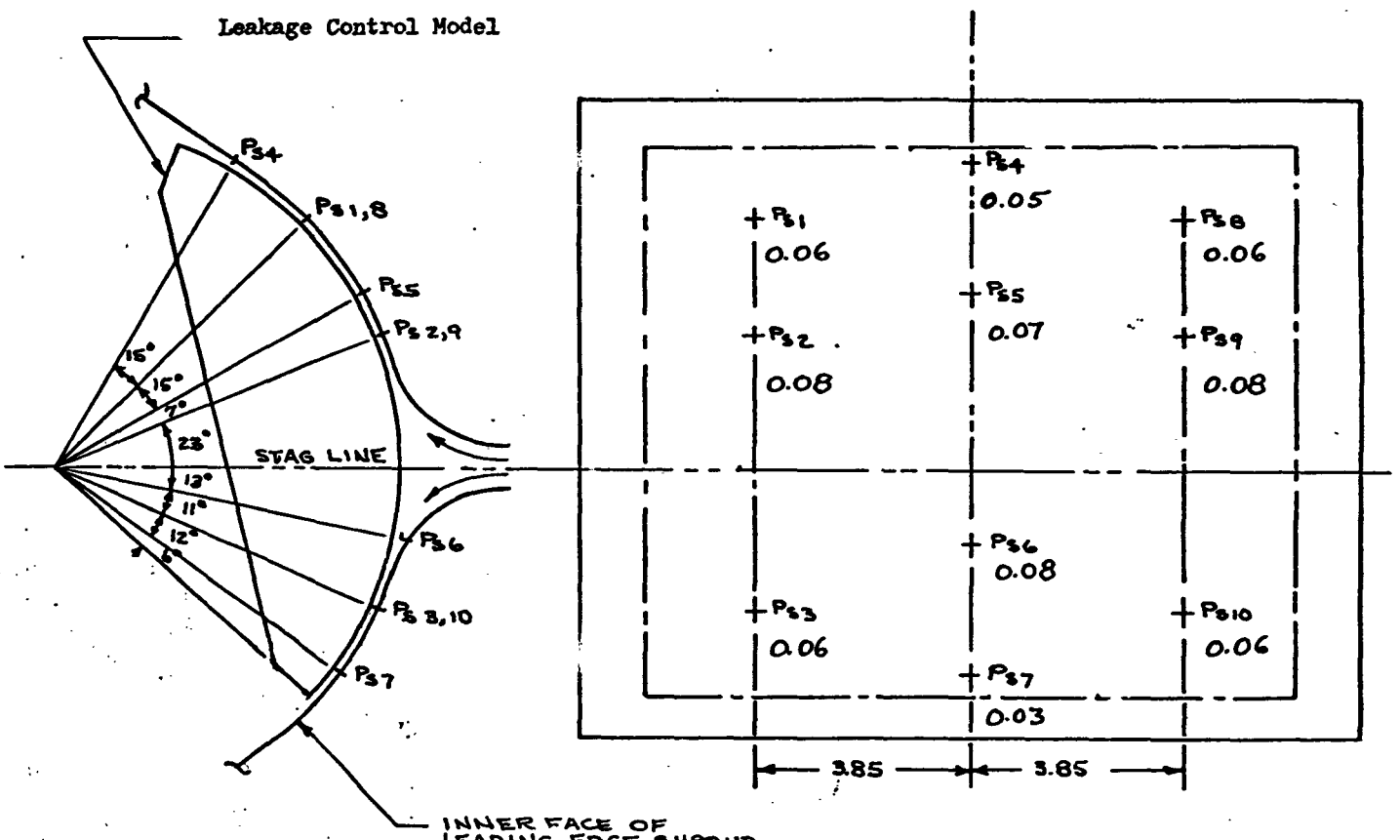

RUN No. 107 – 1
CHAMBER PRESSURE : 0.1 PSIG
(STAG. LINE PRESSURE)
STEP 1

CALC	CHECK	APR	APR	APR	REVISED	DATE
CAH	WMG					
6/2/62	6/2/62					

LEADING EDGE SHROUD PRESSURES
LEAKAGE CONTROL MODEL
TWA S-607 TEST 2224
THE BOEING COMPANY
D2-8006
Figure 2-
PAGE 2a75

US 4038 0000

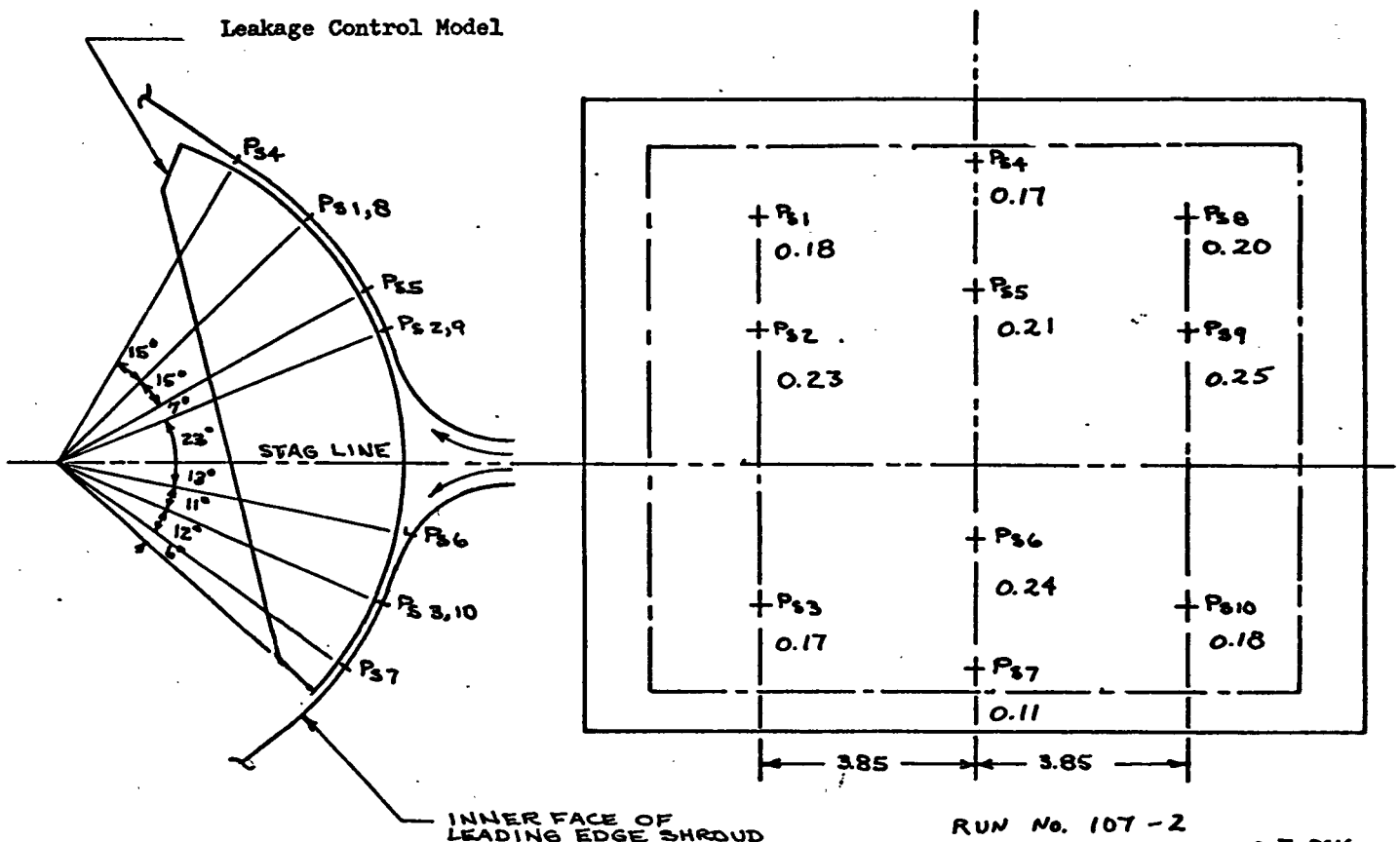

CALC	CAK	6/22/62			
CHECK	W.M.L.	6/22/62			
APP					
APP					
			REVISED	DATE	

LEADING EDGE SHROUD PRESSURE — D2-80085

LEAKAGE CONTROL MODEL

RMA 5-609 TEST 222.4

THE BOEING COMPANY

PAGE 2-76

Figure 2-51

US 4080 8000

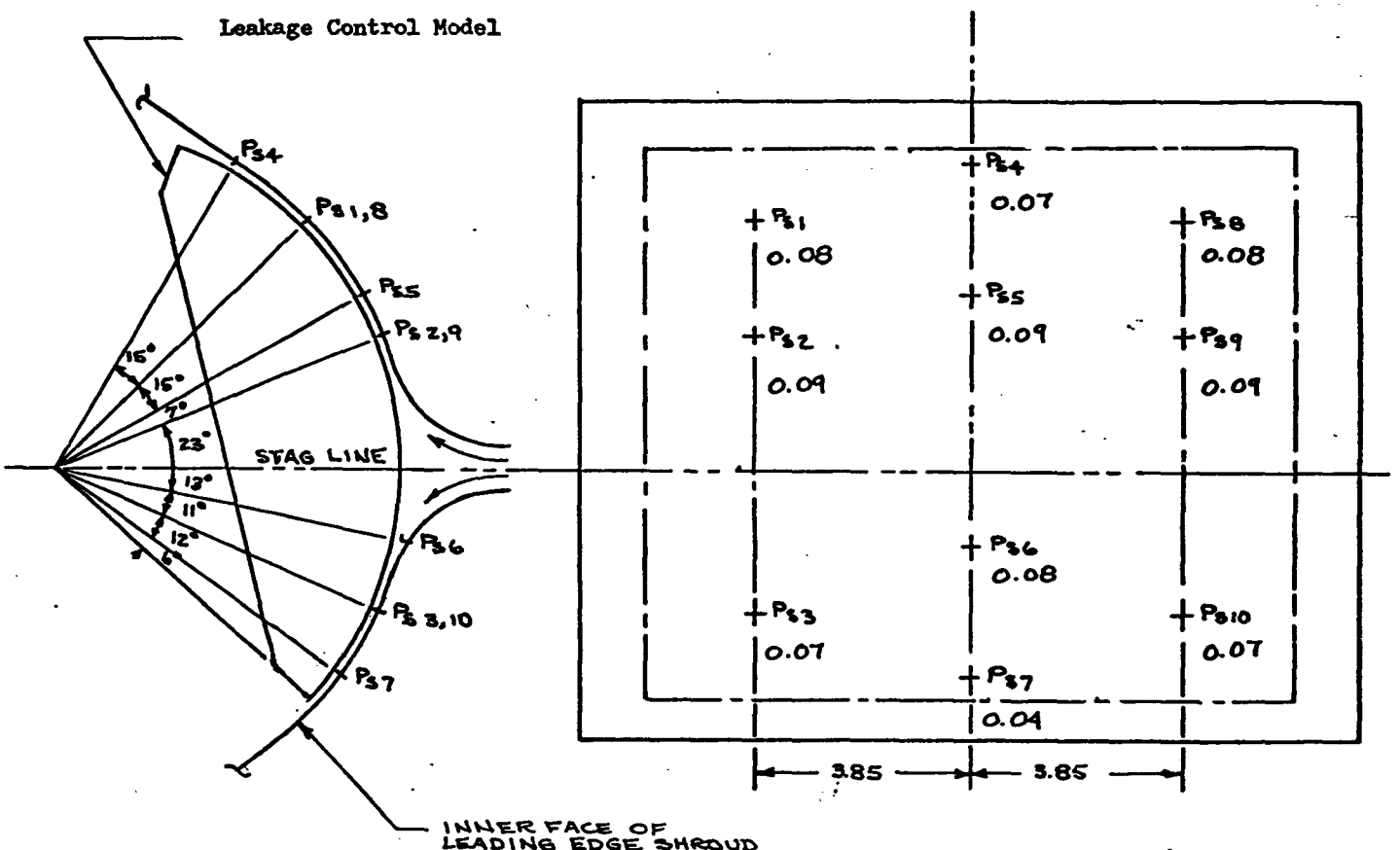

RUN No 107-5
CHAMBER PRESSURE : 0.1 PSIG
(STAG. LINE PRESSURE)

STEP 5

CALC	CAK	6/22/62		
CHECK	W.H.G.	6/22/62		
APP				
APP				
			REVISED	DATE

LEADING EDGE SHROUD PRESSURE — LEAKAGE CONTROL MODEL

EWA 6-409 TEST 222.4

THE BOEING COMPANY

D2-80085

Figure 2-

PAGE 2-72

U3 4038 8000

CALC	CAK	6/22/62	REVISED	DATE
CHECK	U.M.G.	6/22/62		
APR				
APR				

LEADING EDGE SHROUD PRESSURE
LEAKAGE CONTROL MODEL
EWA 5-609 TEST SPECIMEN
THE BOEING COMPANY

D2-80085
Figure 2-53
2-78

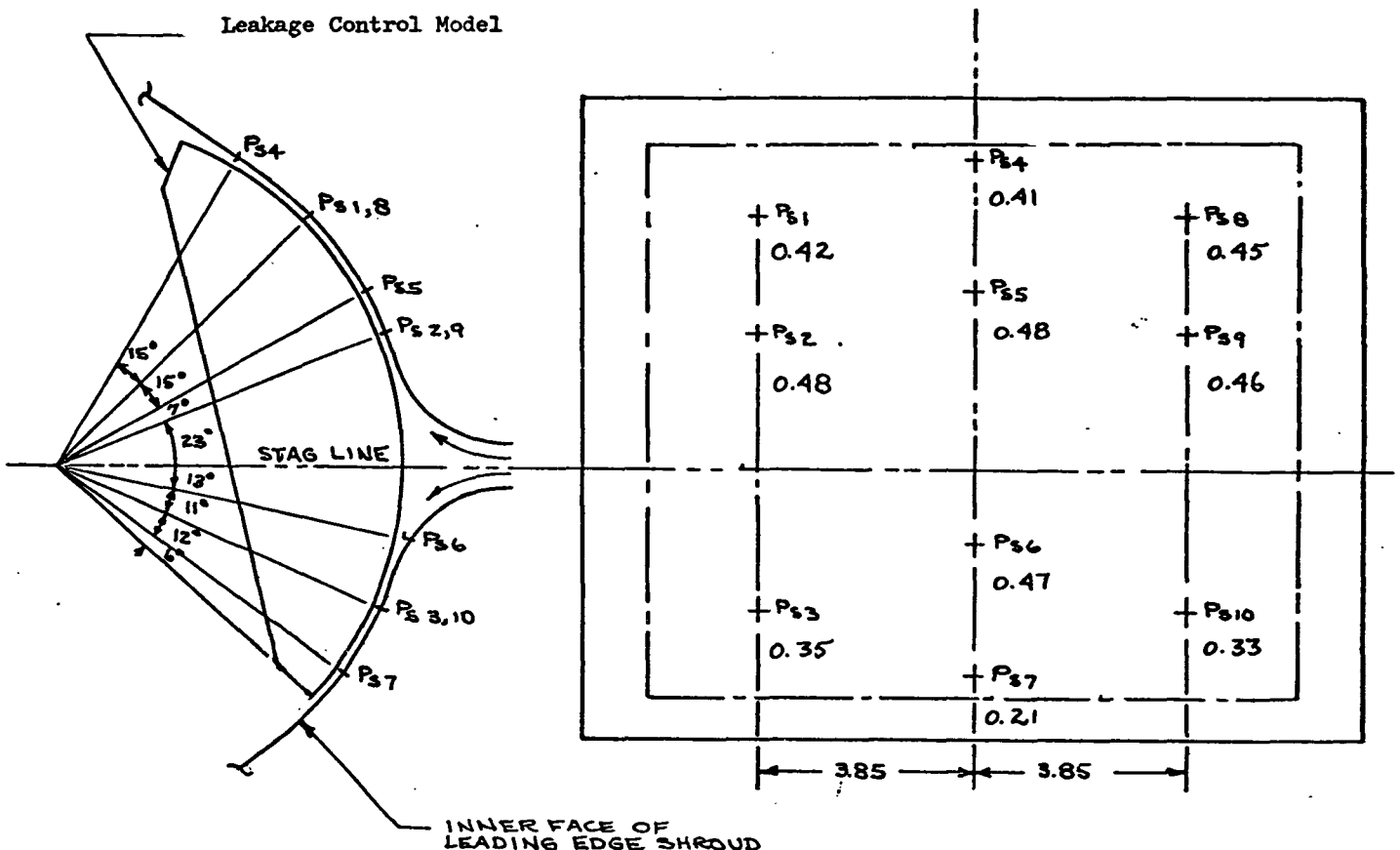

RUN No. 107-7
CHAMBER PRESSURE : 0.6 PSIG
(STAG. LINE PRESSURE)

STEP 7

CALC	CHECK	APR	APR	REVISED	DATE
CAK	W.M.G.	6/22/62	6/22/62		

LEADING EDGE SHROUD PRESSURE
LEAKAGE - CONTROL MODEL
RWA S-609 TEST 222.4
THE BOEING COMPANY

D2-30035

PAGE 2-79

Figure 2-57

U3 4038 0000

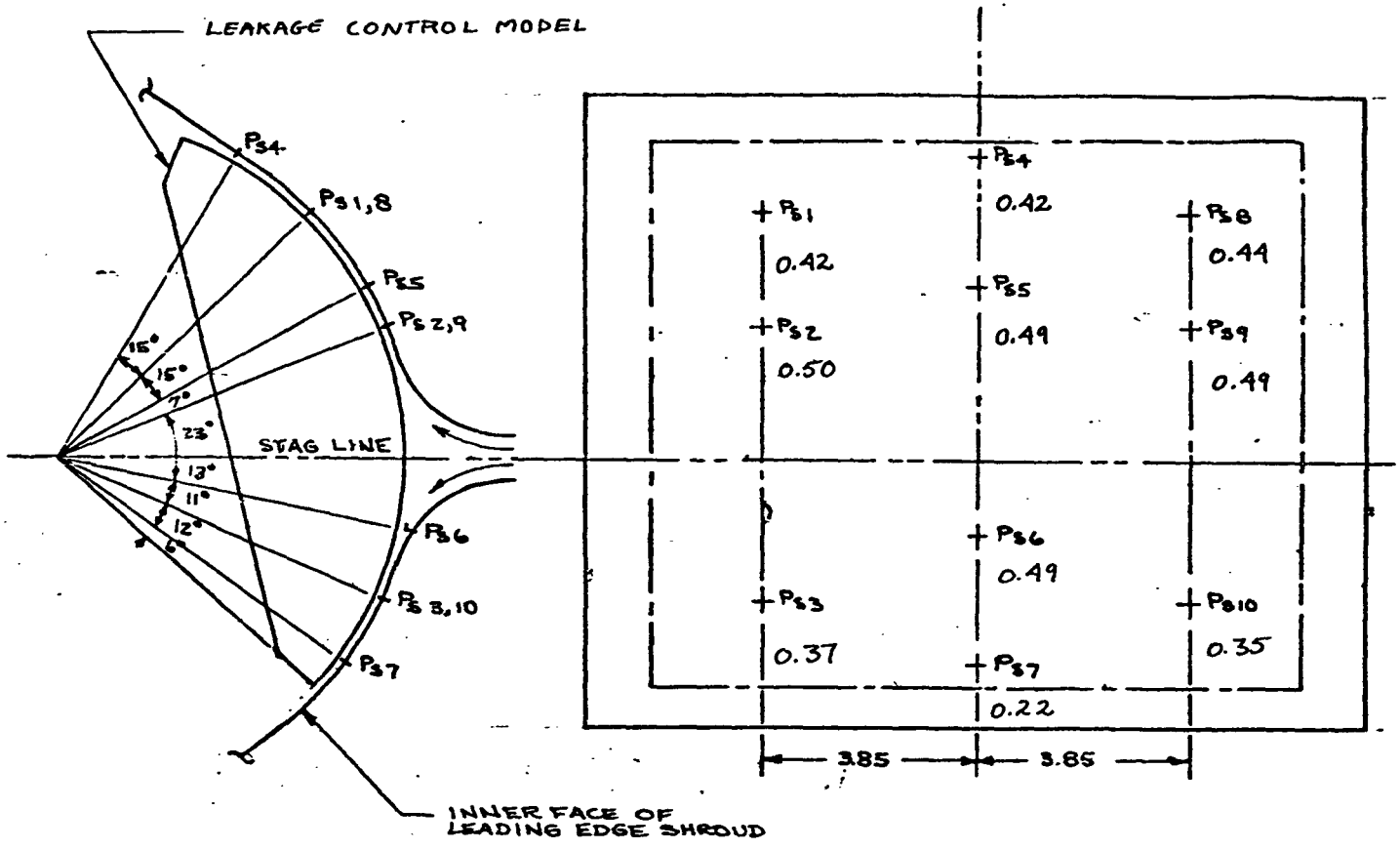

RUN No. 107 – 9
CHAMBER PRESSURE : 0.6 PSIG
(STAG. LINE PRESSURE)

STEP 9

CALC	CAK	6/22/62	REVISED	DATE	
CHECK	W.M.G.	6/22/62			
APR					
APR					

LEADING EDGE SHROUD PRESSURES
LEAKAGE CONTROL MODEL
EWA 5-609 TEST 2224
THE BOEING COMPANY
D2-80035
PAGE 2-80
Figure 2-

2-80

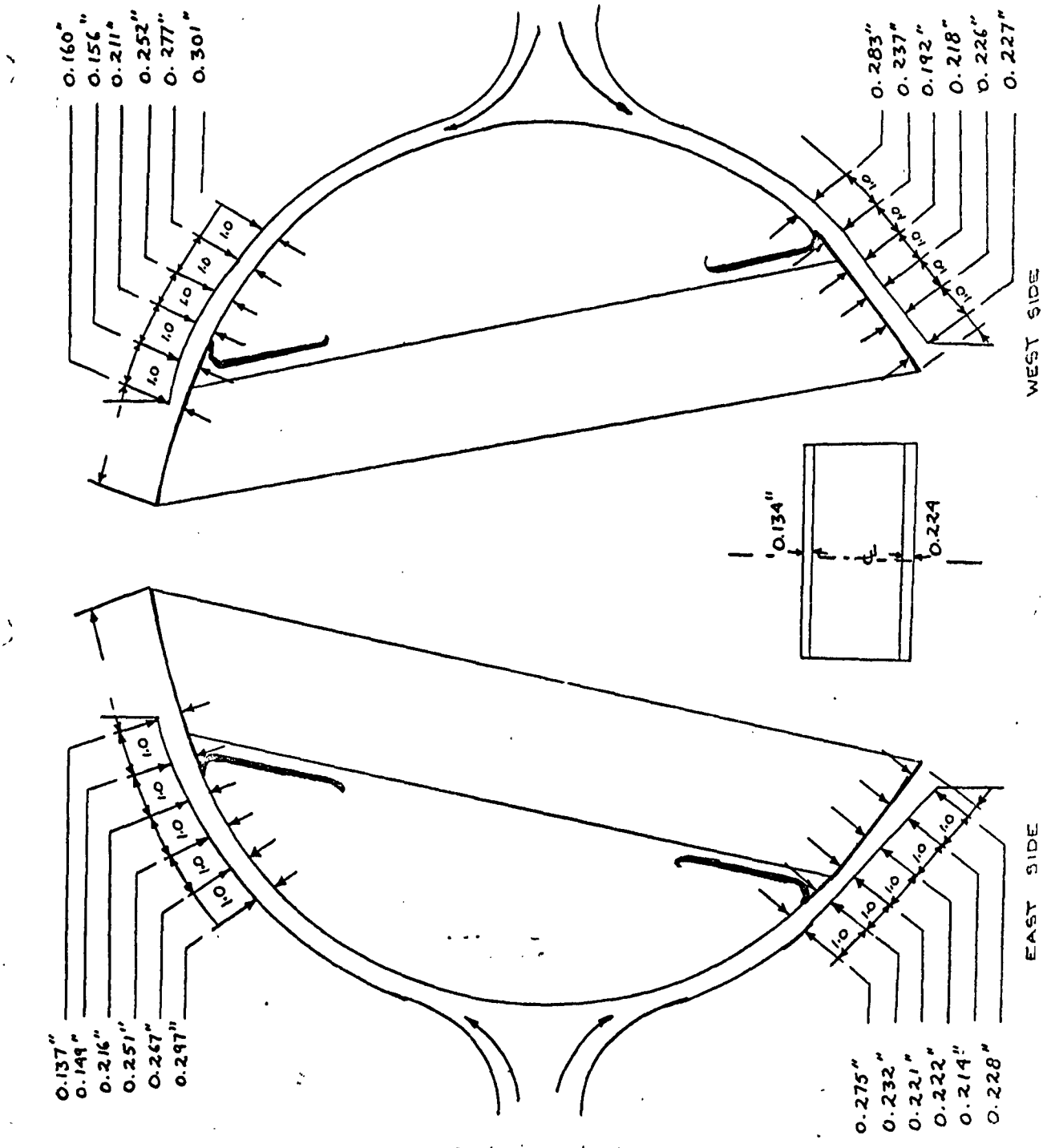

CALC.	U.M.G.	6/21/62	REVISED	DATE	LEAKAGE CONTROL MODEL GAP MEASUREMENTS TEST 2224 RUN No. 107 EWA 5-609	D2-80085
CHECK						Fig. 2-55
APPR.						
APPR.					THE BOEING COMPANY SEATTLE, WASHINGTON	2-81

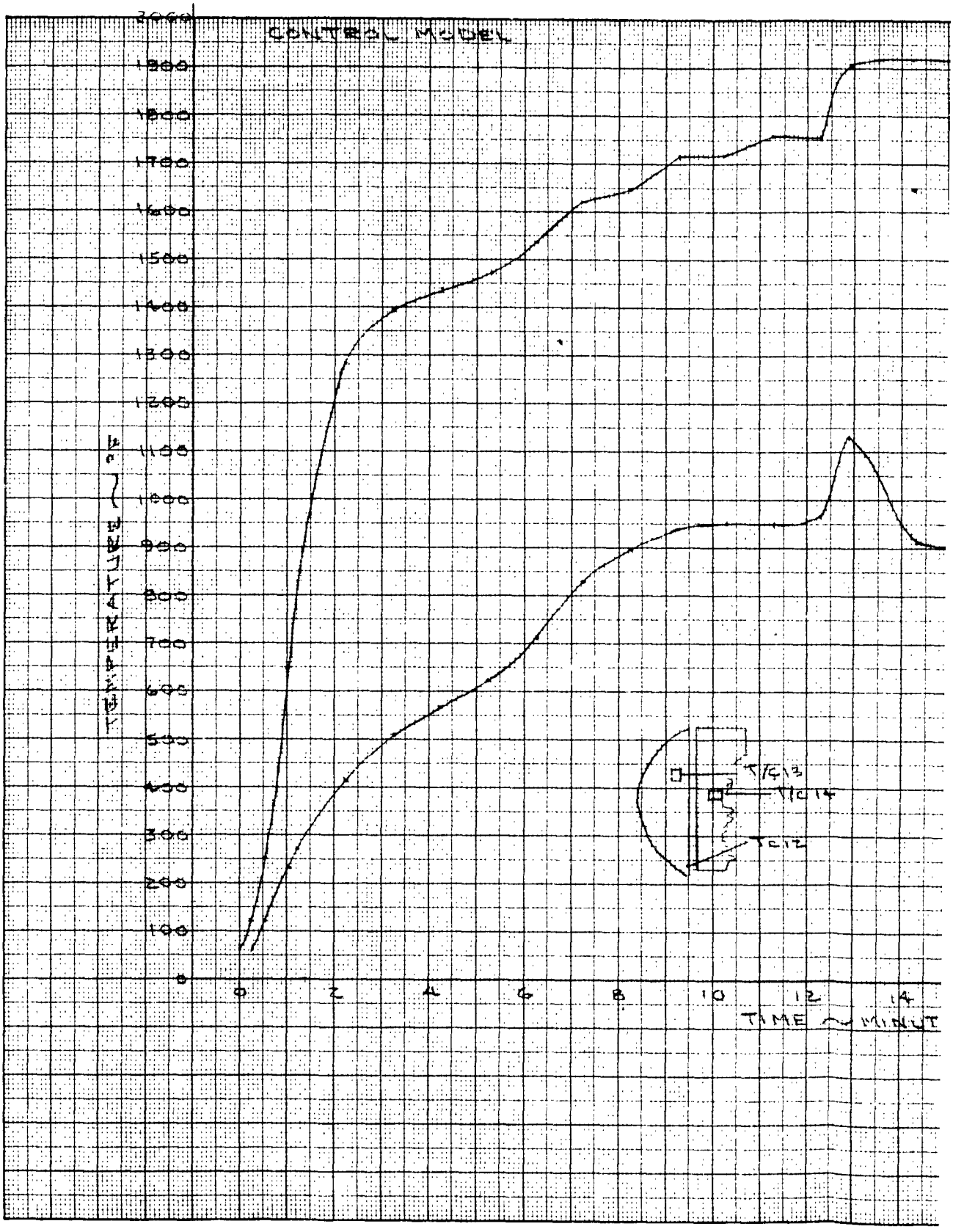
CONTROL MODEL
2000
1900
1800
1700
1600
1500
1400
1300
1200
1100
1000
900
800
700
600
500
400
300
200
100
0
0
2
4
6
8
10
12
14
TIME ~ MINUT
TC 13
TC 14
TC 12

1

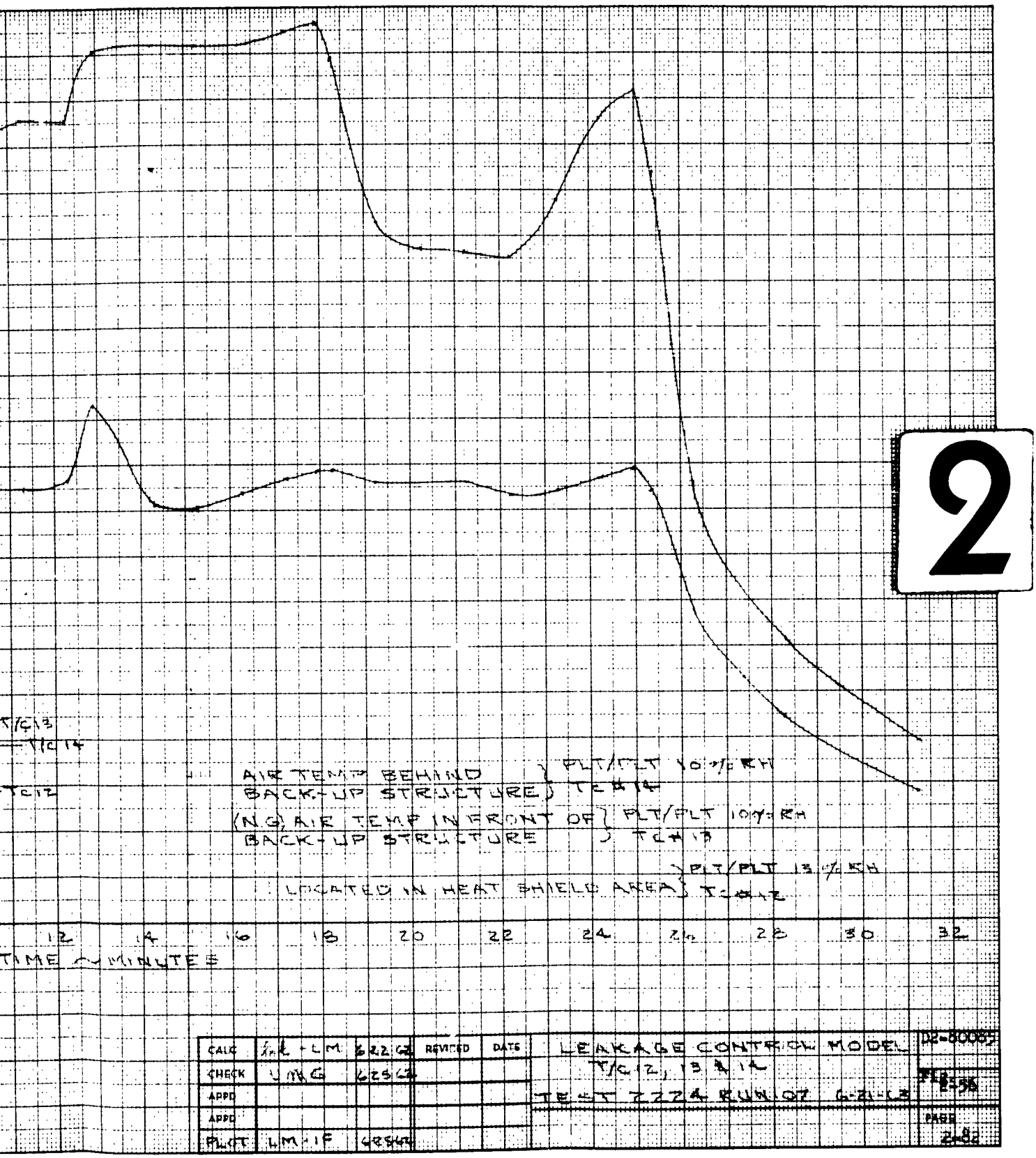

CALC	J.M.L + L.M.	6-22-64	REVISED	DATE	LEAKAGE CONTROL MODEL T/C 12, 13 & 14 TEST 2224 RUN-OF 6-21-64
CHECK	L.M.G.	6-25-64			
APPD					
APPD					
PLOT	L.M.-I.F.	6-25-64			

D2-80085
PAGE 2-58

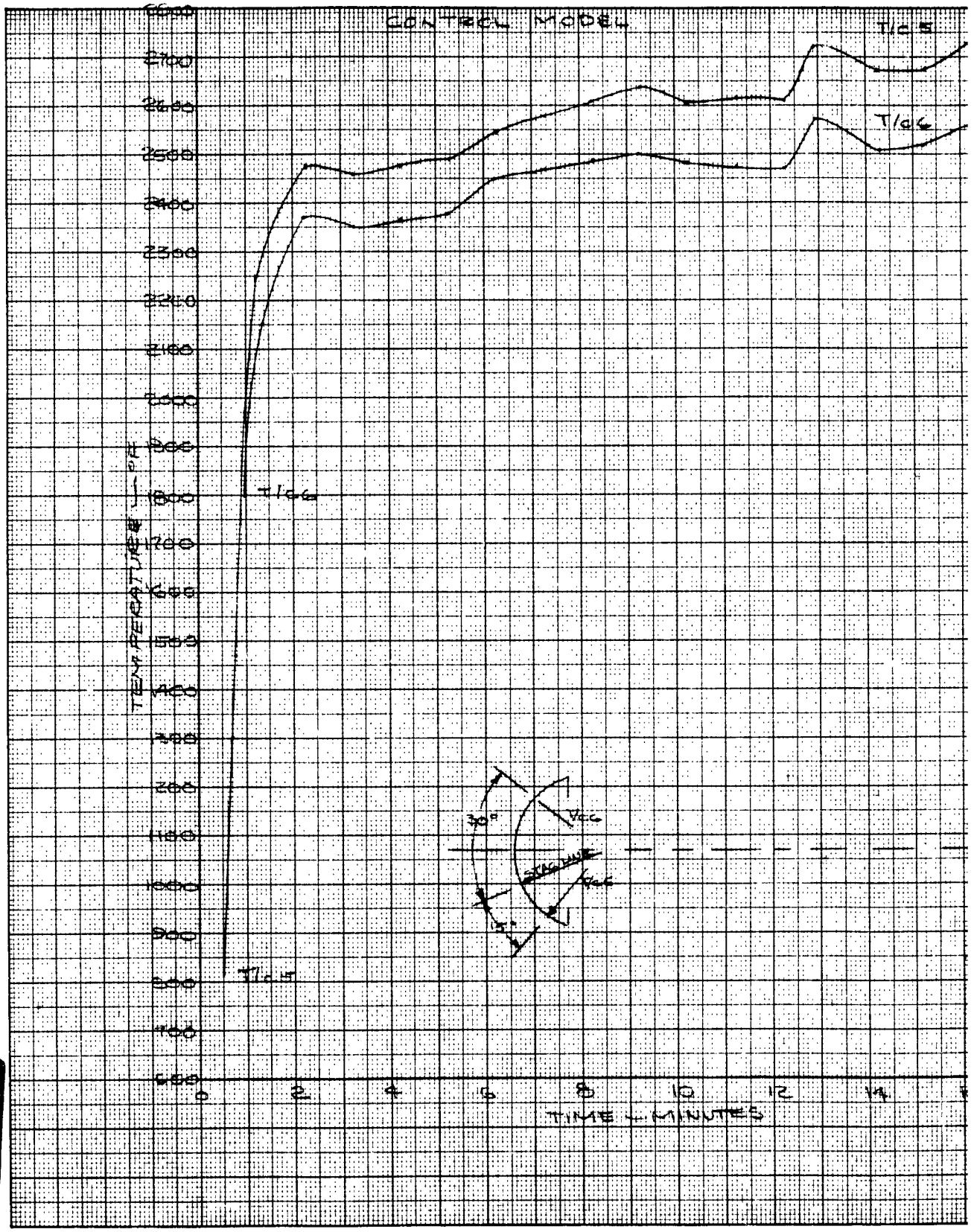
CONTROL MODES
T/C 5
T/C 6
TEMPERATURE °F
TIME - MINUTES
0
2
4
6
8
10
12
14
2700
2600
2500
2400
2300
2200
2100
2000
1900
1800
1700
1600
1500
1400
1300
1200
1100
1000
900
800
700
600
30°
Vcc
Vcc

1

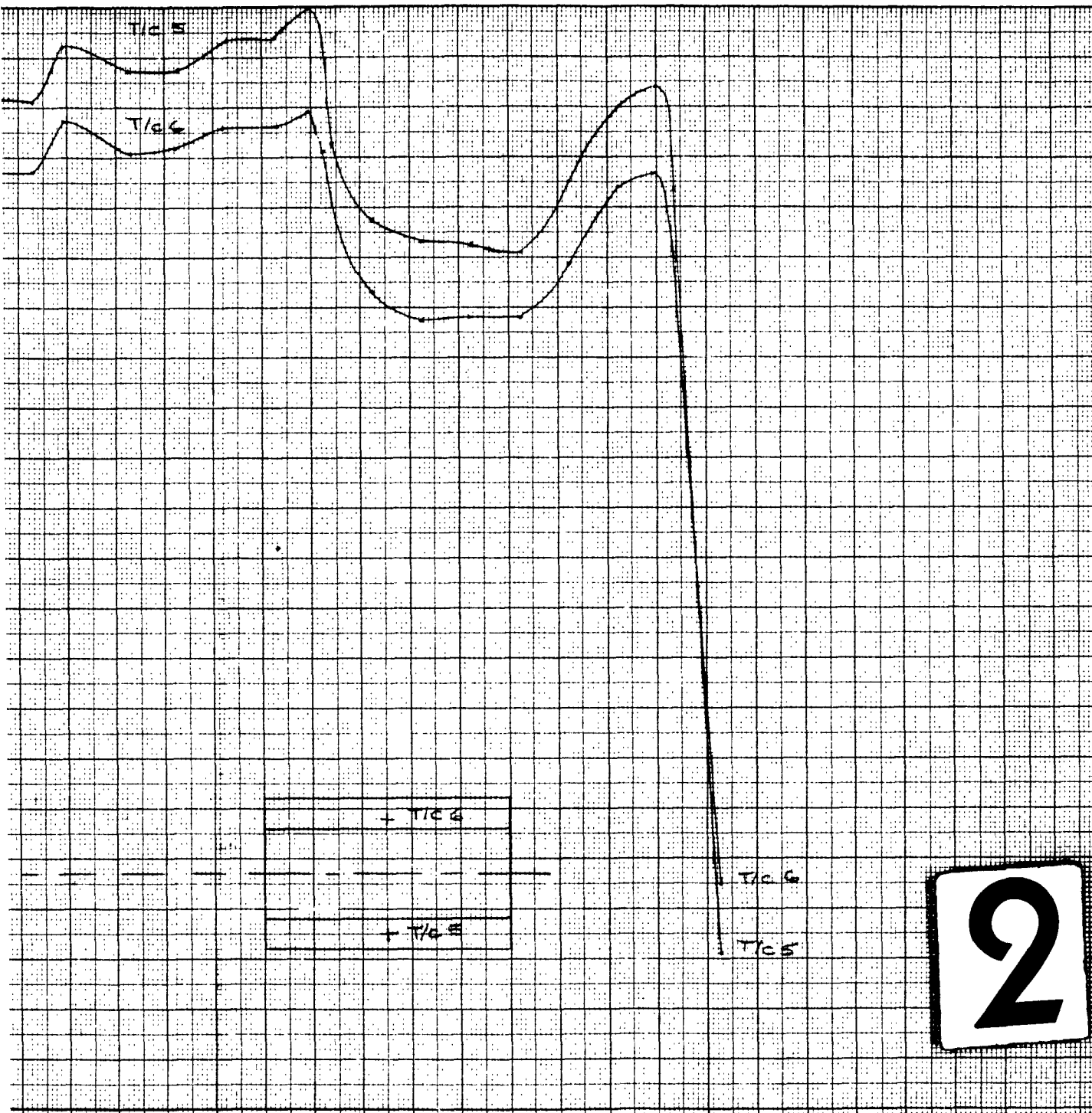

2

CALC	[illegible]	4-22-63	REVISED	DATE	LEAKAGE CONTROL MODEL	22-40085
CHECK					T/C 5 & 6	
APPD					TEST 2224 PUNCH 6-21-63	
APPD						
DRAFT	[illegible]	4-25-63				

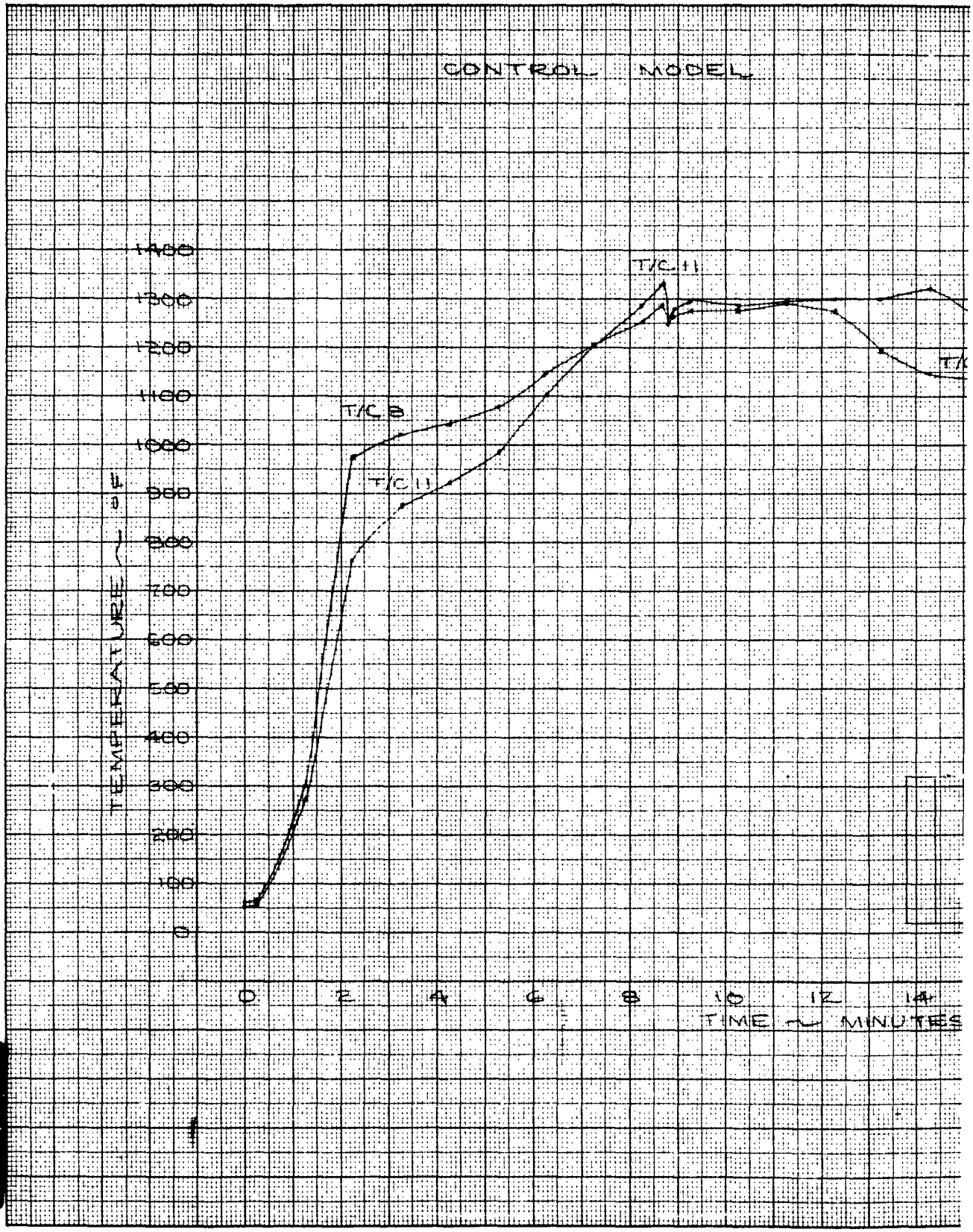
CONTROL MODEL
T/C 11
T/C 8
T/C 11
TEMPERATURE
1400
1300
1200
1100
1000
900
800
700
600
500
400
300
200
100
0
0
2
4
6
8
10
12
14
TIME — MINUTES

1

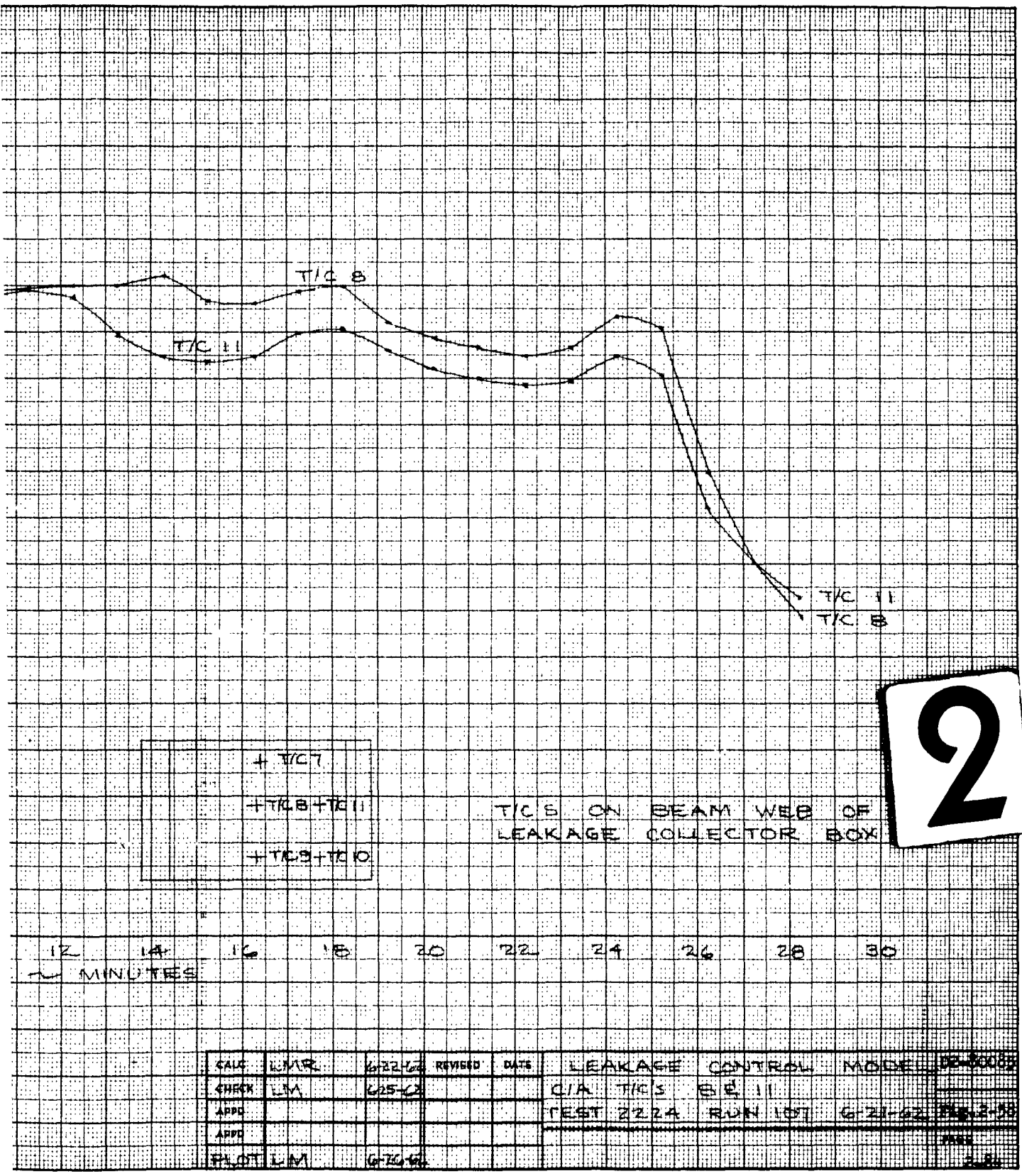

2

CALC	L.M.R.	6-22-62	REVISED	DATE
CHECK	L.M.	6-25-62		
APPD				
APPD				
PLOT	L.M.	6-26-62		

LEAKAGE CONTROL MODEL DS-XXXX
C/A T/C'S SE 11
TEST 2224 RUN 107 6-21-62

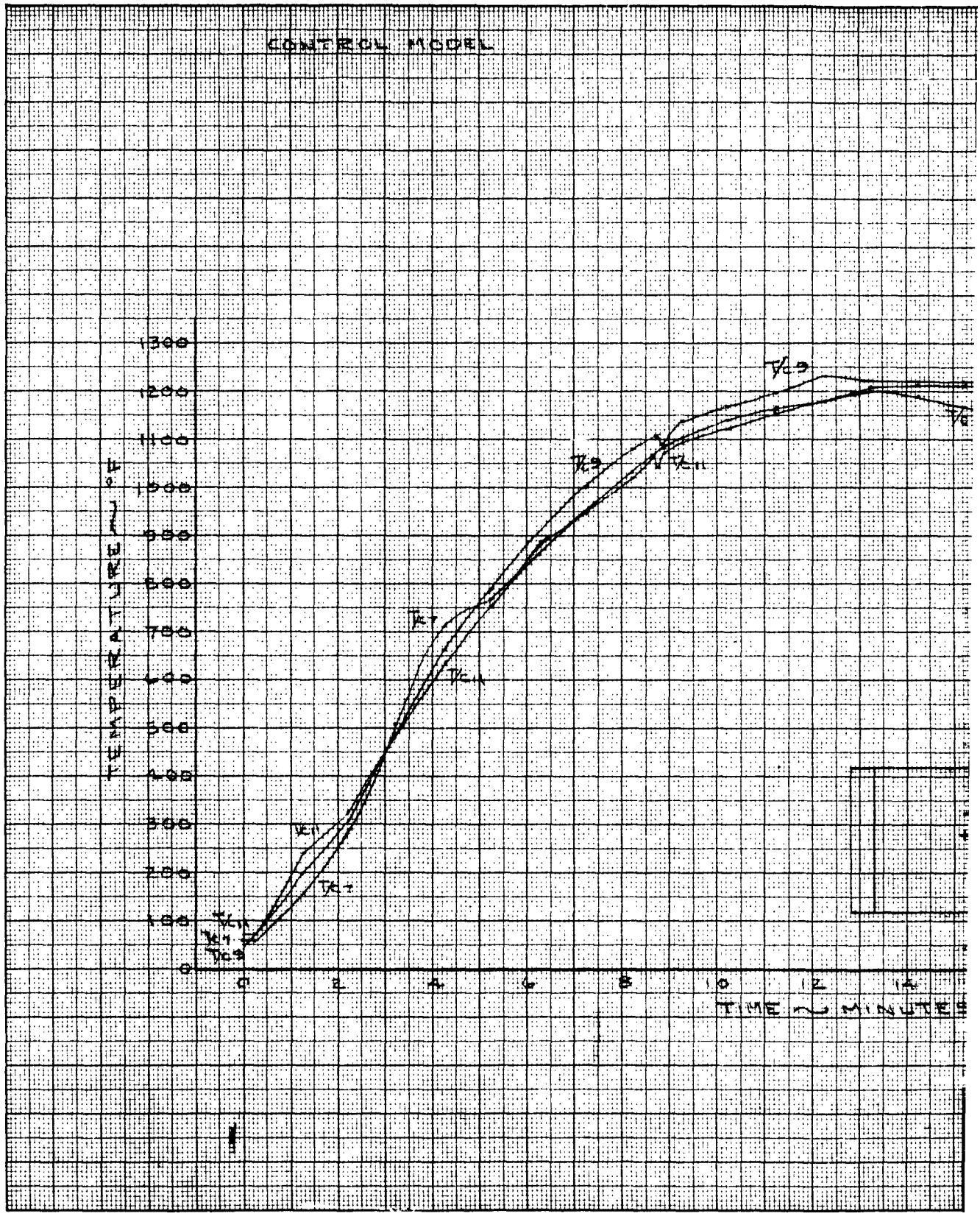
CONTROL MODEL
TEMPERATURE °F
1300
1200
1100
1000
900
800
700
600
500
400
300
200
100
0
0
2
4
6
8
10
12
14
TIME — MINUTES
Tc9
Tc11
Tc7
Tc1

1

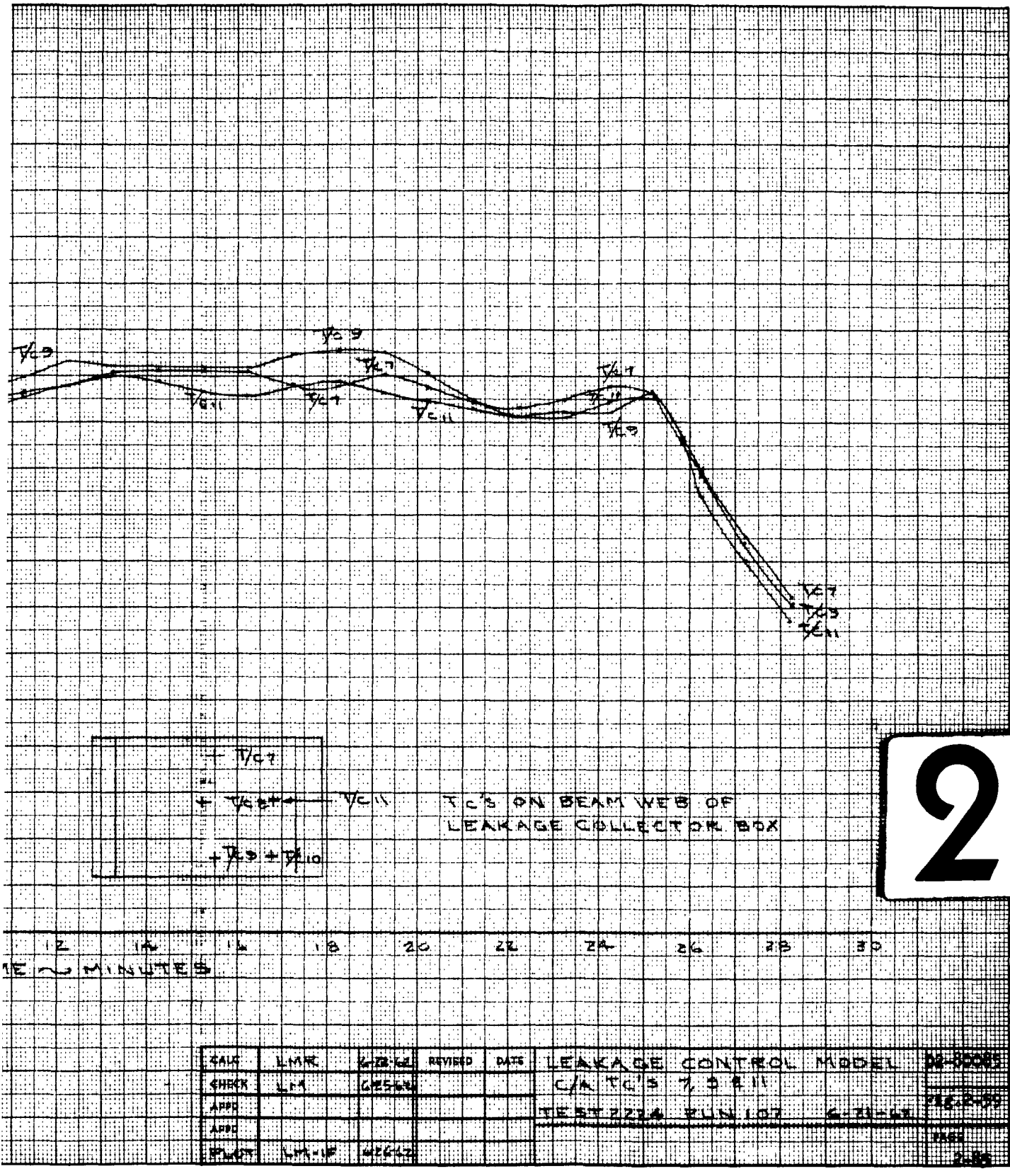

2

CALC	LMM	6-28-62	REVISED	DATE	LEAKAGE CONTROL MODEL	62-00065
CHECK	LMM	6-28-62			C/A T/C'S 7, 9 & 11	
APPD					TEST 2224 RUN 107 6-21-62	FIG. 2-89
APPD						PAGE
PILOT	LMM-JF	6-28-62				2-86

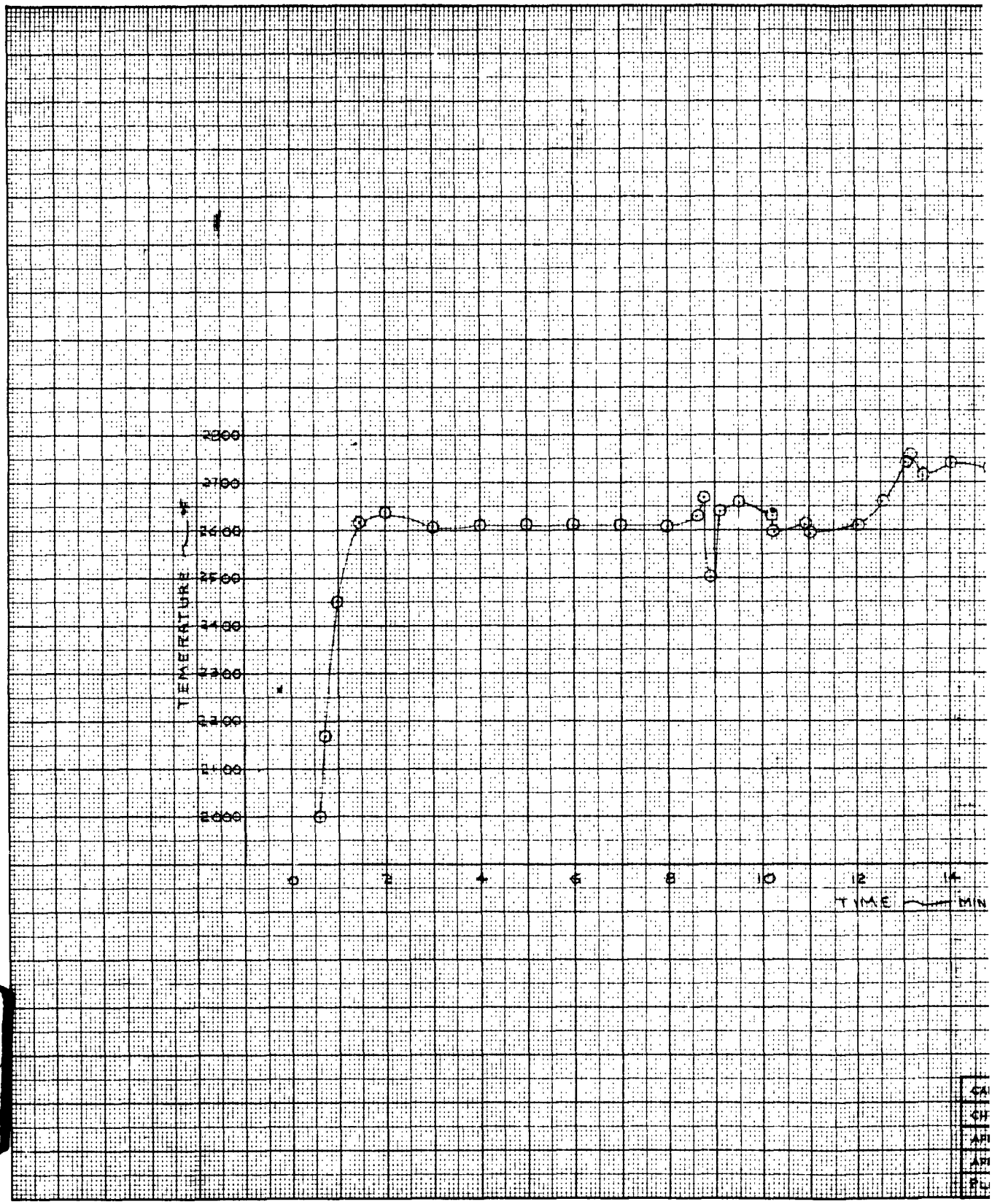
TEMERATURE °F
2200
2700
2600
2500
2400
2300
2100
2000
0
2
4
6
8
10
12
14
TIME MIN

1

2

CALC	JP	4-27-62	REVISED	DATE	PYROMETER LEAKAGE CONTROL MODEL
CHECK					
APPD					TEST 2224 RUN 107 6-20-62
APPD					
PLOT	RTW	4-30-62			

D2-80085
PAGE 2-36

SEGMENTED DOUBLE SHELL MODEL

DS- DOUBLE SHELL MODEL LEADING EDGE
POST RUN #10 - TOP VIEW 7-13-62 2411-084

U3-4071-1000 (was BAC 1546-L-R3)

FIGURE 2-61

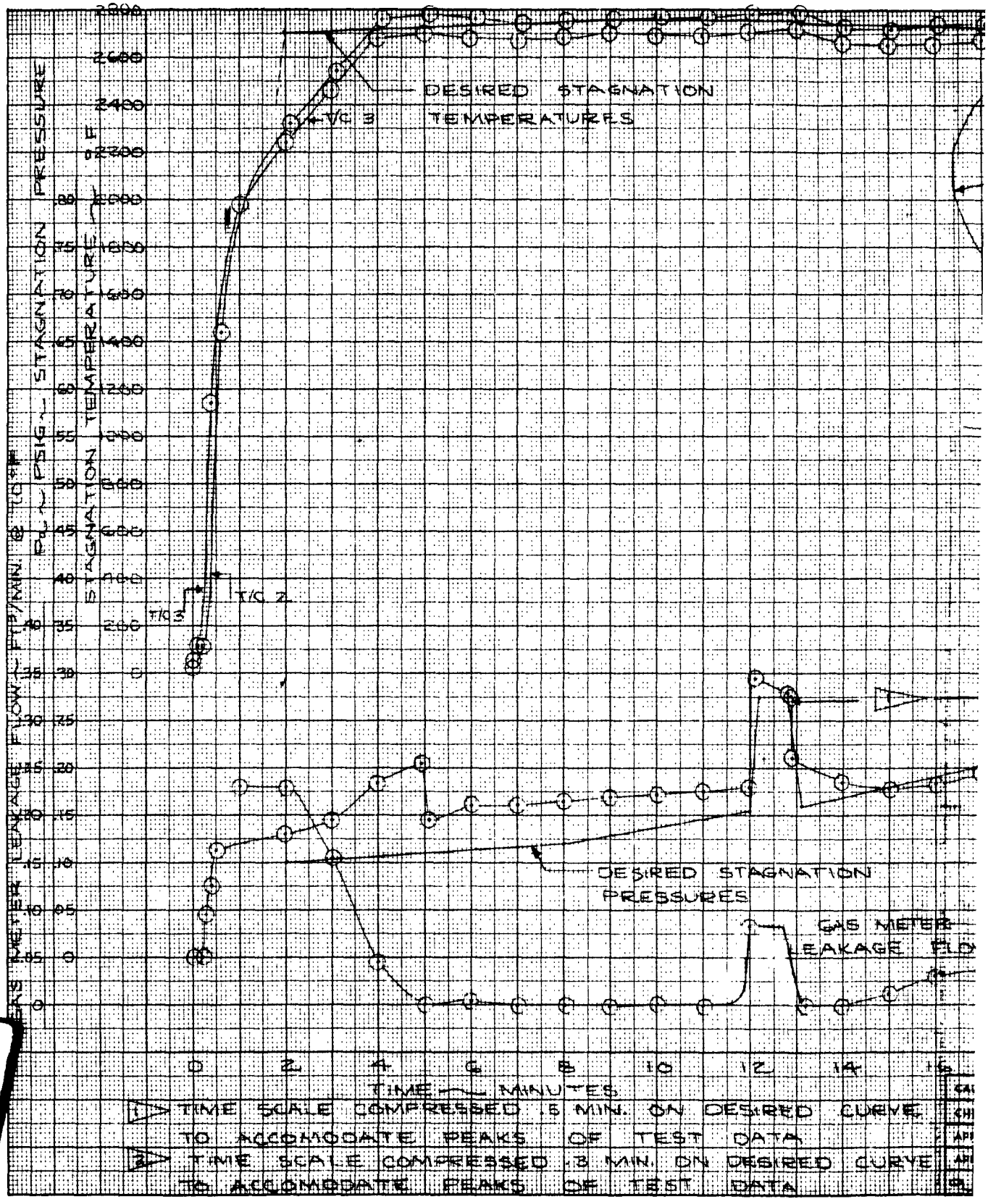
DESIRED STAGNATION
TEMPERATURES
T/C 3
T/C 2
T/C 1
DESIRED STAGNATION
PRESSURES
GAS METER
LEAKAGE FLO
STAGNATION PRESSURE
STAGNATION TEMPERATURE
GAS METER LEAKAGE FLOW FT³/MIN @ STD °F
0 2 4 6 8 10 12 14
TIME — MINUTES
1 TIME SCALE COMPRESSED .5 MIN. ON DESIRED CURVE TO ACCOMODATE PEAKS OF TEST DATA
2 TIME SCALE COMPRESSED .3 MIN. ON DESIRED CURVE TO ACCOMODATE PEAKS OF TEST DATA

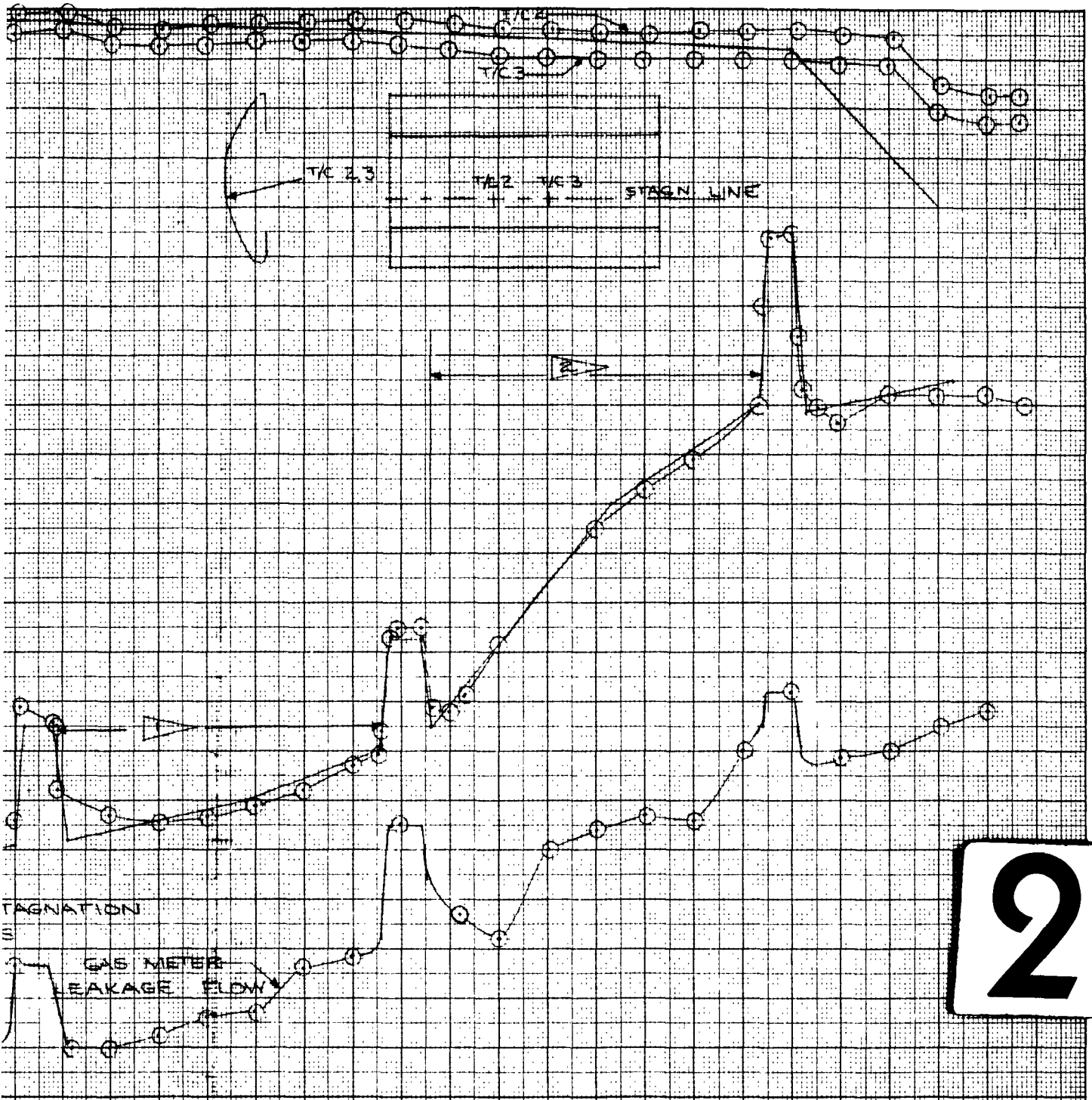

2

CALC				REVISED	DATE	SEGMENTED DOUBLE SHELL MODEL	D2-30085
CHECK						LEAKAGE FLOW, STAG. TEMP & PRESS.	FIG. 2-68
APPD						EWA 3-609 TEST 2224	
APPD							PAGE
PROJECT	LEC	4234-2					2-88

SIRED CURVE
DATA
ESIRED CURVE
DATA

U I 4041 7000

K·E ALBANENE 1951 TRACING PAPER 6x7/8

			REVISED	DATE
CALC				
CHECK				
APR				
APR				
Plot	P.C.T.	4-15-3		

LEADING EDGE SHROUD PRESSURES, SEGMENTED DOUBLE SHELL MODEL, PLASMA JET TEST

EWA 5-609 TEST 2224

THE BOEING COMPANY

D2-80085

FIGURE 2-

PAGE 2-89

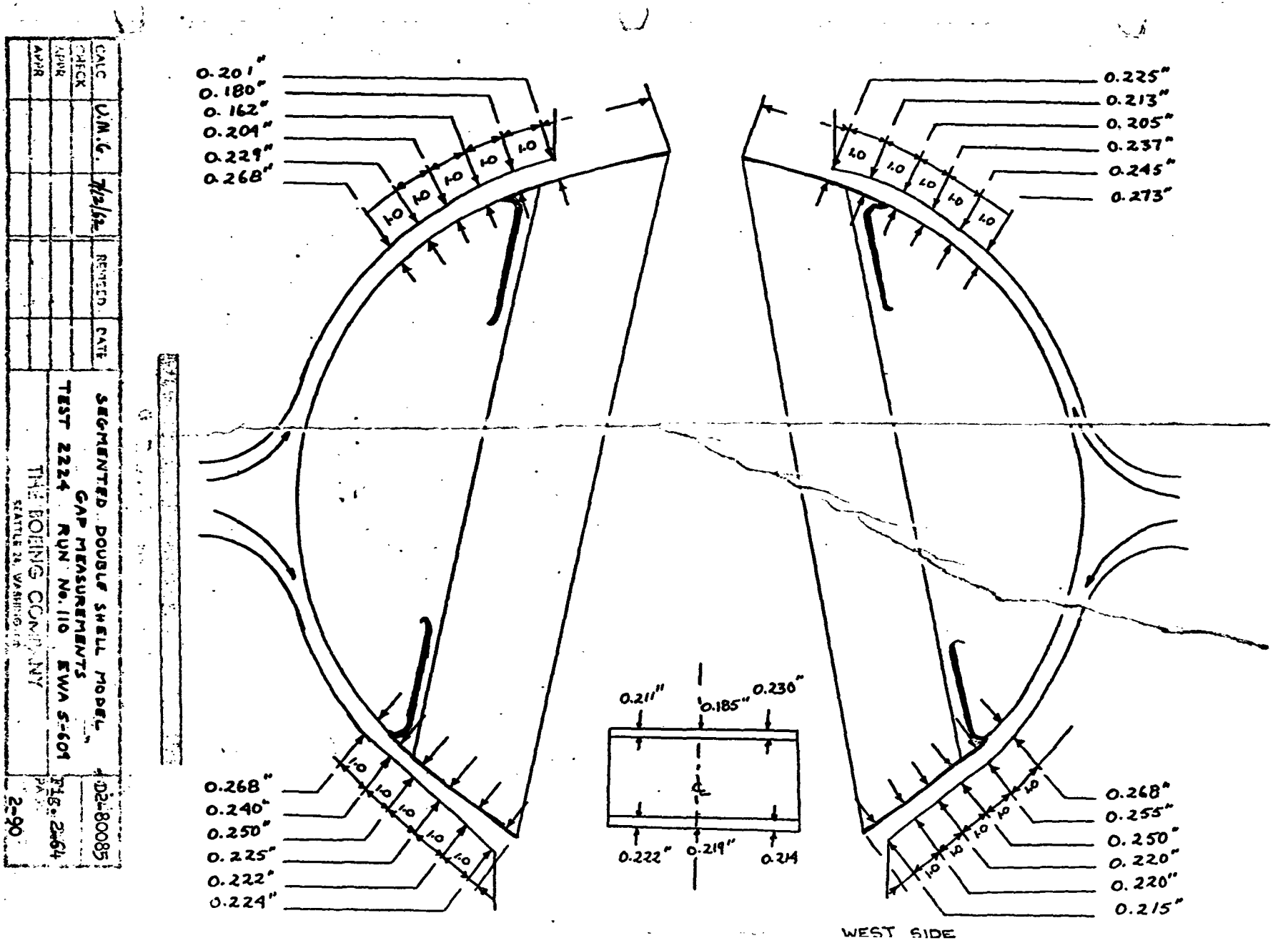

	CALC	U.M.G.	7/2/62	REVISED	DATE
	CHECK				
	APPR				
	APPR				

SEGMENTED DOUBLE SHELL MODEL
GAP MEASUREMENTS
TEST 2224 RUN No. 110 EWA S-601

THE BOEING COMPANY
SEATTLE 24, WASHINGTON

D2-80085
PAGE 2-64
2-90

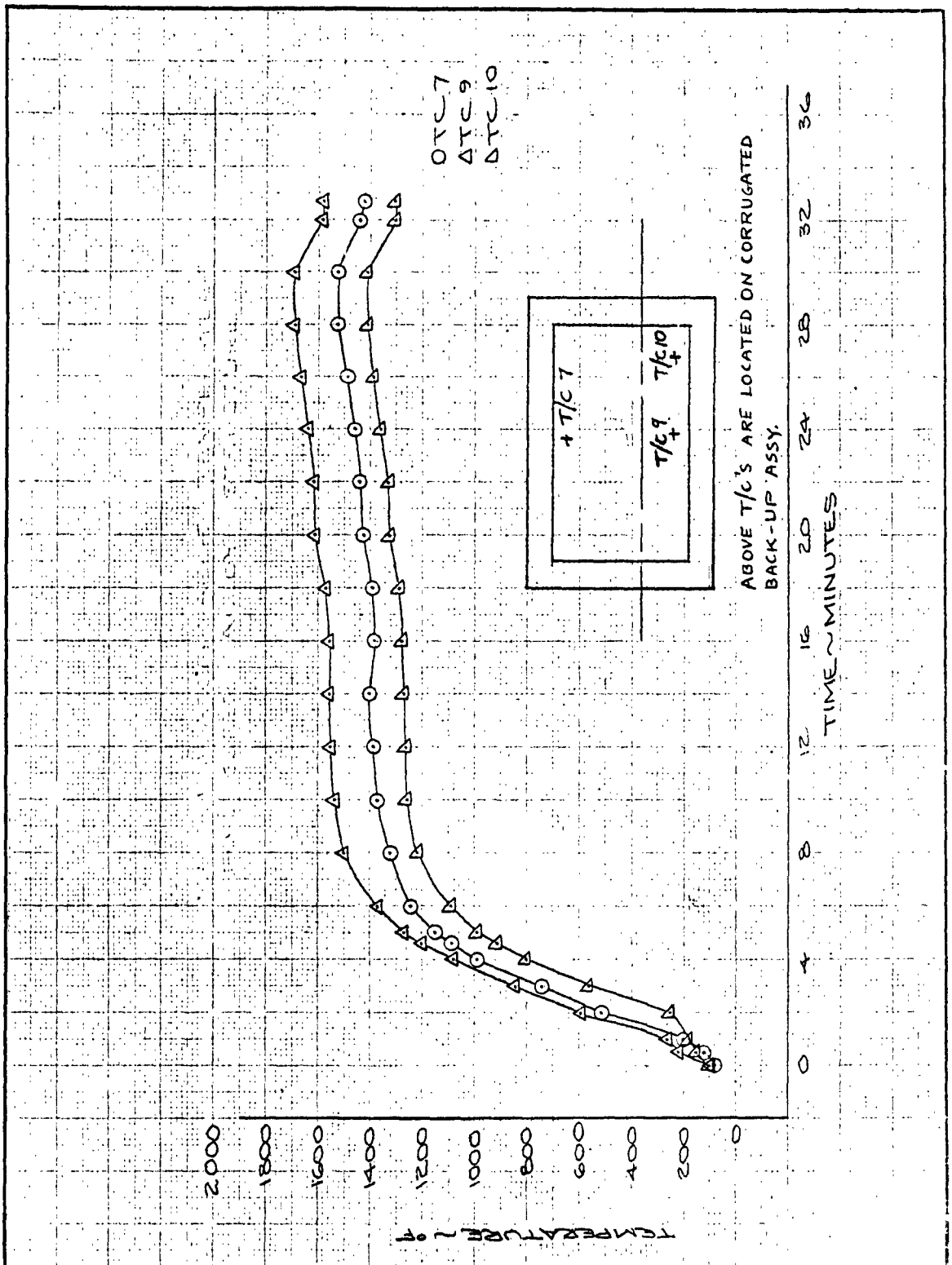

CALC		7-17-62	REVISED	DATE	SEGMENTED DOUBLE SHELL MODEL - C/A T/C'S # 7, 9 & 10	D2-80085
CHECK					TEST 2224 RUN 10 7-12-62	Fig. 2-6
APR					THE BOEING COMPANY	PAGE 2-91
APR						

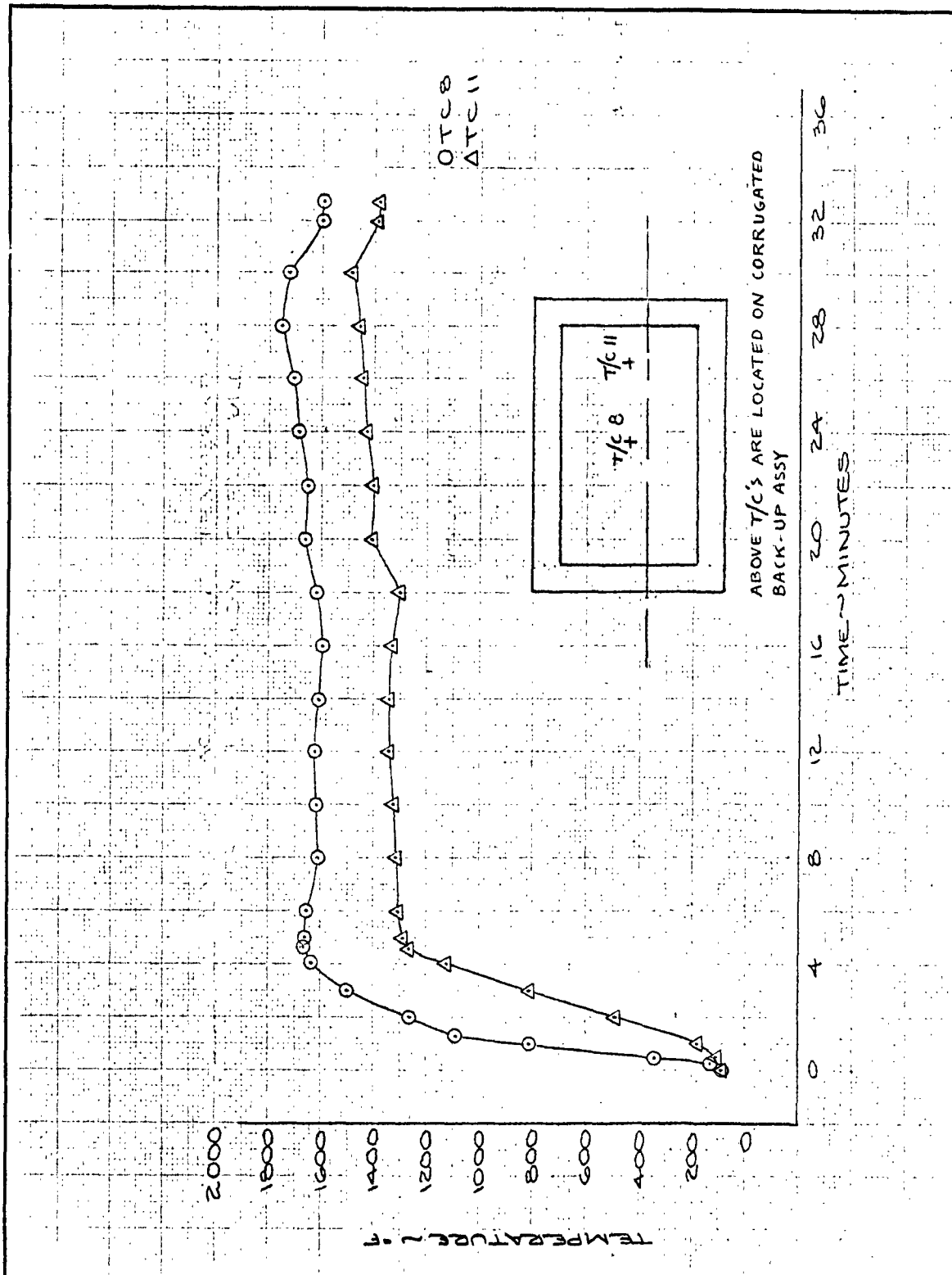

CALC		7-17-62	REVISED	DATE	SEGMENTED DOUBLE SHELL MODEL C/A T/C's # 8 & # 11 TEST 222A RUN 110 7-12-62	D2-80085
CHECK						
APR						
APR						
					THE BOEING COMPANY	PAGE 2-92

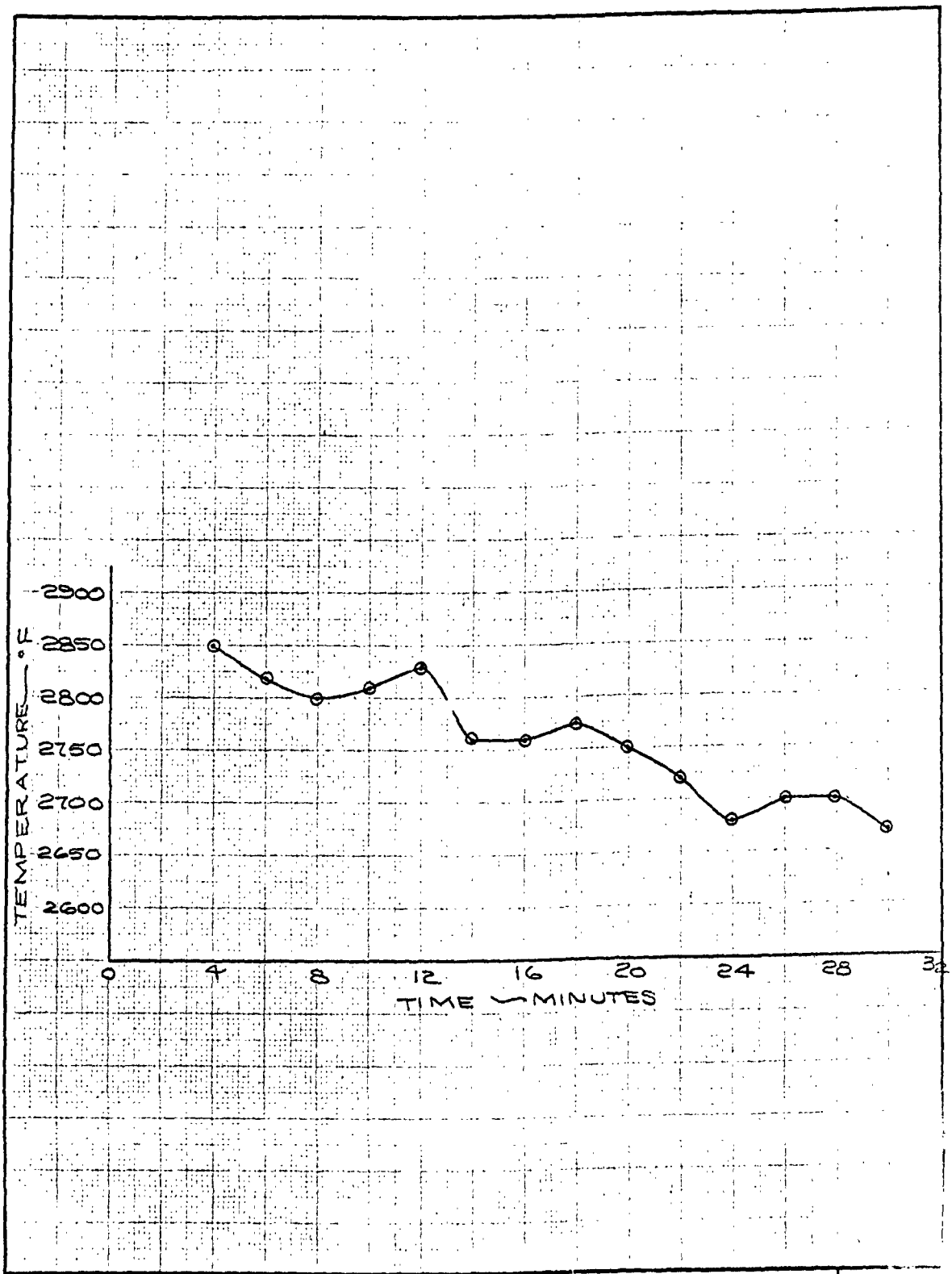

			REVISED	DATE	SEGMENTED DOUBLE SHELL MODEL PYROMETER TEMPERATURES PLASMA JET TEST EWA 5-609 TEST 2224	D2-80085
CALC						FIGURE 2-(
CHECK						
APR						
APR					THE BOEING COMPANY	PAGE 2-93
PLOT	lwa	4-23-63				

U3 4013 8000

K+E ALBANENE 1981 68587